Experimental Research on BFRP Confined Concrete Columns

by

Arngrímur Konráðsson

Thesis in civil engineering with
emphasis on structural engineering
Master of Science

March 2011

Experimental Research on BFRP Confined Concrete Columns

Arngrímur Konráðsson

Thesis in civil engineering with emphasis on
structural engineering submitted to
the School of Science and Engineering
at Reykjavík University in partial fulfillment
of the requirements for the degree of
Master of Science

March 2011

Supervisor:

Eyþór Rafn Þórhallsson,
Associate professor, Reykjavík University, Iceland

Examiner:

Dr. Baldvin Einarsson,
Associate professor (part time), University of Iceland
Director, Efla Consulting Engineers

Abstract

Many older structures today are in the need of strengthening their existing civil engineer infrastructure. The reasons are deterioration by ageing or corrosion caused by environmental factors, load increase because of change of function in the structure or poor design which does not meet the current more strict design requirements such as in earthquake areas. The most practical solutions for rehabilitation are often those that minimise the risk of structural collapse which can be done by upgrading selected critical structural components.

The primary objectives of this research are to investigate the behaviour of axially loaded concrete columns confined with an obscure material in civil engineer for strengthening, basalt fibre reinforced polymer jacket (BFRP), and to compare calculation predictions to the test results using available guidelines. Eighteen standard cylinder specimens and six reinforced columns of square cross-section were confined with various BFRP thicknesses to investigate the confinement effectiveness for ductile behaviour. Unjacketed control specimens were also tested. Thereto, the columns had different corner radius in order to examine the influence of rounding of corners on confinement effectiveness. Tensile coupon tests were made to evaluate the ultimate strength and strain of the BFRP material. Design approaches for FRP confinement of reinforced concrete columns of three design guidelines were introduced and their different approaches discussed. The experimental results were compared to the theoretical calculations obtained by each guideline.

The experimental results clearly demonstrate that BFRP wrapping can enhance the structural performance of concrete columns under axial load. Available guidelines can be considered to be able to predict the compressive strength enhancement with satisfactory accuracy. However, more scatter occurred in the prediction of the axial strain. Reduced strain efficiency of 60% can be considered to be valid for BFRP jacket on concrete columns.

Keywords: Basalt fibre, BFRP, concrete column, confinement, square columns, strengthening.

Ágrip

Eldri byggingar fullnægja í mörgum tilvikum ekki kröfum gildandi staðla auk þess sem mögulegt er að burðarkerfi þeirra hefur orðið fyrir skemmdum. Ýmsar ástæður geta verið fyrir þessu, m.a. öldrun, hrörnun vegna veðrunaráhrifa, aukið álag vegna breyttrar notkunar, skemmdir vegna óhappaálágs eða hönnunin stenst einfaldlega ekki nútíma hönnunarkröfur eins og til dæmis á jarðskjálftasvæðum. Til að lágmarka hættu á hruni eldri bygginga er því mikilvægt að styrkja viðkvæmustu hluta hennar.

Megin markmið þessa verkefnis er að rannsaka styrktar súlur undir lóðréttu álagi. Súlurnar eru styrktar með trefjastyrktu epoxý efni (FRP) með basalttrefjum (BFRP) og niðurstöður prófana bornar saman við útreikninga samkvæmt leiðbeinandi hönnunarstöðlum fyrir FRP efni í steyptum mannvirkjum. Basalttrefjar er nýtt efni á sviði mannvirkjahönnunar sem ekki hefur verið tekið fyrir í stöðlum. Í formi trefjamotta er þeim vafið umhverfis súlur og þær þannig gerðar bendiluktar. Átján sívalningssýni og sex járnbentar ferhyrndar súlur, bendiluktar með mismunandi fjölda laga af basalttrefjamottum voru prófaðar til þess að rannsaka virkni mottanna á steyptum byggingahlutum. Óstyrkt sýni voru einnig prófuð til samanburðar. Ferhyrndu súlurnar voru rúnnaðar á hornum til þess að skoða áhrif þversniðslögunar á bendilukta styrkinn. Togþolspróf voru gerð á basaltmottunum til þess að meta togstreitu og togþol efnisins. Hönnunarstaðlar sem taka á bendiluktum súlum með FRP efnum voru kynntir og farið í gegnum mismunandi reikniaðferðir. Niðurstöður tilrauna voru að lokum bornar saman við útreiknaðar styrktaraukningar.

Niðurstöður tilrauna sýna að með því að vefja basalttrefjamottum um súlur má auka burðareiginleika steyptra súlna gagnvart lóðréttu álagi. Þeir staðlar sem skoðaðir voru áætla aukið þrýstiþol með viðunandi nákvæmni, það á hinsvegar ekki við um útreikninga á auknu streituþoli þar sem dreifnin var nokkuð meiri. Lækkun togstreitu í basalttrefjamottum um 60% virðist vera raunhæf í hönnun á steyptum súlum styrktum með slíkum mottum.

Lykilorð: Basalttrefjar, BFRP, bendilukt steypa, steyptar súlur, styrkingar,

Experimental Research on BFRP Confined Concrete Columns

Arngrímur Konráðsson

Thesis (30 ECTS) submitted to
the School of Science And Engineering
at Reykjavík University in partial fulfillment
of the requirements for the degree of
Master of Science in Civil Engineering with Specialization in Structural Design

March 2011

Student: Arngrímur Konráðsson

Arngrímur Konráðsson

Supervisor: Eyþór Rafn Þórhallsson

Eyþór Rafn Þórhallsson

Examiner: Baldvin Einarsson

Baldvin Einarsson

Acknowledgements

The research presented in this thesis was worked in collaboration with the Innovation Center Iceland and funded by the Technology Development Fund of Rannís.

I would like to thank my supervisor Eyþór Rafn Þórhallson, civil engineer M.Sc. and associate professor at Reykjavik University, for his guidance and inspiration through the entire thesis work. I would like to thank Stefan Kubens, research engineer & scientist Ph.D. at the Innovation Center Iceland for his assistance and motivation through the experimental work.

Special thanks go to the people that made the experimental work possible: Björgvin Smári Jónsson, civil engineering student M.Sc., Einar Einarsson, managing director of concrete production at BM-Vallá, Gísli Freyr Þorsteinsson, mechanician at Reykjavik University, Gunnlaugur Jónason, civil engineer B.Sc., Hrannar Traustason, electronics engineer at Reykjavik University, Indriði Ríkharðsson, mechanical engineer M.Sc. and assistant professor at Reykjavik University, Ívar Hauksson, civil engineering student M.Sc. and the technical staff at Mannvits´s laboratory.

I would also like to thank Fjóla Guðrún Sigtryggsdóttir, head of the Civil Engineering department at Reykjavik University, Hlíf Þ. Jónsdóttir pharmacist M.Sc., Konráð Erlendsson geographer B.Sc., Sigurður Unnar Sigurðsson doctoral candidate in earthquake engineering for reading and correcting and Sigurður Guðjón Jónsson, civil engineering student M.Sc. for his valuable comments and support through the writing of the thesis.

Finally, I would like to thank my fiancée, Hildur B. Jónsdóttir and son, Hákon Logi Arngrímsson for their patience and support through my M.Sc. study.

Table of Contents

List of Figures

List of Tables

Notation

Latin Upper Case Symbols

A_g	=	Gross area
$A_{s,l}$	=	Cross-sectional area of longitudinal reinforcement
$A_{s,t}$	=	Cross-sectional area of transverse reinforcement
D	=	Diameter of circular column
D′	=	Hoop diameter
$D^* = b$	=	Diameter of equivalent circular column in the case of rectangular column
E_c	=	Modulus of elasticity of concrete
E_f	=	Modulus of elasticity of FRP
F_c	=	Axial load capacity of unconfined column at peak
F_{cc}	=	Axial load capacity of confined column at ultimate
F_{cc1}	=	Axial load capacity of confined column at first peak
F_{cu}	=	Axial load capacity of unconfined column at ultimate
F_{max}	=	Maximum compressive force
F_t	=	Ultimate tensile force
MCR	=	Confinement ratio of rectangular column
N_c	=	Unconfined axial load capacity
N_{cc}	=	Confined axial load capacity
R_{max}	=	Ratio of obtained maximum FRP strain on concrete specimens to the ultimate FRP strain from tensile coupon test specimen

Latin Lower Case Symbols

b	=	Width of rectangular cross-section, shorter side
b_f	=	Width of FRP strap
f_c	=	Compressive strength of concrete
f_{cc}	=	Confined compressive strength at ultimate
f_{cc1}	=	Confined compressive strength at first peak
f_f	=	Ultimate tensile strength of FRP
f_l	=	Confinement pressure
$f_{l,a}$	=	Actual confinement pressure
f_y	=	Yield strength of reinforcement
h	=	Width of rectangular cross-section, longer side
k_s	=	Shape factor for rectangular cross-section
k_ε	=	Strain efficiency factor
n	=	Number of FRP layers
r	=	Corner radius of cross-section
s	=	Hoop spacing
t_f	=	Nominal thickness of FRP
$t_{f,tot}$	=	Total nominal thickness of FRP

w	=	Width of FRP tensile coupon test specimen
ø	=	Diameter of reinforcement bar

Greek Symbols

ε_{c1}	=	Compressive strain in the concrete at the peak stress f_c
ε_{cc1}	=	Compressive strain in the concrete at the peak stress f_{cc1}
ε_{cu}	=	Compressive strain in the concrete at the confined compressive stress f_{cc}
$\varepsilon_{cu,s}$	=	Compressive strain in the concrete at the ultimate compressive stress f_{cc} in the case of confinement with steel hoops
ε_f	=	Ultimate tensile strain of FRP
$\varepsilon_{f,a}$	=	Actual tensile strain of FRP
ε_y	=	Tensile strain in steel at yield stress
ρ_f	=	Reinforcement ratio for FRP
ρ_l	=	Reinforcement ratio for longitudinal reinforcement
ρ_t	=	Reinforcement ratio for transverse reinforcement

Abbreviations

FRP	=	Fibre reinforced polymers
AFRP	=	Aramid fibre reinforced polymers
BFRP	=	Basalt fibre reinforced polymers
CFRP	=	Carbon fibre reinforced polymers

1 Introduction

1.1 Background

Many older structures today are in the need of strengthening their existing civil engineer infrastructure. The reasons are deterioration by ageing or corrosion caused by environmental factors, load increase because of change of function in the structure or poor design which does not meet the present more stringent design requirements such as in earthquake areas. The low probability of major seismic events and high cost of structural rehabilitation make it difficult to justify economically. The most practical solutions for rehabilitation can often be those that minimise the risk of structural collapse which can be done by upgrading selected critical structural components. Strengthening or retrofitting of older structures to resist higher design loads or increase ductility has been accomplished with traditional materials such as externally bonded steel plates and steel jackets since in the 1960s [1].

Concrete columns are important structural elements which are vulnerable for exceptional loads. In older structures, columns often have insufficient transverse reinforcement which is unable to provide sufficient confinement to the concrete core or to prevent buckling of the longitudinal reinforcement. This can lead to unacceptable premature strength degradation. Confinement is required to delay the softening of concrete under ultimate load conditions and to allow a ductile response of the column. Numbers of retrofit techniques have been developed for strengthening columns which have led to improvement in both axial strength and ductility and to prevent buckling of the longitudinal reinforcement. Techniques with traditional materials include confinement with steel jackets or reinforced concrete jackets [2]. More recent technique is external confinement by wrapping fibre reinforced polymer (FRP) sheets around columns to form an external reinforced jacket. The wrapping of FRP composite sheets around concrete columns is a promising method for structural strengthening and repair, based on FRP´s unique properties in terms of strength, lightness, chemical resistance and ease of application. This strengthening technique is of practical interest for given its fast execution and low labour costs. The sheets provide a passive confinement to the concrete core and react against the lateral dilation of the column under compression which delays the softening of the concrete and has shown to enhance both strength and ductility of the column [3].

Extensive work has been done in the experimental and analytical fields on concrete specimens of circular columns since the development of FRP wrapping started in the 1980s, and later on, columns of square and rectangular cross-sections. The experimental work have mostly focused on the common FRP materials on the market which are carbon(CFRP), glass(GFRP) and aramid(AFRP) fibres. Among them, CFRP is the most used but the price of it is high and despite the lower price of GFRP and AFRP their mechanical properties are not as good [3-10].

Fardis and Khalili [8] were among the first to test concrete cylinders wrapped with FRP. They tested several cylinders confined with GFRP jacket and their test results showed strength gain from 1,5 to 5 times the unconfined compressive strength depending on the

jacket thickness. From their results they developed an analytical model to trace the behaviour of confined cylinders with increasing axial compression [11].

Saadatmanesh [4] studied reinforced columns of both circular and rectangular cross-sections. The columns were wrapped with FRP straps with clear spacing of 152-305 mm and applied in concentric rings or a continuous spiral. The results showed increase in ultimate compressive strength and ductility which increased linearly with increase in strap thickness. It also resulted in decreasing ductility as the strap spacing was increased. An analytical model was developed with the same stress versus strain relation for confined concrete as proposed by Mander [12].

Several reports on the design and construction of internally and externally reinforced concrete have been published which provide information on the use of FRP materials [13-15]. Analytical models derived for cylinder specimens have shown to predict the confinement strength quite well. However, the corner sharpness of square and rectangular cross-sections has an influence on the distribution of the confining stress which reduces the compressive strength of the columns and creates a certain uncertainty in predicting the compressive strength of non-circular columns.

Basalt fibre (BFRP) is a new material in civil engineering compared to carbon, glass and aramid and has shown to be a promising material for infrastructure strengthening. The fibres are made from basalt rocks through melting process and contain no other additives in the manufacturing process which makes advantages in cost. Basalt fibres show comparable mechanical properties to glass fibres at lower cost and exhibit good resistance to chemical and high temperature exposure [16]. The ultimate strain of BFRP is higher compared to other common FRP materials and thus it is interesting to use these advantages in column strengthening to enhance the seismic performance. However, there is still little research concerning the application of basalt fibre in civil engineering and its strengthening efficiency on concrete elements.

Much research has been done on concrete columns and cylinders confined with common FRP jackets, such as carbon, glass and aramid. Insufficient research has been done on FRP jackets made from basalt and thus it is important to research their efficiency on concrete members as a strengthening material in civil engineering.

1.2 Aim and Objectives of this Research

The main aim of this study is to increase knowledge on concrete columns strengthened with FRP jackets and investigate the efficiency of basalt fibre sheets as a strengthening material.

The objectives of this research are:

1. Investigate and review the strength properties of BFRP.
2. Investigate the ultimate compressive strength and axial strain capacity of axially loaded concrete cylinders confined with BFRP jackets.

3. Investigate the ultimate compressive strength and axial strain capacity of axially loaded reinforced concrete members of square cross-section confined with BFRP jackets.
4. Estimate the strain efficiency of the BFRP on confined concrete.
5. Compare designers guide calculations to test results in order to evaluate their accuracy in predicting strength of concrete confined with BFRP jackets.

1.3 Summary of Approach

Experimental work is done to investigate the strength improvement and axial strain capacity of axially loaded BFRP confined specimens. Concrete cylinder specimens are tested to study the actual behaviour of BFRP confined concrete and to review the efficiency of the BFRP jacket. Concrete columns of square section are also tested to investigate the behaviour of columns with low amount of transverse reinforcement which will be compared to BFRP confined columns with the same reinforcement but different amount of external reinforcement. Cylinders and columns are tested under axial load until failure.

Available design guidelines, considering FRP confined columns, are reviewed and their calculation methods used to estimate the strength gain of the concrete specimens. The test results are then compared to the calculation results and their accuracy estimated for predicting the strength of columns confined with an obscure FRP material in civil engineering.

1.4 Thesis outline

This research is divided into seven chapters and the main chapters are as follows:

Second chapter covers information and background relevant to the work of this research. The theory of confinement is explained and the use of FRP jackets for confined concrete. Main factors that have an impact on the FRP confinement performance are reviewed and previous researches relevant to those factors are specified.

Third chapter summarizes available design guidelines and their calculation methods introduced for confined columns.

Fourth chapter details the experimental work and the material properties of the concrete and BFRP material used.

Fifth chapter summarizes the results of the experimental work.

Sixth chapter discusses the test results, the efficiency of the BFRP jacket and the strength prediction by the design guidelines.

Seventh chapter includes a summary of the main conclusions drawn from the experimental work. Future research involving confinement of concrete columns using BFRP is discussed.

2 Review of relevant Literature

This chapter gives background information on topics relevant to this research work. FRP composite is briefly introduced and its possibilities in civil engineering following the main subject of retrofitted columns. Basalt fibres are compared to common FRP materials and its advantage as a strengthening material reviewed. The use of FRP composite for retrofitted columns is discussed and previous research reviewed. Theory of confined concrete is introduced and the main factors that influence the efficiency of FRP confined concrete.

2.1 FRP Composite

2.1.1 General Description of FRP Composite

FRP composite consists of a matrix material, such as epoxy, that is reinforced with fibres. The epoxy binds the fibres together and transfers stresses to the fibres by adhesion and protects them from environmental damage [17]. These fibres are indefinitely long and are generally mentioned as continuous fibres.

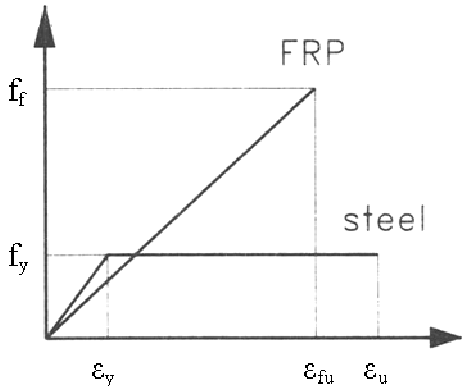

Figure 2-1: Stress-strain model of FRP compared to steel [15].

Compared to steel, fibres do not exhibit yielding during tension but instead the stress-strain model of FRP materials is modelled as linearly elastic to failure as shown in Figure 2-1. Failure initiates when the fibres reach their ultimate strain. It is assumed that all fibres in a composite fail at the same time in theoretical models, however in reality fibres rupture at various strain levels. Some regions of the cross-section become weaker as number of fibres rupture which causes the failure of the composite along that region. If the fibre volume in a composite is not sufficient, the matrix cannot support the entire load when the fibres rupture and composite failure will then instantly take place. Generally FRP composite suffer internal failures before it ruptures. These failures consist of micro cracking of matrix, rupture of fibre, fibre separation from the matrix, which is generally mentioned as debonding, and separation of layers which is called delamination [18]. Volume ratio of fibres in a composite is normally between 20 to 60 percent [19].

2.1.2 FRP Composite in Civil Engineering

The use of FRP composite in civil engineering can be categorized into two types. The former type is strengthening where the original structure´s strength is enhanced because of change of function in the structure or to make the structure capable of resisting possible earthquakes which most recent structures are designed for because of more stringent design codes. Repair is another type where existing structures are repaired to bring back the load capacity which it was designed for. The necessity for repairing can be caused by environmental deterioration or by damage in service. These two types are known as retrofitting applications. This technique has been successfully used for flexural strengthening in beams and slabs, shear strengthening of beams and for axial strengthening and ductility enhancement of columns [19]. In column retrofitting, the FRP makes an external jacket which provides confinement to the column. This confinement can be either active or passive and the confinement is achieved where the confining pressure is engaged by transverse dilation of the column under compression. This technique has many advantages over steel which has been used for strengthening since in the 1960s. Some of the advantages are:

- FRP composite materials have higher ultimate strength and lower density than steel, therefore the strength to weight ratio is higher for FRP composites.
- Higher corrosion resistance.
- Lighter unit weight which makes handling and installation easier than steel which leads to less expensive equipment needed for application.
- Faster field installation and no risk of damaging the existing reinforcement because of no mechanical anchors.
- Capability of following curved lines of the structure in retrofitting.

However, the use of FRP composite has some limitations such as uncertainties about the durability in long term performance, risk of fire and accidental damage unless the composite is protected [20].

2.1.3 FRP System

The most widely used method in structural engineering for applying FRP composite to structural elements is the hand layup process. Fibre sheet is impregnated with epoxy resin using handheld rollers, then pressed on the concrete surface to form the FRP composite and cured at ambient temperature. The fabrication procedure starts by applying a layer of resin on the concrete surface with rollers and then the dry sheet is placed on the surface. Rollers are then used to depress the sheet into the resin and an overcoat of resin layer is applied to finish the impregnation. If an additional layer is required the process is repeated. A finishing layer such as painting can then be provided for better appearance.

2.1.4 Basalt Fibre

Basalt fibres are made from basalt rocks which are the most common rock type in the earth´s crust. The fibres are manufactured from melted rock which is then extruded through small nozzles to produce continuous basalt fibre. The manufacturing process requires less energy compared to other FRP materials and the raw material needed in the process is available widely around the world. Basalt fibres do not contain any other additives in the producing which makes them environmentally friendly. These elements in the manufacturing process give basalt fibre some advantages in cost over commonly used FRP materials.

The elastic modulus of basalt fibre is low compared to carbon and aramid fibre which has disadvantages considering flexural strengthening. However the ultimate tensile strain is high which makes it promising in retrofitting of columns to enhance seismic performance. Several researches have shown that basalt fibre is good replacement for glass fibre in terms of strength, failure strain, corrosion and cost [16, 21-23]. Sim [16] showed that basalt fibre has better weathering resistance compared to glass fibre. They tested carbon, glass and basalt fibre under ultra-violet exposure for 4000 hours, which represents 20 years under natural conditions. The tensile strength of the fibres was measured where the strength of carbon fibre was merely affected by the exposure but the glass and basalt fibres did lose their strength. However the strength reduction in the glass fibre was two times faster than that of the basalt fibre. Good thermal stability was also shown in the experiment where the test specimens were heated for two hours at, 100, 200, 400, 600 and 1200°C. The carbon and glass fibre started to lose their strength rapidly at 200°C but the basalt fibre retained about 90% of the normal temperature strength up to 600°C. A comparison of typical material properties can be seen in Table 2-1 below.

Table 2-1: Typical dry fibre properties. Properties of carbon, aramid and glass from [14]. Properties of basalt from manufacturer (Basaltex).

Fibre	**Elastic modulus (GPa)**	**Tensile strength (MPa)**	**Ultimate tensile strain (%)**	**Density (g/cm^3)**
Carbon				
High strength	230-240	4300-4900	1,9-2,1	1,8
High modulus	294-329	2740-5490	0,7-1,9	1,78-1,81
Ultra high modulus	540-640	2600-4020	0,4-0,8	1,91-2,12
Aramid	124-130	3200-3600	2,4	1,44
Glass	70-85	2400-3500	3,5-4,7	2,6
Basalt	84	2500	3,15	2,6

2.2 Confined Concrete

2.2.1 Confined Concrete by Steel Reinforcement

For the survival and minimal damage of structures suffering lateral forces, the structure must be capable of sustaining large deformations caused by major earthquakes which can be well beyond the elastic limit of the structure [24]. This ability of the structure is called ductility. Ductile behaviour of concrete columns can be obtained by sufficient transverse hoop reinforcement which makes the concrete under compression confined. At higher axial compressive load on the column the greater amount of confining reinforcement is necessary to achieve ductile performance. Deformability of concrete above the peak stress is affected by the behaviour of longitudinal reinforcement where the transverse hoops provide lateral restrain against buckling. When unconfined concrete column subjected to axial compression approaches its compressive stress capacity at peak, the transverse strain reaches its maximum value. That will lead to instability of the compression area, longitudinal bars will buckle which then leads to failure of the column. If sufficient transverse reinforcement is installed, the hoops will act to restrain the lateral displacement of the concrete core and prevent buckling of the longitudinal bars. This enables higher compression stresses and more axial strain above the peak stress before failure of the column. When the defined compressive strength of the column is reached the concrete cover will be inactive and start spalling but the concrete core, surrounded by the hoops, will continue to carry axial stress until the hoops reach their ultimate stress and cannot restrain the lateral displacement any more. This combination of axial and transverse stress results in a triaxial state of stress (shown schematically in Figure 2-2).

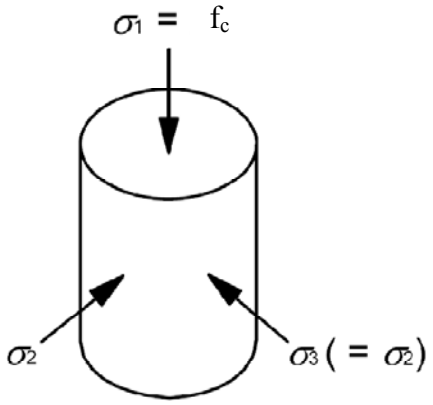

Figure 2-2: Triaxial state of stress [25].

In circular columns, the hoops provide a uniform line load around the circumference. As previously described the concrete core is under triaxial compressive stresses where the major compressive stress σ_1 is in the longitudinal direction of the column and two stresses σ_2 and σ_3 are in the transverse direction. Under concentric loading, the two lateral stresses are equal in the whole cross-section of a circular column and the maximum effective lateral confining pressure is when the hoops reach their yield strength, Figure 2-3, and can be calculated by:

$$f_l = \frac{2 f_y A_{s,t}}{D' s} \tag{2.1}$$

where f_y is the hoops yield strength, $A_{s,t}$ is the hoop section area, D' is the diameter of the hoop and s is the vertical spacing of hoops. After reaching the maximum value corresponding to the yield stress the confinement pressure is constant and shows a strain softening response, Figure 2-4.

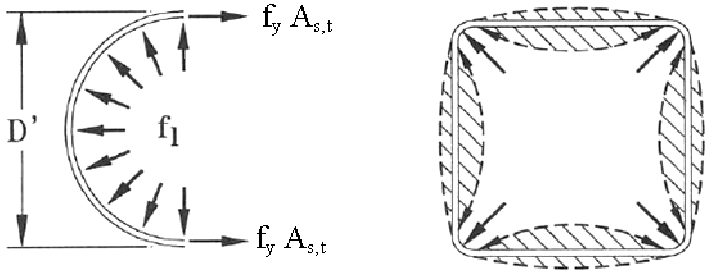

Figure 2-3: Confining pressure from circular hoop and a square hoop [2].

Rectangular or square hoops are only capable of providing full confining reactions at the corners of the hoop and are therefore less effective than circular hoops. The performance can be improved by the use of overlapping hoops that crosses the column section. Confinement effectiveness for square columns is further discussed in section 2.2.3.

Through extensive experimental tests on concrete cylinders under lateral fluid pressure, Richart [26] studied the strength enhancement of confined concrete cylinders and showed that the axial strength and ductility of the concrete increased with higher lateral pressure. He developed an expression to predict the axial compressive strength enhancement:

$$\frac{f_{cc}}{f_c} = 1 + k_1 \frac{f_l}{f_c} \tag{2.2}$$

where k_1 is the confinement effectiveness coefficient and was proposed as 4,1, f_c is the concrete strength and f_{cc} is the confined concrete strength. A stress-strain approach for confined concrete was developed for the ascending part of the compressive stress by Mander [12] which is the most widely used confinement model to day. The confined compressive stress f_{cc} is given by:

$$f_{cc} = f_c \left(-1{,}254 + 2{,}254 \sqrt{1 + \frac{7{,}94 f_l'}{f_c}} - 2\frac{f_l'}{f_c} \right) \tag{2.3}$$

where f_l' is the effective lateral pressure and is given by:

$$f_l' = k_e f_l \tag{2.4}$$

where k_e is the confinement effectiveness coefficient that takes into account the effective confined core area and the ratio of longitudinal reinforcement to the concrete core area of the section.

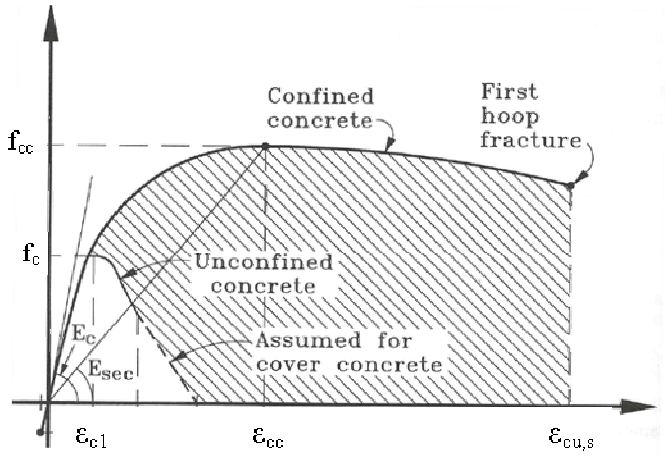

Figure 2-4: Compressive strain of unconfined and confined reinforced concrete [2].

The compressive strain of confined concrete where the steel starts yielding is given by:

$$\varepsilon_{cc} = \varepsilon_{c1}\left[1 + 5\left(\frac{f_{cc}}{f_c} - 1\right)\right] \tag{2.5}$$

where ε_{c1} is the compressive strain corresponding to the unconfined concrete strength at peak and is assumed to be 0,002 [12].

2.2.2 Confined Concrete by FRP Composites

In the previous section the relevance of confined concrete columns for civil engineering infrastructure has been explained and calculation model for confinement by sufficient internal reinforcement revealed. Generally in the case of confinement with FRP composites the lateral reinforcement is not sufficient for confining, so by wrapping a FRP sheet around a column it acts as an external reinforcement where the circumferential fibre confine the concrete. Different hoop spacing is not considered in this study as it has been shown that different hoop spacing has no effect on the compressive behaviour if it is not able to provide sufficient confinement [5]. The lateral expansion of the concrete under axial compression increases drastically when it has reached the maximum unconfined strength where micro cracks have developed. At that point the FRP has been fully activated for confinement and applies pressure on the concrete core until the FRP jacket ruptures. This means that the FRP jacket has no structural purpose before the concrete starts to dilate and crack. Unlike confinement with steel hoops the FRP jacket acts as linear to failure so the strength of confined column with a strain hardening response continues to increase until the FRP jacket rupture in tension or delamination at the overlap [19]. Figure 2-5 shows the behaviour of FRP confined concrete cylinders where point A is the peak point of a strain softening response in the case of low amount of confining pressure. Point B is the transition point of a hardening response where the FRP jacket is fully activated and applies continuous pressure until the FRP ruptures.

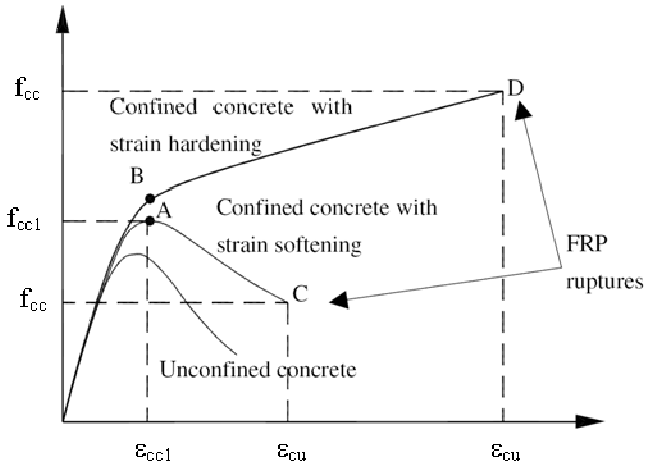

Figure 2-5: Stress-strain behaviour of FRP confined concrete [27].

The linear behaviour is caused by the elastic behaviour of the FRP jacket and the confining pressure increases as the dilation of the concrete increases. Because of external wrapping the effective confining area is the overall cross-section of the column but not only the concrete core as in the case of confinement by transverse steel hoops. Therefore the thickness of the concrete cover has little effect on column behaviour and is not considered as a design parameter.

Most of the models for FRP confinement today are based on the previous research on reinforced confined concrete which was revealed in previous section [12, 28]. Similar to equation (2.1) the uniform lateral confining pressure for a fully wrapped column can be calculated by:

$$f_l = \frac{2 f_f t_f n}{D} \tag{2.6}$$

where f_f is the ultimate tensile strength of the FRP composite and can be written as:

$$f_f = E_f \varepsilon_f \tag{2.7}$$

E_f is the elastic modulus of FRP, ε_f is the longitudinal strain of the FRP, t_f is the nominal thickness of one FRP layer, n is the number of layers and D is the column diameter.

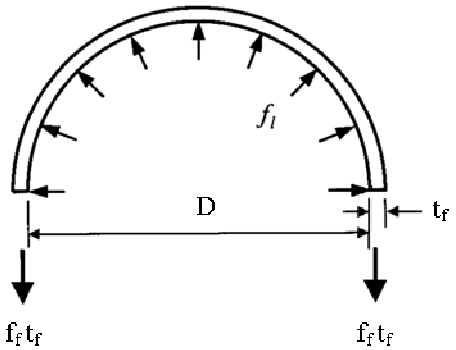

Figure 2-6: Confining pressure of FRP composite [29].

Several factors have great influence on the behaviour and performance of FRP confined concrete and need to be considered to obtain satisfactory confinement in concrete columns

such as shape of the column, ultimate rupture strain of the FRP and the concrete strength. These factors will be discussed in the next section.

2.2.3 Shape Effect

2.2.3.1 Circular Section

For a circular section the dilation of concrete inside the FRP jacket increases the perimeter length of the section. To resist this dilation the FRP jacket provides uniform confinement pressure so the stress in the jacket is constant around the cross-section perimeter. The quantity of confinement offered by the FRP jacket is often represented by the confinement ratio which can predict whether the stress-strain response of FRP confined concrete has a strain softening or a strain hardening response after reaching the peak stress. For a strain softening response the confined concrete has insufficient confinement to provide gain in axial strength but will provide gain in axial strain. After reaching the maximum compressive stress it will decrease until the FRP ruptures. For sufficient confinement a strain hardening response will occur with both gain in axial strength and strain. The FRP is activated after reaching the maximum unconfined strength and applies continuously increasing pressure on the concrete core with increase in the compressive stress until the FRP ruptures. Lam and Teng [30] showed that the criterion for sufficient confinement on concrete cylinders by Spoelstra and Monti´s [31] can be used with the maximum confining pressure being the actual value rather than the nominal value. According to Lam and Teng, the confinement ratio for FRP confined concrete of circular section can be taken as 0,07 to be sufficiently confined to obtain increase in compressive strength.

$$For\ a\ strain\ hardening\ response\ \ \frac{f_{l,a}}{f_c} \geq 0{,}07 \qquad (2.8)$$

$f_{l,a}$ is the lateral confining pressure based on the actual rupture strain of the FRP which is discussed further in section 2.2.4. From this expression it can be shown that the confined performance of a circular section is a strong function of the FRP jacket thickness.

2.2.3.2 Rectangular and Square Section

It has been shown that confined columns of rectangular and square cross-sections are less efficient than confined circular sections [12, 32].

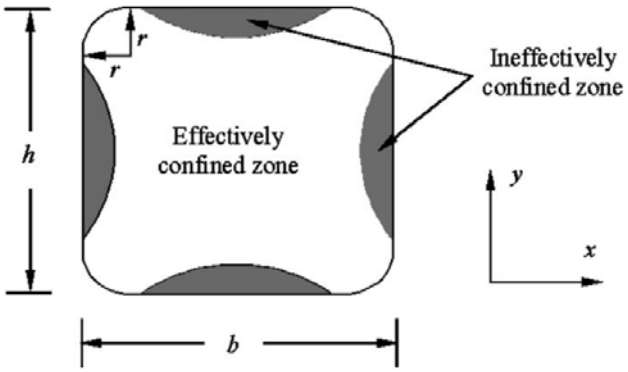

Figure 2-7: Effectively confined concrete in a square cross-section [9].

FRP jacket around rectangular section provides a non-uniform confining pressure and as shown on Figure 2-7 the confinement is concentrated at the corners rather than over the cross-section perimeter. The maximum confining pressure varies from the corners to a minimum between edges so the confinement level is affected both by the corner radius and the dimension of the cross-section. The theoretical approach is to define the effective area by four parabolas which intersect the edges at 45° and the confining pressure is based on equivalent circular column diameter as has been done in confinement with steel [12]. From this effective area a shape factor is defined which reduces the effectiveness of the FRP jacket. Shape factor of square and rectangular sections is based on geometry, aspect ratio and the longitudinal steel reinforcement. In general the shape factor is defined as in equation (2.9) with slight changes between researches:

$$k_s = 1 - \frac{(b-2r)^2 + (h-2r)^2}{3bh(1-\rho_l)} \tag{2.9}$$

In equation (2.9), b is the shorter side of the section and h is the longer side, r is the corner radius and ρ_l is the ratio of longitudinal steel reinforcement area to the cross-sectional area of the column. By adding the shape factor to equation (2.6) for the confining pressure of circular section the confining pressure of square and rectangular cross-section is defined by:

$$f_l = \frac{2 f_f t_f n k_s}{D^*} \tag{2.10}$$

where D^* is the equivalent column diameter.

The corner radius of the cross-section is an important factor of FRP confined rectangular and square columns and it has been shown that by increasing the corner radius more effective confinement is obtained. Columns of square and rectangular cross-sections with sharp corners are ineffective in increasing their axial strength but effective in increasing

the ductility. Columns with corner radius more than 30 mm can be expected to enhance increase in axial strength with sufficient confinement ratio [33]. Increased corner radius minimises the risk of premature rupture of the FRP jacket which is further discussed in section 2.2.4. Rochette and Labossière [32] stated that the confinement effect is related to the shape of the column for a given confinement ratio around the column. They tested square columns with 152 mm sides, height of 500 mm and corner radius of 5, 25 and 38 mm. A rapid decrease of the curve was shown for radius of 5 mm after reaching the maximum compressive strength. For radius of 25 mm a good plastic behaviour, or strain-softening response, was obtained and for the radius of 38 mm stress behaviour was a hardening response until the FRP ruptured. This important effect of increased corner radius has also been revealed by other researchers [33-35].

As in columns with circular section the confinement ratio of the square and rectangular FRP confined columns can predict whether strength enhancement can be expected. Mirmiran [36] suggested that enhancement in compressive strength of a confined column should not be expected if the confinement ratio *MCR* is less than 0,15:

$$MCR = \frac{2r}{D^*} \cdot \frac{f_l}{f_c} \tag{2.11}$$

Lam and Teng [34] stated that their criterion value of 0,07 in equation (2.8) for a strain-hardening response of circular columns is also valid for columns of square and rectangular cross-section. However, this criterion does not guarantee even ascending stress-strain curve to rupture of the FRP. Test results indicate that descending stress-strain curves are more commonly found in square and rectangular columns than in circular columns [34].

2.2.4 Tensile Strain of FRP

An important factor to be able to predict the strength gain in FRP confined columns is the tensile strain of the FRP. Existing test results show that the rupture of FRP jacket is generally observed at strain less than the ultimate strain recorded from coupon tensile test [6, 30, 33]. Two causes have been suggested for this phenomenon. The former is that a non-uniform strain distribution occurs in the FRP jacket because of deformation where the jacket crosses for example a splitting crack in the concrete. At this location the concrete does not carry stress resulting in increased local strain in the jacket. This gain in strain is attributing to the shear that is transferred across the interface between the jacket and the concrete because the jacket is bonded to the concrete. If the jacket is not bonded to the concrete the interface is frictionless which may lead to uniform strain distribution. The latter is the curvature of the FRP jacket which has an effect on its tensile strength.

For square and rectangular columns the curvature of rounded corners is important because of its effectiveness on the FRP tensile strength, especially on corners with a small radius. The FRP jacket ruptures at lower strain on columns with sharp corners and a premature failure occurs generally in the corner area. By increasing the corner radius a higher strain

occurs in the jacket and a premature failure at the corners is prevented. Rupture of the FRP jacket is more likely to occur on side surface by increased corner radius [37].

To be able to estimate the confinement strength of concrete column the effective strain level has to be known which can be determined from a confined cylinder test. A strain efficiency factor has been suggested by Pessiki [6]:

$$k_\varepsilon = k_{\varepsilon 1} k_{\varepsilon 2} \tag{2.12}$$

where, $k_{\varepsilon 1}$ is the ratio of the average jacket strain, ε_{ja}, to the maximum strain in the jacket at rupture, ε_{jr}.

$k_{\varepsilon 2}$ is the ratio of ε_{jr} to the strain capacity measured from tensile coupon test, ε_f.

Several tests have been done on confined cylinders to determine the strain efficiency factor of CFRP, GFRP and AFRP jackets. Lam and Teng [30] determined the average jacket strain efficiency factor in 52 CFRP cylinders, 9 GFRP cylinders and 7 AFRP cylinders. The efficiency factor was 0,586, 0,624 and 0,851 respectively with an average value of 0,63 when all specimens were considered together. Information about the efficiency factor in BFRP confined cylinders has not been found in the available literature.

To take into account reduced ultimate strain in FRP jackets on confined columns the actual rupture strain should be taken as [30]:

$$\varepsilon_{f,a} = k_\varepsilon \varepsilon_f \tag{2.13}$$

and the lateral confining pressure is then calculated by:

$$f_{l,a} = \frac{2 t_f n \varepsilon_{f,a} E_f k_s}{D} \tag{2.14}$$

2.2.5 Concrete Strength

It has been shown that the confined compressive strength and strain are related to the unconfined concrete strength [38, 39]. This is because low strength concrete has larger deformability than high strength concrete due to its lower modulus of elasticity. As described earlier, in confinement the FRP jacket provides pressure on the specimen and restrains the lateral expansion of the concrete until the jacket reaches its ultimate tensile strength. For the same amount of confining pressure, different enhancement in strength and strain are obtained for different concrete strength and the confinement efficiency of lower strength concrete is higher. Wu [27] has developed equations for predicting the confined strength of FRP confined concrete. In his research he suggested that for concrete strength lower than 30 MPa an efficiency factor should be used because of the higher deformability of low strength concrete. This makes the use of FRP jacket for strengthening older structures more efficient because older structures are generally made from low strength concrete.

3 Review of Design Guidelines

In this section three design guidelines are introduced and their design methods reviewed. The design guidelines are as follows: "*Guide for the Design and Construction of Externally Bonded FRP Systems for Strengthening Concrete Structures*" reported by the American Concrete Institute [13], "*Design Guidance for Strengthening Concrete Structures Using Fibre Composite Materials*" Technical Report No.55 by the Concrete Society [14] and "*Externally Bonded FRP Reinforcement for RC Structures*" Technical Report by the Federation Internationale du Beton [40].

The main object of this section is to summarize the design guidelines for calculating the maximum confined column strength and strain and view their limitations. Some of the calculation models may not be able to give appropriate stress-strain curve for FRP confined columns, however in design the maximum strength is generally needed which is then considered as the critical parameter. For convenience the same symbols are used in this discussion for all design guidelines but they may be different from the original ones.

3.1 American Concrete Institute

The guideline provided by ACI Committee 440 (ACI) recommends the use of FRP for axial strengthening, only for non-slender circular columns. Strengthening in axial strain capacity is provided by the ACI for circular and square columns. The confined compressive strength model is a steel based model proposed by Mander [12].

3.1.1 Circular Sections

The axial compressive strength of a concrete column with steel tie reinforcement is calculated by:

$$N_{Ed} = 0{,}8\varphi\left(0{,}85\Psi_f f_{cc}\left(A_g - A_s\right) + f_y A_s\right) \tag{3.1}$$

where 0,8 is a reduction factor for unintended eccentricity, φ is a strength reduction factor, ψ_f is a reduction factor for FRP strength corresponding to exposure conditions, f_{cc} is the confined compressive strength, A_g is the gross area of concrete, A_s is the cross-sectional area of longitudinal reinforcement and f_y is the yield strength of longitudinal reinforcement.

The approach that is recommended for the confined compression is based on the model developed by Mander [12] that was discussed earlier for steel confined concrete. Up to the yielding point, steel behaves linearly elastic like FRP so by using Mander model the compressive strength is calculated corresponding to the maximum confining pressure provided by the FRP jacket which is limited by the actual rupture strain of the FRP. The maximum confinement pressure is given by:

$$f_{l,a} = \frac{k_s \rho_f \varepsilon_{f,a} E_f}{2} \tag{3.2}$$

where the shape factor, k_s, can be taken as 1,0 for circular section, ρ_f is the FRP reinforcement ratio, $\varepsilon_{f,a}$ is the actual rupture strain of the FRP and E_f is the elastic modulus of the FRP.

The reinforcement ratio is given by:

$$\rho_f = \frac{4nt_f}{D} \tag{3.3}$$

where D is the column diameter, n is the number of FRP layers and t_f is the nominal FRP thickness. Equation (3.3) is only applicable for fully wrapped columns.

The confined compressive strength is then calculated by:

$$f_{cc} = f_c \left(2{,}25 \sqrt{1 + 7{,}9 \frac{f_l}{f_c}} - 2 \frac{f_l}{f_c} - 1{,}25 \right) \tag{3.4}$$

where f_c is the concrete compressive strength.

As discussed in section 2.2.4 the FRP ultimate strain from tensile coupon test is not reached in a FRP jacket that confines a concrete column. To take into consideration the strain efficiency factor k_ε, ACI limits the strain level with the criteria given by:

$$\varepsilon_{f,a} = min \begin{cases} 0{,}004 \\ 0{,}75\varepsilon_f \cdot C_E \end{cases} \tag{3.5}$$

where C_E is an environmental reduction factor. This criterion is not based on experimental evidence on the actual rupture strain in a FRP jacket providing confinement.

For increased ductility of a column, gain in axial compressive strain is needed. For the ultimate compressive strain ACI provides the following definition:

$$\varepsilon_{cu} = \frac{1{,}71(5f_{cc} - 4f_c)}{E_c} \tag{3.6}$$

where E_c is the elastic modulus of concrete and the ultimate strain, ε_{cu}, corresponds to a stress-strain curve with a strain hardening response.

3.1.2 Square and Rectangular Sections

For increase in ductility, ACI recommend that the ultimate compressive strain should be calculated by equation (3.6) where equations (3.2), (3.4) and (3.5) are also valid. The reinforcement ratio is found by:

$$\rho_f = \frac{2nt_f(b+h)}{bh} \tag{3.7}$$

and is only valid for a fully wrapped column. The efficiency factor is based on geometry, aspect ratio, longitudinal steel reinforcement and is defined by:

$$k_s = 1 - \frac{(b-2r)^2 + (h-2r)^2}{3bh(1-\rho_l)} \tag{3.8}$$

3.1.3 Limitations and Safety Factors

Limitations of using the recommendations provided by ACI for strengthening of confined columns manly concern columns of square and rectangular sections. Confining effect of FRP jacket should not be considered for a cross-section that does not satisfy the criteria for aspect ratio:

$$h/b \leq 1{,}5 \tag{3.9}$$

and the side dimension should not exceed 900 mm. Corners should be rounded to a minimum radius of 13 mm to prevent premature rupture of the FRP jacket. For a sufficient overlap of the FRP jacket no limits are suggested by ACI, however for a sufficient overlap the required overlap provided by the material manufacturer should be followed.

ACI provides a strength reduction factor which is multiplied to the calculated nominal capacity, φ = 0,7. Considering the FRP an environmental reduction factor, C_E, is provided by the ACI which varies from 0,5 to 0,95 depending on the FRP type and exposure conditions. This reduction factor should be used for reducing the ultimate tensile strength and strain. When estimating the exposure conditions, regard should be taken to the protective coat applied on the FRP jacket. No minimum limit for the confining pressure is provided but the load carrying capacity is reduced to 95% by the reduction factor ψ_f which indirectly provides a minimum limit for the FRP jacket.

In the case of damaged FRP system the structure should be capable to resist a reasonable level of load without collapsing. Therefore it is recommended that the existing strength of the structure should be sufficient to resist a level of load as described by:

$$(\phi R_n)_{existing} \geq \left(1{,}2F_G + F_Q\right)_{new} \tag{3.10}$$

where R_n is the nominal strength of member, F_G is the permanent action and F_Q is the variable load.

3.2 Concrete Society

The Concrete Society provides a guideline for strengthening circular columns in axial strength and strain. Concerning guidelines of square and rectangular columns, only axial strengthening is suitable with some limitations. The calculation model proposed by the Concrete Society may be classified as an empirical model which was originally developed by Lam and Teng [30]. Their model is calibrated against currently available test data and is only suitable for a strain hardening response.

3.2.1 Circular Sections

Design strength of confined concrete under concentric compression is given by:

$$f_{cc} = f_c + \frac{0{,}05 \cdot 2nt_f E_f}{D} \tag{3.11}$$

The confined compressive strength is not calculated directly from the maximum confining pressure provided by the FRP jacket as in many other models.

Ultimate axial strain of confined concrete is calculated by:

$$\varepsilon_{cu} = \varepsilon_{c1}\left(1{,}75 + 12\left(\frac{2E_f nt_f}{E_{cm}D}\right)\left(\frac{0{,}6\varepsilon_f}{\varepsilon_{c1}}\right)^{1{,}45}\right) \tag{3.12}$$

where ε_{c1} is the axial strain in unconfined concrete at peak stress and E_{cm} is the secant modulus of elasticity of concrete. Because of the fact that at concrete compressive strain over about 0,01 the concrete is crushed and has lost all cohesion, the Concrete Society, recommends that if the ultimate strain from equation (3.12) is more than 0,01 the maximum compressive stress should be taken from a stress-strain curve corresponding to the axial strain at 0,01. The stress-strain curve is defined as follows:

$$f_{cc}{}^{*} = E_c\varepsilon_c - \frac{(E_c - E_2)^2\varepsilon_c^2}{4f_c} \qquad for\ 0 \le \varepsilon_c \le \varepsilon_t \tag{3.13}$$

and

$$f_{cc}{}^{*} = f_c + E_2\varepsilon_c \qquad for\ 0 \le \varepsilon_c \le \varepsilon_t \tag{3.14}$$

where ε_c is the compressive concrete strain, ε_t is the position between the parabola and straight line and is defined by:

$$\varepsilon_t = \frac{2f_c}{(E_c - E_2)} \tag{3.15}$$

E_c is the modulus of elasticity of concrete and E_2 is the slope of the ascending part of the curve:

$$E_2 = \frac{(f_{cc} - f_c)}{\varepsilon_{cu}} \tag{3.16}$$

The Concrete Society considers the strain efficiency of the FRP jacket by limiting the FRP strain to 60% of the ultimate FRP strain by adding a reduction factor in equation (3.12). This recommendation is based on the experimental results of Lam and Teng where test results of CFRP, AFRP and GFRP confined cylinders were considered [30].

3.2.2 Square and Rectangular Sections

Axial strength of square and rectangular sections can be estimated, however it is noted that the confinement model is based on concentrically loaded columns and should be used with caution in the case of load eccentricity. In that case the stress distribution will be such that the confined area will be more highly stressed than predicted by the model. The model has been calibrated against small scale specimen of 150 mm x 150 mm for square and up to 150 mm x 225 mm for rectangular columns and therefore a care should be taken for columns of larger cross-sections and independent testing is recommended.

The axial strength of a confined column is given by:

$$f_{cc} = f_c + 2k_s f_l \tag{3.17}$$

where the confining pressure is given by:

$$f_l = \frac{2f_f n t_f}{\sqrt{b^2 + h^2}} \tag{3.18}$$

the shape factor k_s is the product of the aspect ratio and the ratio of the effective confined area and the total gross area of the column and is given by:

$$k_s = \frac{b}{h} \cdot \frac{A_e}{A_g} \tag{3.19}$$

The ratio A_e/A_g is given by:

$$\frac{A_e}{A_g} = \frac{1 - ((b - 2r)^2 + (h - 2r)^2 - 3A_{ol})/(3A_g) - \rho_l}{1 - \rho_l} \tag{3.20}$$

where A_g is the gross area of the column and A_{ol} is the inactive confined area defined by the overlap of the parabolas in the case of high aspect ratio.

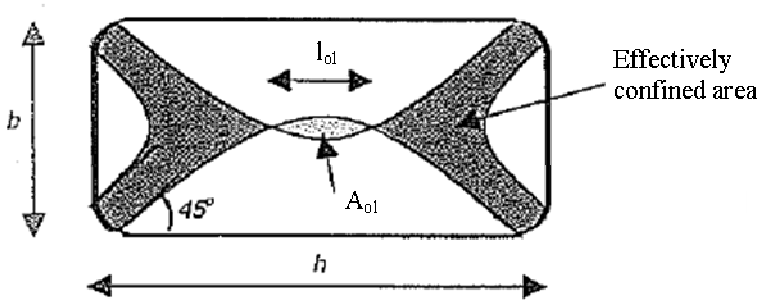

Figure 3-1: Inactive area in the case of high aspect ratio [14].

The inactive confined area can be calculated by:

$$A_{ol} = \frac{4{l_{ol}}^3}{3(h-2r)} + l_{ol}\big(2b - (h-2r)\big) \tag{3.21}$$

where

$$l_{ol} = \sqrt{\frac{(h-2r)^2}{4} - \frac{b(h-2r)}{2}} \tag{3.22}$$

and is valid when

$$2b < (h-2r) \tag{3.23}$$

Recommendations for calculating the ultimate axial strain of square and rectangular columns are not provided at this point.

3.2.3 Limitations and Safety Factors

As the model provided by the Concrete Society is only suitable for a strain hardening response the following criteria should be met for a sufficient confinement:

$$\frac{2nt_f E_f}{Df_c^2} > 0{,}183\ (MPa) \tag{3.24}$$

No recommendations can be found for a sufficient confinement of square and rectangular columns.

For strengthening of square and rectangular columns the following conditions should be met: Loading should be concentric, side dimension should not be greater than 200 mm, the aspect ratio should be less than 1,5 and the corners should be rounded to minimum radius of 15 mm.

Because of uncertainty of material properties, several safety factors are provided. Design value of elastic modulus of FRP is given by:

$$E_f = \frac{E_{fk}}{\gamma_{mE}} \tag{3.25}$$

where γ_{mE} is the product of γ_E and γ_{mm}. γ_E is a safety factor for different materials and is 1,1 for CFRP and 1,8 for GFRP. γ_{mm} is a safety factor applied to manufactured composites and for a wet lay-up procedure of sheet the safety factor is 1,2.

Design value of ultimate strain of FRP is given by:

$$\varepsilon_f = \frac{\varepsilon_{fk}}{\gamma_{m\varepsilon}} \tag{3.26}$$

where $\gamma_{m\varepsilon}$ is the product of γ_ε and γ_{mm}. γ_ε is a strain safety factor which is 1,25 for CFRP and 1,95 for GFRP.

The material safety factors for concrete and steel is $\gamma_c = 1{,}5$ and $\gamma_s = 1{,}05$.

3.3 Federation International du Beton

Similar to ACI Committe 440, the model provided by the Federation International du Beton (fib) is a steel based model. This model is developed by Spoelstra and Monti [31] which takes into account the behaviour of FRP confinement and is based on the model developed by Mander [12]. The model provides two sets of equations for calculating the maximum confined compressive strength and strain which are referred to as "exact" and "practical" formulas. The "exact" formulas require the calculations of confined compressive strength and strain from Mander´s model with equation (2.3) and (2.5) but for the "practical" formulas only the confined pressure f_l is needed. Guidelines are provided for strengthening of axial stress and strain of both circular columns and as well as square and rectangular columns. The axial compressive strength of columns is recommended to calculate according to appropriate model as given by EC2 [25].

3.3.1 Circular Sections

Recommendations for calculating the confined concrete strength are as follows.

"Exact"

The confinement pressure is given by:

$$f_{l,a} = \frac{2nt_f E_f \varepsilon_{f,a} k_e}{D} \tag{3.27}$$

where $\varepsilon_{f,a}$ is the actual rupture strain and should be decided according to experimental evidence. The coefficient k_e consider the less effective confining pressure in the case of partially wrapped column. This coefficient is defined by:

$$k_e = \frac{\left(1 - \frac{s'}{2D}\right)^2}{1 - \rho_l} \tag{3.28}$$

where k_e is lower than 1,0 in the case of partially wrapped column and s' is the clear spacing between FRP straps. The ultimate strain is given by:

$$\varepsilon_{cu} = \varepsilon_{cc}^{*}\left(\frac{2\beta\varepsilon_{f,a}E_{cc}}{E_c - E_{cc}}\right)^{1-E_{cc}/E_c} \tag{3.29}$$

where

$$E_{cc} = \frac{f_{cc}^{*}}{\varepsilon_{cc}^{*}} \tag{3.30}$$

and f_{cc}^{*} and ε_{cc}^{*} are given by equation (2.3) and (2.5). The parameter β accounts for the degradation of concrete subjected to loading and is defined by:

$$\beta = \frac{5700}{\sqrt{|f_c|}} - 500 \tag{3.31}$$

The ultimate confined compressive strength can then be calculated by:

$$f_{cc} = E_{sec,u}\varepsilon_{cu} \tag{3.32}$$

where the secant modulus at ultimate is given by:

$$E_{sec,u} = \frac{E_c}{1 + 2\beta\varepsilon_{f,a}} \tag{3.33}$$

"Practical"

With the practical formulas, the ultimate confined compressive strength is given by:

$$f_{cc} = f_c\left(0{,}2 + 3\sqrt{\bar{f}_{l,a}}\right) \tag{3.34}$$

where

$$\bar{f}_{l,a} = \frac{f_{l,a}}{f_c} \tag{3.35}$$

The ultimate confined strain is given by:

$$\varepsilon_{cu} = \varepsilon_{c1}\left(2 + 1{,}25\bar{E}_c\varepsilon_{l,a}\sqrt{\bar{f}_{l,a}}\right) \tag{3.36}$$

where

$$\bar{E}_c = \frac{E_c}{f_c} \tag{3.37}$$

In the case of no confinement, equation (3.34) results in 20% of the unconfined concrete strength and equation (3.36) results in ultimate strain of 0,004 if ε_{c1} is equal to 0,002.

3.3.2 Square and Rectangular Sections

Confined strength and strain of square and rectangular columns should be calculated similar to circular columns with equations (3.29) to (3.37). The confining pressure can be calculated by:

$$f_{l,a,x,y} = \frac{\rho_{f,x,y} E_f \varepsilon_{f,a} k_s}{2} \tag{3.38}$$

where the confining pressure is calculated in the x and y direction of the section, Figure 2-7. In the case of square columns the confining pressure is equal in each direction. The guidelines do not include coefficients for partially wrapped columns, only the shape factor k_s is considered which is given by:

$$k_s = 1 - \frac{(b-2r)^2 + (h-2r)^2}{3bh(1-\rho_l)} \tag{3.39}$$

The volumetric ratio of confining reinforcement is given by equation (3.40) where partially wrapped column is considered:

$$\rho_{f,x} = \frac{2b_f n t_f}{sb} \quad and \quad \rho_{f,y} = \frac{2b_f n t_f}{sh} \tag{3.40}$$

where b_f is the width of the FRP strap and s is the centre to centre length between straps.

3.3.3 Limitations and Safety Factors

Considering the effective ultimate strain of the FRP jacket, fib does not provide a strain efficiency factor that reduces the ultimate strain because of limited data available on this issue. However, it is recommended that the reduced ultimate strain should be taken into account and a proper strain value could be justified by experimental evidence. Value of sufficient confinement is not provided but to be able to provide confinement for square and rectangular columns the corners should be rounded to a radius of 15 mm to 25 mm or as suggested by the FRP manufacturer.

General design rules and safety factors for concrete structures and steel reinforcement provided by EC2 are recommended but fib provides the FRP material safety factor γ_f. Values for this factor are mainly based on long term behaviour of different FRP materials and the influence of different application methods. In the case of wet lay-up system under normal quality control conditions the material factor is 1,35 for CFRP, 1,45 for AFRP and 1,5 for GFRP.

4 Experimental Program

The experimental program includes testing of standard concrete cylinder specimens confined with BFRP jacket and reinforced concrete columns of square cross-section confined with BFRP jacket. The objective of the tests was to study the axial strength and strain capacity enhancements provided by the BFRP jacket and the ultimate tensile strength and strain of plain BFRP test specimens. Concrete cylinders were tested with and without BFRP jacket to study the efficiency of the jacket on plain concrete specimens. Reinforced columns were fabricated to study the jacket efficiency on structural components. In this chapter the experimental work is described and the material properties of relevant material reviewed. Section 4.1 describes the procedure of tensile test made on the BFRP material and the material properties of the basalt fibre and epoxy resin used. Sections 4.2 to 4.3 provide a description of the procedure of casting, wrapping and testing of the concrete cylinders and columns. The material properties of the concrete and reinforcing steel used in the experiment are also reviewed. The experimental results are reported in chapter 5.

4.1 Tensile Coupon Test

Tensile coupon tests were made to determine the actual material strength of the BFRP composite according to ASTM standard [41]. Material properties reported by the basalt fabric manufacturer are only the properties of the dry fibre which cannot be used in calculations for the BFRP composite unless a proper reduction factor is known. Therefore it is necessary to find the actual strength of the composite which is then used in further calculations. Two test groups were tested with two different basalt fabric types and each group consisted of a minimum of five tests as required by the standard.

4.1.1 Material Properties

The two types of BFRP were made from different types of basalt fibre fabric sheets and the same epoxy resin was used for both types. The sheets were of one unidirectional type with the main fibre in the longitudinal direction and one biaxial type with the same amount of main fibre in the longitudinal and transverse directions, both were supplied by Basaltex, Belgium (http://www.basaltex.com). The epoxy resin was supplied by Sika, Denmark (http://www.sika.dk).

4.1.1.1 Basalt Fibre

Unidirectional fabric sheet, BAS UNI 600

This woven fabric sheet is made from basalt roving and is provided in 1270 mm wide rolls. The surface weight is 657 g/m^2 but the weight of the main fibre in the longitudinal direction is 600 g/m^2 which corresponds to the fabric type name, BAS UNI 600. The

longitudinal fibres are held together by a stitched grid and transverse fibres of surface weight 57 g/m^2 on one side of the fabric. The nominal thickness of the BAS UNI 600 is 0.65 mm which is the thickness used in calculations.

Biaxial fabric sheet, BAS 220

The biaxial fabric has the same amount of fibres in both directions which is in the longitudinal direction, 0°, and the transverse direction, 90°. This type of fabric is particularly useful when 90° orientation is needed, but in confinement the 0° fibres are the main bearings and the efficiency of the 90° fibres considered to be negligible. As for the BAS UNI 600, this woven fabric sheet is made from basalt roving and is provided in 1270 mm wide rolls. The surface weight is 220 g/m^2, 110 g/m^2 in the 0° direction and 110 g/m^2 in the 90° direction. The nominal thickness of the BAS 220 is 0,2 mm.

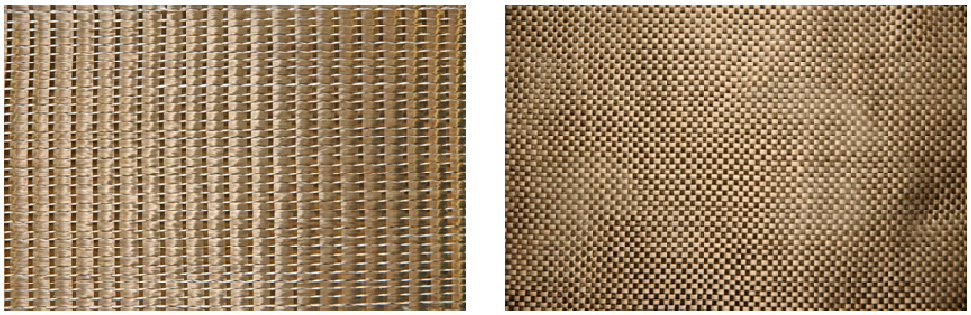

1) *2)*

Figure 4-1: Basalt fabric sheets. 1) BAS UNI 600, 2) BAS 220.

4.1.1.2 Epoxy Resin

For the production of BFRP composite a Sikadur-330 epoxy resin was used. It consists of two parts which are mixed in a 4:1 ratio of resin to hardener for a mixture weight of 0,7-1,5 kg/m^2 on concrete surface. This recommendation however depends on the roughness of the surface. According to the manufacturer, the epoxy resin has reached its maximum strength after 5 days of curing at 23°C. The tensile strength is 30 MPa and the elastic modulus is 4,5 GPa.

Table 4-1: Material properties reported by manufacturer.

Material	Nominal thickness (mm)	Surface weight (g/m^2)	Tensile strength (MPa)	Elastic modulus (GPa)	Tensile strain (%)
BAS UNI 600	0,65	657	2500	84	3,15
BAS 220	0,2	220	2500	84	3,15
Epoxy resin	-	-	30	4,5	-

4.1.2 Fabrication Procedure of Specimens

The dimensions of the tensile specimens were determined according to the ASTM standard recommendations and can be seen on Figure 4-2 [41]. Recommended width of specimen is 15 mm for unidirectional fabric with 0° orientation but it is also stated that specimens should contain a sufficient number of fibre in the cross-section to get an optimum result. Therefore, it was decided that a width of 25 mm would be more appropriate for the tensile specimens and the fabrication would be easier than of a smaller specimen.

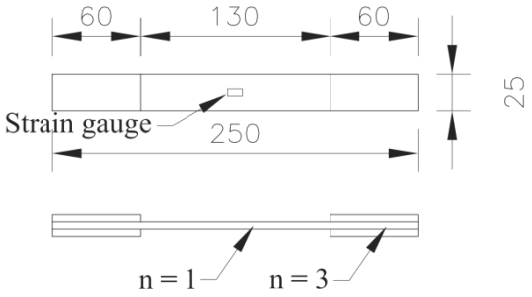

Figure 4-2: Dimension of BFRP tensile specimen.

All of the basalt fabric sheets were cut down into pieces of the same dimension shown in Figure 4-2. Each piece of 250 mm length was impregnated with epoxy resin with a narrow paint roller and placed on a flat surface where an additional layer of tab was applied on each end of the specimen. The end tabs are for more strength at gripping zones and are of the same material as the test specimen. Before the end tab was applied a second coat of resin was attached on the end surface and the end tab was then applied and a roller used to work the resin into the sheet. Final coat of epoxy resin was then worked into the sheet on the outer surface to make a successful composite. This procedure was repeated for each end tab. Each specimen was then stringed up where each end was held so the specimens would be as straight and parallel as possible. The tensile test specimens were let to cure for seven days at room temperature. Three specimens of each group with an overall length of 130 mm were also fabricated to estimate the amount of epoxy resin in one layer of the composite. Estimation of the volume fraction can be seen in appendix E.

Table 4-2: Test matrix of tensile specimens.

Fabric material	Specimen	Number	Overall length (mm)	Width (mm)	Thickness (mm)
BAS 220	**BB-1-5**	5	250	25	0,2
BAS UNI 600	**BU-1-5**	5	250	25	0,65

At the curing time, strain gauges were attached to specimens BB and BU for measuring the longitudinal strain. One strain gauge with an active gage length of 6,5 mm was attached at mid-section on each side of the specimen. Strain gauge with an active gage length of 6 mm is recommended by the ASTM standard [41].

1) 2)

Figure 4-3: 1) Cut specimens of BAS UNI 600, 2) impregnation of tensile test specimen.

4.1.3 Test Procedure

Before testing of the tensile specimens, width and length of each specimen was measured because some of the specimens suffered a loss of fibre in the fabrication procedure. The width was measured at three places with a calliper at the active length of the specimen. In the results, the width of each specimen is presented as the average of the three measured widths. All specimens were tested under tensile load at head displacement rate of 2 mm/min according to ASTM [41]. The specimens with BAS 220 material were tested in a testing machine with load capacity of 10 kN and the BAS UNI 600 specimens were tested in a testing machine with load capacity of 100 kN at the Innovation Center Iceland. The longitudinal strain was measured simultaneously using two strain gauges at opposite sides of the specimens. In the results, the strain is the average of the two strain gauges. Two computers were used for data reading, one for the load reading and one for the strain reading.

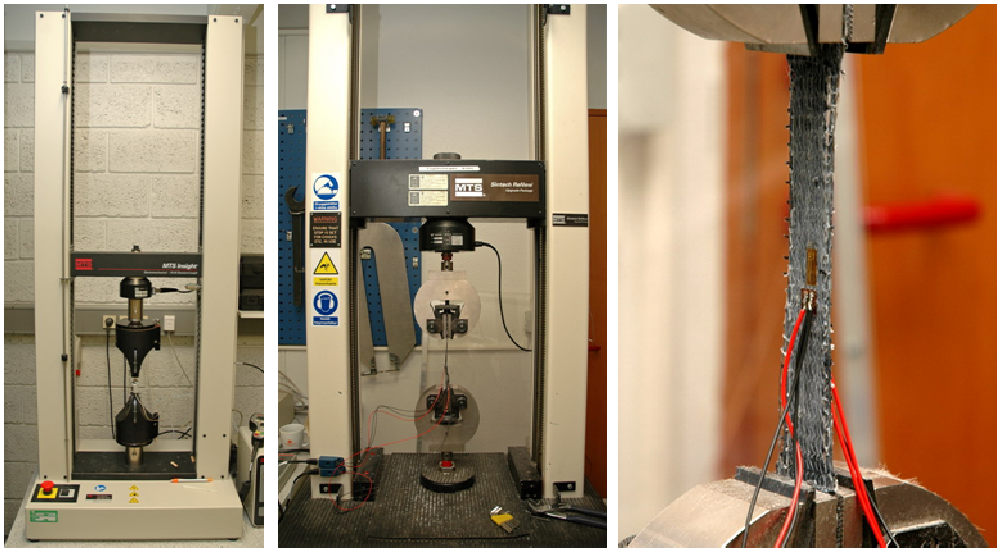

1) 2) 3)

Figure 4-4: 1) Testing machine of 10 kN capacity, 2) testing machine of 100 kN capacity, 3) tensile test specimen installed in the grip head of the testing machine of 100 kN capacity.

4.2 Cylinder Specimens

4.2.1 Description of Cylinder Specimens

Two groups of concrete cylinders were tested where one group, SBB, contained cylinders confined with BFRP jacket of the BAS 220 material and the other, SBU, contained cylinders confined with BFRP jacket of the BAS UNI 600 material. Total of 24, 100mm x 200mm concrete cylinders, were casted but the fabrication was not done simultaneously and therefore each group contained three unconfined cylinders as a reference for the concrete cylinders strength. Cylinders confined with the BAS 220 material were tested before the tensile coupon test was performed. The specimens were designed based on information provided by the basalt manufacturer and estimated volume fraction of fibres in the composite. That test did not show a successful result and therefore a new test series was designed following the results from the tensile test. To examine the confinement stiffness variation, the specimens were wrapped with different numbers of basalt sheets. One basalt sheet refers to one layer of BFRP jacket. Three identical cylinder specimens were made for each number of BFRP layers. The number of applied layers on each cylinder were based on Lam and Teng´s criterion for sufficient confinement [30]. As shown by equation (2.8) the confinement ratio should not be less than 0,07 for a strain hardening response and as shown in Table 4-3, two specimens fall under the criteria for a strain softening response. The other specimens are expected to show a good strain hardening response. For calculating the confinement pressure in equation (2.8), the strain efficiency factor was chosen as 0,6 as recommended by the Concrete Society. Different concrete strength was not considered as a parameter in this study but to simulate older concrete buildings under the need of strengthening their existing infrastructure, a concrete strength of 25 MPa was chosen which is generally considered as a normal concrete strength in older structures. Table 4-3 provides details of the cylinders.

Table 4-3: Details of concrete cylinder specimens.

Specimen[#]	f_c* (Mpa)	n	$t_{f,tot.}$ (mm)	$f_{l,a}/f_c$	ρ_f (%)	Number of specimens
S-BB0	30,7	0	-	-	-	3
S-BB1	30,7	1	0,20	0,03	0,8	3
S-BB2	30,7	2	0,40	0,06	1,6	3
S-BU0	35,8	0	-	-	-	3
S-BU1	35,8	1	0,65	0,17	2,6	3
S-BU2	35,8	2	1,30	0,34	5,2	3
S-BU3	35,8	3	1,95	0,51	7,8	3

[#] Unsuccessfull test series of the first cylinder test is revealed in appendix B.
[*] Concrete strength determined by standard cylinder test [42].

4.2.2 Material Properties

4.2.2.1 Concrete

Concrete supplied by the concrete supplier BM-Vallá was used for casting all cylinders. The concrete was from two C25 mix designs for a local customer so the concrete used in the experiment was representative for a normal structural concrete of 25 MPa compressive strength. The compressive strength was determined by tests performed on three standard 100mm x 200 mm concrete cylinders together with the BFRP confined cylinders in each specimen group. Results of the cylinder compressive tests are presented in section 5.2.2. Properties of the fresh concrete were determined by a staff member at the supplier´s laboratory.

Table 4-4: Concrete mix reported by the supplier.

Group	Concrete	Sand (kg/m^3)	Rock (kg/m^3)	Aalborg cement (kg/m^3)	Water (kg/m^3)	Admixtures (kg/m^3)	Maximum aggregate size (mm)
SBB	C25	993	831	300	126	2,25	25
SBU	C25	975	740	303	130	2,45	25

Table 4-5: Properties of fresh concrete.

Group	Slump (mm)	Air (%)	W/C ratio	Strength (Mpa)
SBB	800	8,5	0,53	30,7
SBU	800	9	0,44	35,8

4.2.2.2 External Reinforcement

The material used to fabricate the external reinforcement jacket is described in detail in section 4.1.1 where the BFRP tensile specimens are described. The material strength is presented in Table 5-1.

4.2.3 Fabrication Procedure

4.2.3.1 Casting

Both test groups were constructed in the laboratory of the concrete supplier BM-Vallá where the cylinder specimens were cast in steel forms. The concrete was placed in the steel forms in two layers and each layer was packed 25 times according to standard [42]. The specimens were cured in a horizontal position for 24 hours before being removed from the forms and stored in a humidity room at Innovation Center Iceland for at least 14 days until they were prepared for wrapping with basalt sheets.

4.2.3.2 BFRP Application

The procedure of applying the fabric sheets can be considered to consist of the following three main steps: 1) preparation of concrete surface; 2) preparation of sheets; and 3) application and impregnation of the basalt sheets. The cylinder specimens were let to dry for 24 hours after being removed from the humidity room. Before the wrapping procedure began, the concrete surface of the specimens was wire brushed to remove loosely held powders and then cleaned with compressed air and water and left to dry. The fabric sheets were cut to lengths of 0,46 m for one layer, 0,78 m for two layers and 1,09 m for three layers The width was cut to 0,19 m which provided 5 mm gap on each end of the cylinder in order to prevent axial load on the BFRP jacket. As the sheets were wrapped in a continuous way, these lengths allowed for an overlap of 150 mm.

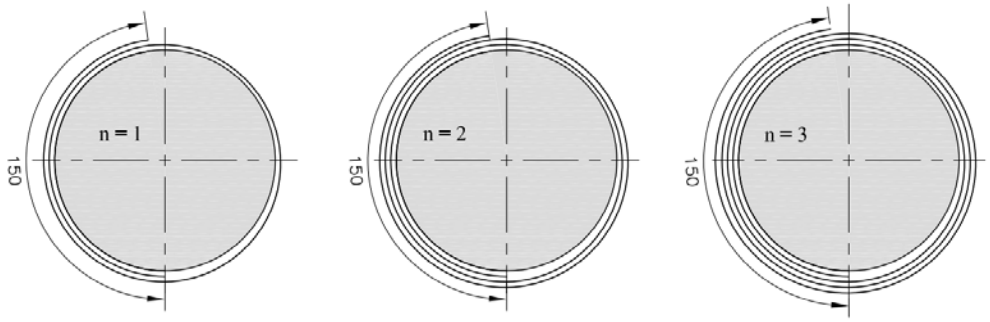

Figure 4-5: Distribution of continuous wrapped cylinders.

The final step of the procedure involved three tasks which were repeated for each layer of the basalt sheet: a) application of inner resin coat; b) application of the basalt sheets; and c) application of an outer resin coat. The epoxy resin consisted of two parts, resin and a hardener, and was mixed in a 4:1 ratio. The epoxy resin was distributed evenly on the concrete surface with a paint roller for the inner resin coat. Next step was to wrap the basalt sheet around the specimen in a continuous way forming one to three layers of BFRP jacket. The resin was worked into the sheets by light pressure with hand and followed by a roller. Care was taken to ensure a perpendicular alignment to the axial direction of the specimen. Final step for each layer was to apply the outer epoxy resin coat to the sheet for good impregnation. Once the appropriate number of layers had been placed, the outermost layer was extended by an additional overlapping length of 150 mm to prevent slip between layers. The wrapped specimens were then left standing in the laboratory environment at room temperature for the BFRP to cure for at least seven days before testing.

In the wrapping procedure, care had to be taken so fibres did not separate from the sheet at the edges. This was especially the case when wrapping the BAS 220 material because of its fineness and because no stitch grid held the fibres in place.

1) *2)* *3)* *4)*

Figure 4-6: The BFRP application procedure. 1) Cured concrete cylinder, 2) prepared concrete surface, 3) epoxy resin worked into fabric sheet and 4) applied outer layer of resin.

4.2.4 Test Procedure

All specimens were axially loaded in a universal testing machine with a compressive capacity of 2500 kN at Mannvit´s laboratory, which is a local engineering firm. The specimens were tested under displacement control mode with a constant speed of 0,5 MPa/s according to standard [42]. For each specimen the axial load and axial deformation was recorded. Axial load was recorded from an output signal from the test machine and the axial deformation was measured as the displacement of the loading base plate. For specimens SBB1 and SBU1, four strain gauges were glued to the BFRP surface at middle region for measuring the actual BFRP jacket longitudinal strain. The same strain gauges were used as for the tensile coupon test specimens. The strain gauges were located 90 degrees from each other as shown in Figure 4-7 where two strain gauges were located at the end and middle of the overlap zone, 2E and 2M, and other two at the actual one layer area, 1E and 1M. Before the specimens were tested, the cylinder ends were sanded for smooth and levelled surface for even stress distribution in the test. The specimen was then centred under the crosshead and load applied as the base plate moved up, towards the fixed crosshead.

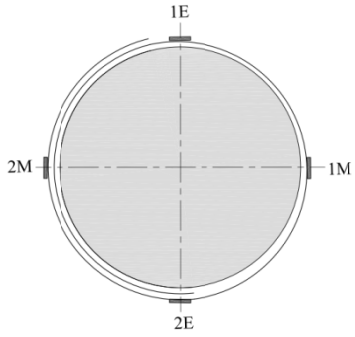

Figure 4-7: Distribution of strain gauges.

Figure 4-8: Test set up for cylinders.

4.3 Column Specimens

4.3.1 Description of Column Specimens

The primary variables in this experimental work were the thickness of the BFRP jacket and the corner radius. Two groups of columns were prepared and tested where group CA contained four columns with a corner radius of 20 mm and group CB contained four columns with a corner radius of 35 mm. Corner radius of 20 mm represents the minimum corner radius recommended by the epoxy resin manufacturer and the corner radius of 35 mm was chosen to investigate the performance of a confined column with increased corner radius and to find out if a larger corner radius might be better than adding a single BFRP layer for better confinement. Each group contained a column wrapped with one, two and three layers of BFRP jacket and one column without BFRP jacket as a reference. Each column is comprised of a centre test region of 900 mm length along the column height and two heavily reinforced ends where load is applied. All columns had 180 mm x 180 mm square section and an overall height of 1400 mm. At the centre test region, four longitudinal bars were placed in each corner and transverse hoops were placed with centre to centre length of 180 mm. Details of longitudinal and transverse reinforcement are provided in section 4.3.2.2. Normal concrete strength of 25 MPa was chosen. Table 4-6 provides details of the columns where r is the corner radius, b and h is the cross-section width, ρ_l is the longitudinal reinforcement ratio, ρ_t is the transverse reinforcement ratio, n is the number of BFRP layers, $t_{f,tot.}$ is the total nominal jacket thickness and MCR is the confinement ratio defined by Mirmiran [36].

Table 4-6: Details of concrete columns.

Column	f_c^* (Mpa)	r (mm)	b = h (mm)	ρ_l (%)	ρ_t (%)	n	$t_{f,tot.}$ (mm)	MCR	Number of columns
CA0	25,8	20	180	1,4	0,31	0	-	-	1
CA1	25,8	20	180	1,4	0,31	1	0,65	0,05	1
CA2	25,8	20	180	1,4	0,31	2	1,30	0,09	1
CA3	25,8	20	180	1,4	0,31	3	1,95	0,14	1
CB0	25,8	35	180	1,4	0,31	0	-	-	1
CB1	25,8	35	180	1,4	0,31	1	0,65	0,08	1
CB2	25,8	35	180	1,4	0,31	2	1,30	0,17	1
CB3	25,8	35	180	1,4	0,31	3	1,95	0,25	1

[*] Concrete strength determined by standard cylinder test [42].

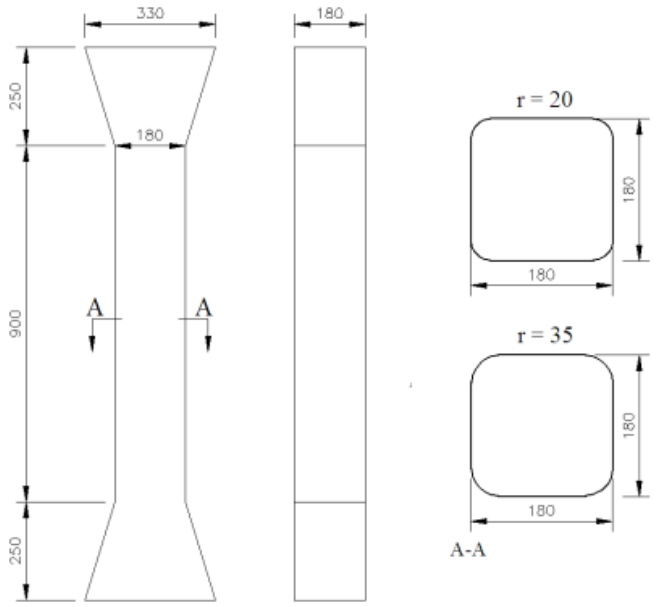

Figure 4-9: Overall dimensions of concrete columns and their cross-section.

4.3.2 Material Properties

4.3.2.1 Concrete

Concrete supplied by the concrete supplier BM-Vallá was used for casting all columns. Because of misunderstanding no tests were made on the fresh concrete at the supplier´s laboratory. The compressive strength was determined by tests performed on three standard 100 mm x 200 mm concrete cylinders. The elastic modulus was also measured on five 150 mm x 300 mm concrete cylinders [43]. Both tests were performed at the Innovation Center Iceland where the concrete strength turned out be 25,8 MPa and the elastic modulus 21,4 GPa which was much lower than expected.

Table 4-7: Concrete mix reported by the supplier.

Concrete	Sand (kg/m^3)	Rock (kg/m^3)	Kraft cement (kg/m^3)	Water (kg/m^3)	Admixtures (kg/m^3)	W/C ratio	Maximum aggregate size (mm)
C25	1080	770	324	148	2,3	0,61	19

4.3.2.2 Internal Reinforcement

Each column was reinforced with four longitudinal ribbed steel bars of steel grade B500C. The steel bars were from the same group as used in the work of J. Fridriksson [44], where tensile tests were made and the average yield strength turned out to be 628 MPa. Longitudinal bars had a diameter of 12 mm and transverse hoops a diameter of 8 mm. Corresponding reinforcement ratio was ρ_l = 1,4% and ρ_t = 0,31%. At the centre region the hoop space was 180 mm, which corresponds to the maximum hoop space for a column of this cross-section according to EC2 [25]. Tapered ends were heavily reinforced with a transverse hoop spacing of 45 mm. Concrete cover was 15 mm for better installation of the reinforcement in a cross-section of this size.

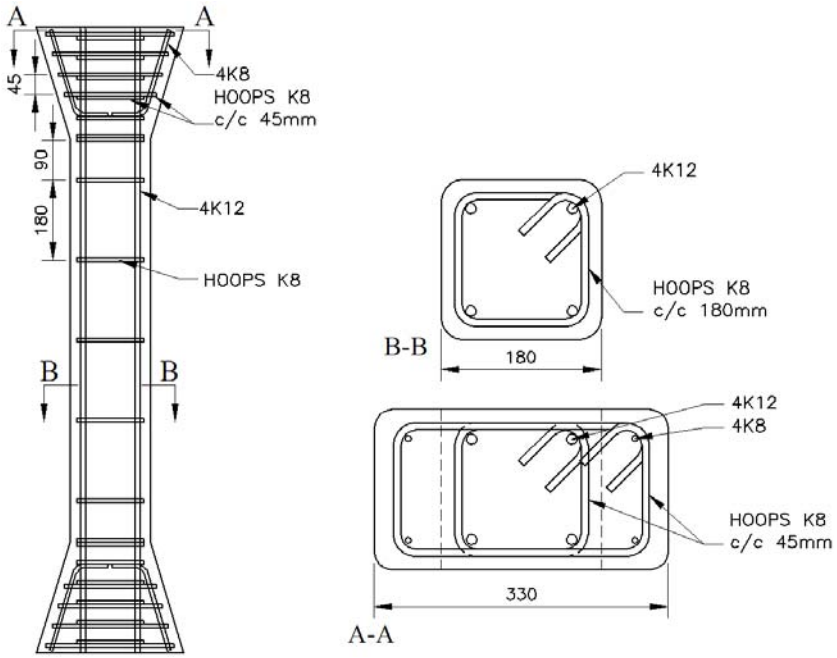

Figure 4-10: Details of reinforced column.

4.3.2.3 External Reinforcement

BAS UNI 600 was used to fabricate the external reinforcement. Material details are listed in section 4.1.1.

4.3.3 Fabrication Procedure

4.3.3.1 Casting

All transverse hoops were fastened to the longitudinal bars using wire ties at the appropriate locations. The columns were made using wood forms. The forms were originally build for another project where columns of different reinforcement were investigated [45]. Inside each corner of the forms at centre region, wood strips were placed to provide rounded corners. One side of each column form was left unassembled to provide access to insert prepared reinforcement cages. As the alignment of cages was done, the formwork was closed and lined up for casting.

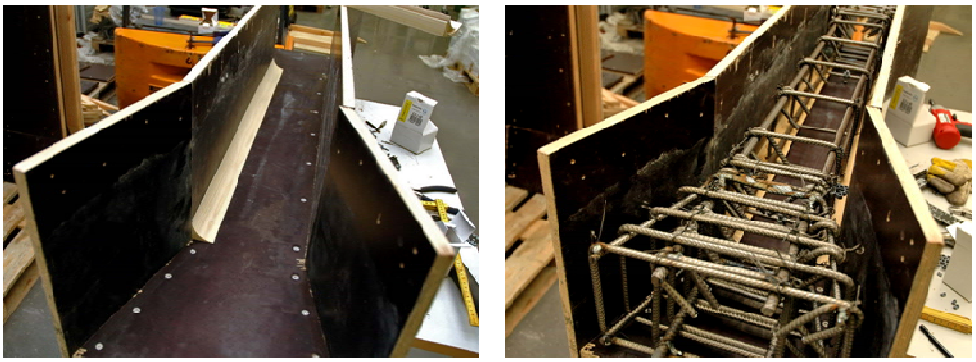

1) *2)*

Figure 4-11: 1) Wood form with corner strip. 2) Inserted reinforcement cage.

The columns were cast vertically outside the structural laboratory of Reykjavik University where the concrete could be poured from a concrete truck along a chute that was placed on the truck. The concrete was placed in the forms in two layers and consolidated by an electrically powered submersion vibrator. Column top surface was aligned before it was covered with plastic sheet. The columns were let to stand outside the laboratory for twelve hours before they were carefully moved with a fork lift inside the laboratory. After five days the columns were removed from the forms and additional water was added to the concrete surface before they were wrapped in plastic sheet. The columns were cured at ambient temperature for 77 days before they were removed from the plastic sheet. In addition to the columns, three 100 mm x 200 mm cylinders and five 150 mm x 300 mm cylinders were cast to estimate the concrete strength and elastic modulus. The cylinders were stored in a humidity room at Innovation Center Iceland for 77 days.

Figure 4-12: Casting of columns.

4.3.3.2 BFRP Application

The procedure of applying the fabric sheets consist of the same three main steps as for the concrete cylinders which is described in section 4.2.3.2, 1) preparation of concrete surface; 2) preparation of sheets and 3) application and impregnation of the basalt sheets. In addition to step one, the corners of tapered ends were rounded with a diamond polishing disc to a proper radius. The rounding was not done with wooden strips in the casting as the original plan was not to wrap the ends with BFRP. The original plan was to confine the ends with bolted steel boxes but because of high cost in fabrication it was not a feasible option. The top surface of the column was also polished for smooth and level surface to get as even stress distribution as possible in the test. In the beginning, only one column, CA2, was prepared and wrapped to evaluate if the BFRP confined ends would ensure that the failure would happen in the middle region of the column which turned out to be successful. The remaining five columns were then prepared in the same manner. In step two, the fabric sheets were cut to a width of 900 mm and suitable lengths in order to allow an overlap of 150 mm at the middle region of the columns. The fabric sheets used on the tapered ends were cut to a width of 260 mm and lengths of 760 mm. In addition to step three, care was taken that unusual voids in the concrete surface were covered with epoxy resin. Unusual voids were of minimum amount. As in the BFRP application on the cylinders, the sheets were wrapped in a continuous way around the middle region of the columns but in the case of tapered ends, two pieces of sheet were used to form one BFRP layer. The sheets were applied from opposite sides which allowed an average overlap of 250 mm on each side. Because of the slope caused by the tapered ends, care was taken that all fibres were perpendicular to the axial direction of the column which was not difficult because of the sheet's flexibility.

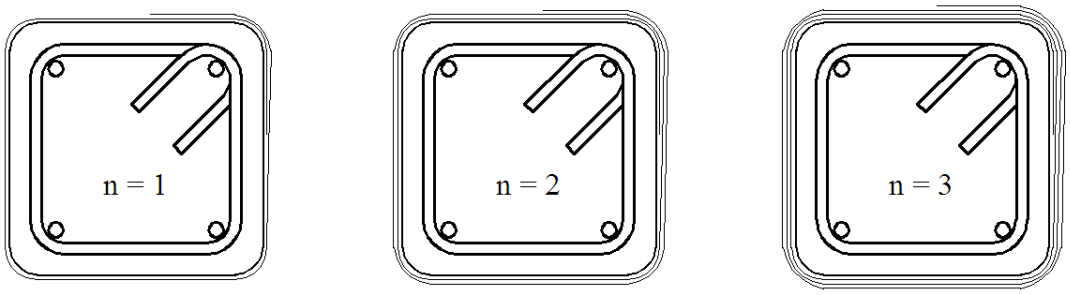

Figure 4-13: Distribution of continuous wrapped columns at their middle region.

1) 2) 3)

4) 5)

Figure 4-14: BFRP application: 1) Application of inner resin coat, 2) BFRP application at middle region. 3) BFRP application at tapered end, 4) Impregnation of fabric sheet, 5) Pre cut fabric sheets.

1) 2) 3) 4)

Figure 4-15: 1) Plain reference column, 2) Column with rounded corners and prepared surface, 2) wrapped column in process, 3) BFRP confined column.

4.3.4 Test Procedure

All columns were axially loaded in a hydraulic pressure testing machine with a compressive capacity of 2000 kN at the structural laboratory of Reykjavik University. Each column was placed in the testing machine with a fork lift and centred under the crosshead. The testing machine was not capable of applying the load at a specific load speed, however the load was applied at even slow speed. Axial load was recorded from the hydraulic pressure with a computer program as the crosshead was forced downward. A steel plate was located at the column top surface´s to provide equal stress distribution where the crosshead applied the pressure. The axial displacement was measured as the movement of the plate. The columns were first loaded up to 30 kN where the data reading started.

Longitudinal jacket strain was measured with strain gauges placed on the surface of the BFRP jacket. The distribution of strain gauges is shown in Figure 4-16 where 1C, 2C, 3C and 1M stand for the centre of corners 1 to 3 and middle of the side face. The strain gauges were applied directly on the jacket which had been sanded for smooth surface. For column CA2, four strain gauges were used and measurements taken at column midheight. The number of strain gauges was subject to the maximum capacity of the measurement equipment used to record the data into a computer. After column CA2 had been tested, distribution of the strain gauges was changed and measurements taken at the middle of the uppermost hoop space of 180 mm as shown in Figure 4-16.

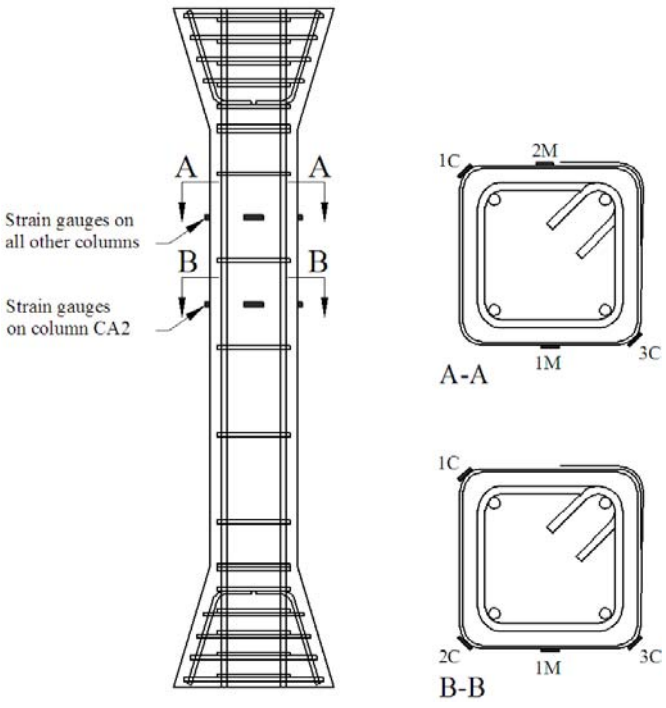

Figure 4-16: Distribution of strain gauges.

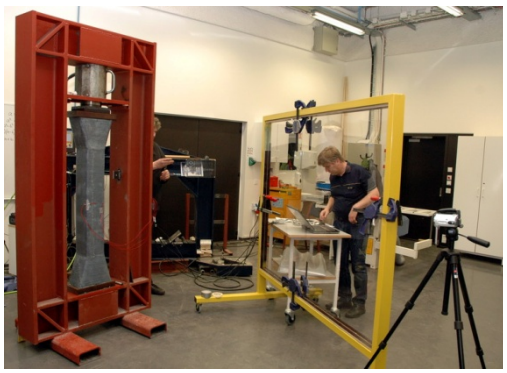

Figure 4-17: Test set up for columns.

5 Experimental Results

This chapter presents the results of the tensile test performed on BFRP tensile coupon test specimens and the axial load tests performed both on the concrete cylinders and columns. Experimental set up is detailed in chapter 4. Section 5.1 summarizes the test results of the BFRP tensile coupon test where the stress-strain behaviour is presented together with the estimation of its elastic modulus. Section 5.2 and 5.3 summarize tests of the confined specimens compared to unconfined specimens. Stress-strain behaviour of cylinders and columns is presented and the ultimate axial load capacity and strain summarized.

5.1 Tensile Coupon Test Specimens

Difference in thickness is generally observed in tested tensile specimen because of variance in the amount of epoxy resin used in a hand layup method which also occurs in the retrofit process of structural components. Therefore, the thickness used in calculations is the nominal thickness of the dry fabric sheet. The BFRP material tensile strength is then calculated by:

$$f_f = \frac{F_t}{w t_f n} \tag{5.1}$$

where F_t is the ultimate tensile force from the test, w is the average width of the specimen, t_f is the nominal thickness of the dry fabric sheet and n is the number of layers in the specimen.

The elastic modulus is estimated according to the ASTM standard [41] where the elastic modulus is calculated within a given strain range from a stress-strain curve. The elastic modulus is given by:

$$E_f = \frac{\Delta\sigma_f}{\Delta\varepsilon} \tag{5.2}$$

where $\Delta\sigma_f$ is the difference in applied stress between the two strain points on the stress-strain curve and $\Delta\varepsilon$ is the difference between the two strain points which is from 0,1% to 0,3% according the standard.

5.1.1 Test Results

All specimens of group BB showed a good linear response between the two strain points for calculating the elastic modulus but around strain at 0,5 % to 0,7 %, a minor change in the slope can be seen which is then linear up to failure. General failure mode of group BB was a sudden rupture in the gage length area generally with a slope around 45°. Specimens BB-2 and BB-4 showed difference from the other three specimens. This difference can be explained as a result of uneven impregnation and misalignment of the fibre in the

fabrication procedure which confirms the importance of accuracy in the fabrication of BFRP composites.

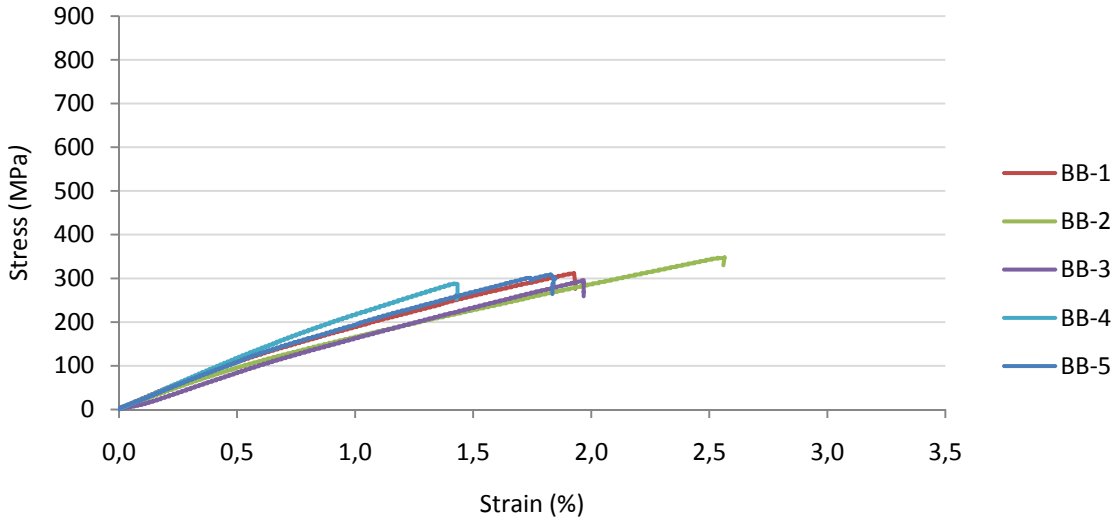

Figure 5-1: Tensile stress versus longitudinal strain of tensile coupon specimens with BAS 220 material.

All specimens of group BU showed a good linear response up to first failure at peak load. At that point the applied stress decreases as the fibres at the edge rupture and the stress starts increasing again until the whole section ruptures. The rupture of the fibres occurred generally from the end of the active gage length of the specimen. The fact that the fibres at the edge rupture first indicates that the orientation of the fibres to the applied tensile load is not perfectly parallel, which however can be the case in structural strengthening. Therefore, the ultimate strength and strain is taken at the peak where the first failure occurs. This is considered to represent the material strength of the BFRP jacket and is shown in Table 5-1.

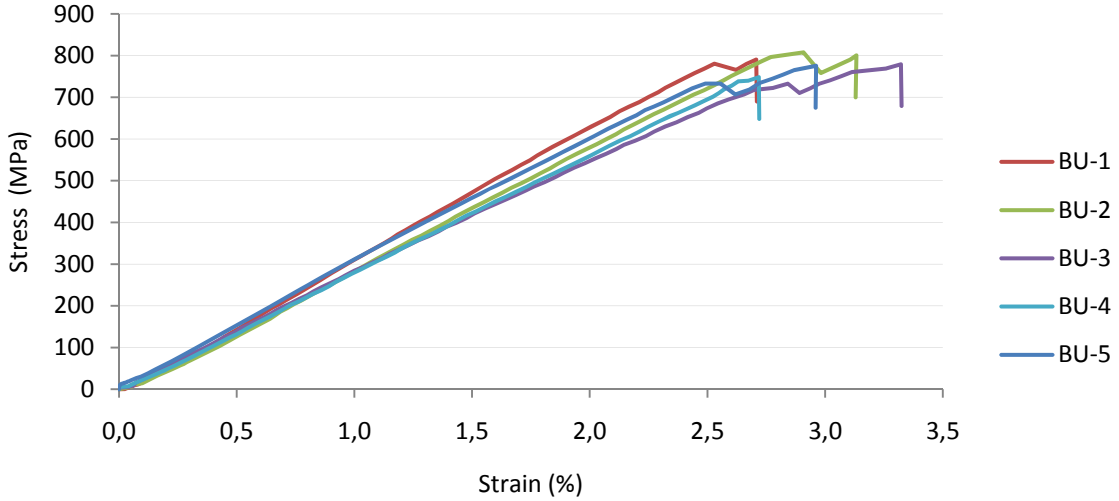

Figure 5-2: Tensile stress versus longitudinal strain of tensile coupon test specimens with BAS UNI 600 material.

Plots of the average stress-strain curves from test groups BB and BU are shown in Figure 5-3. The applied stress is calculated with equation (5.1) and the strain is the average strain from the two strain gauges located on opposite sides on each specimen.

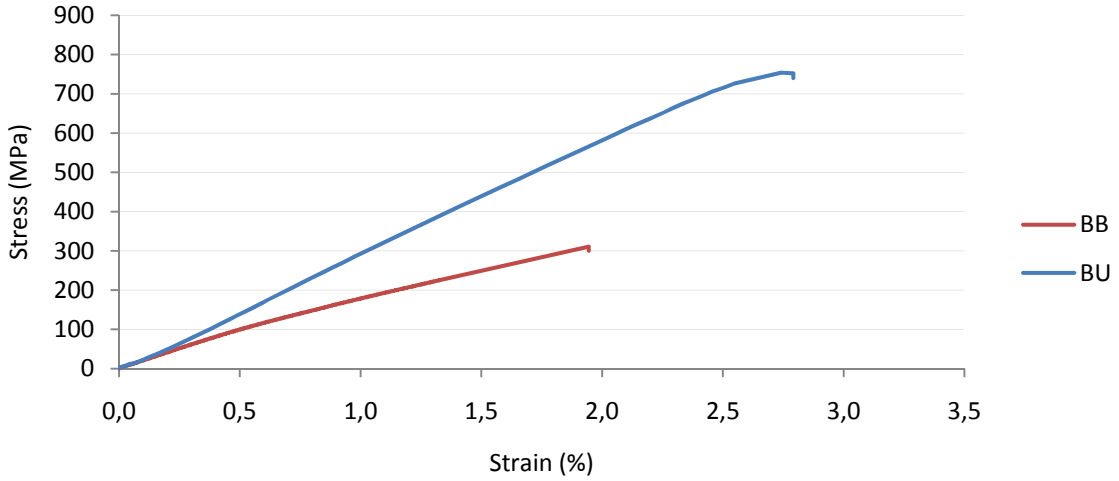

Figure 5-3: Average test results of specimens BB and BU . Tensile stress versus longitudinal strain of tensile coupon test specimens.

Average volume fraction of fibres in the composites turned out to be 31,4 % in BB and 28,5 % in BU. Calculation of volume fraction can be seen in appendix E.

Table 5-1: Results of tensile tests on tensile test specimens.

Specimen	Nominal thickness (mm)	Average width (mm)	Ultimate tensile force (kN)	Tensile stress (MPa)	Strain (%)	Elastic modulus (GPa)
BB-1	0,20	24,58	1,53	311,98	1,93	22,401
BB-2	0,20	25,93	1,81	348,67	2,56	20,185
BB-3	0,20	24,52	1,45	296,02	1,97	16,899
BB-4	0,20	24,65	1,42	288,24	1,43	24,255
BB-5	0,20	22,60	1,40	309,36	1,83	21,423
Average			**1,52**	**310,85**	**1,94**	**21,033**
Standard deviation				**20,81**	**0,36**	**2,46**

Specimen	Nominal thickness (mm)	Average width (mm)	Ultimate tensile force (kN)	Tensile stress (MPa)	Strain (%)	Elastic modulus (GPa)
BU-1	0,65	23,63	11,99	780,58	2,53	31,059
BU-2	0,65	23,37	12,27	807,62	2,91	27,607
BU-3	0,65	24,03	11,44	732,57	2,84	31,489
BU-4	0,65	22,93	11,15	748,20	2,72	24,585
BU-5	0,65	24,48	11,66	732,71	2,56	29,613
Average			**11,70**	**760,34**	**2,71**	**28,871**
Standard deviation				**29,42**	**0,15**	**2,54**

1) 2) 3) 4)

Figure 5-4: Tensile coupon test specimens. 1) Specimen BU, 2) specimen BB, 3) typical failure of specimen BU, 4) typical failure of specimen BB.

5.2 Cylinder Specimens

5.2.1 General Behaviour and Mode of Failure

All BFRP confined specimens had similar stress-strain behaviour in the ascending part of loading before the first micro cracks developed since the lateral dilation was very small. This behaviour confirms that the passive confining pressure provided by the BFRP jacket is negligible during the loading state up to the transition zone where micro cracks start to develop. Increase in compressive strength at the transition point B was observed in all confined specimens. This is because the BFRP jacket activates in the transition zone where micro cracks developed and is fully activated after reaching the unconfined concrete strength where the cracks developed rapidly.

Stress-strain behaviour of a strain softening response was observed on cylinder specimens of test group SBB with a confinement ratio of 0,03 and 0,06 where the ultimate compressive stress was generally lower than the unconfined strength. The axial behaviour can be characterized by a pre-peak ascending branch and a post-peak descending branch. After reaching peak stress at point B, the BFRP jacket was fully activated. The jacket provided pressure to resist the rapid concrete dilation and exhibited a gentle descend slope with a decrease in compressive stress while the axial strain increased. At the end of the post-peak branch, the BFRP jacket reached its maximum bearing capacity and ruptured drastically which resulted in failure of the specimens. The typical failure mode of the cylinder specimens SBB was a tensile rupture of the BFRP jacket at the middle region of the specimens which extended vertically up or down the specimen. The BFRP jacket ruptured generally outside the overlap area. During the loading state no crack sounds were observed in the BFRP jacket until the jacket ruptured.

Distinct hardening response was observed for the stress-strain behaviour of the cylinder specimens in the SBU test group with a confinement ratio of 0,17, 0,34 and 0,51. This behaviour can be characterized by two ascending branches. After reaching the peak stress at point B, the stress-strain relationship continued to increase with a reduced slope. The enhancement in compressive strength was linear from the peak stress, where the BFRP jacket was fully activated, and continued to increase until the BFRP jacket ruptured. This

behaviour was observed in all specimens except in specimens SBU1 with a confinement ratio of 0,17. After reaching the transition point in specimen SBU1, the strength increase consisted of two slopes where the former was of lesser slope and can respond to the beginning of a softening response. In the latter slope, the confinement pressure started to fully resist the concrete dilation and the compressive stress increased until the BFRP jacket ruptured.

1) *2)* *3)* *4)*

Figure 5-5: Typical failure modes of specimens SBB. 1) Explosive rupture of specimen SBU1-2, 2) Explosive rupture of specimen SBU2-2, 3) Combination of delamination and tensile rupture of specimen SBU2-2, 4) Close up of delamination.

The failure of the specimens can be divided into two modes, tensile rupture of the BFRP jacket and a combination of delamination at the overlap and tensile rupture of the BFRP jacket. The former failure mode behaviour of the jackets started with rupture of the first fibres which then extended to other fibres during continued loading in an explosive way, resulting in failure of the specimens with a loud sound. The latter failure mode started in a similar manner but instead of an explosive rupture, a delamination occurred in the overlap following the first rupture of fibre. During the loading state, crack sounds in the BFRP jacket started at approximate 60% of the maximum compressive stress.

5.2.2 Axial Stress versus Strain Response

Axial stress behaviour of cylinder specimens is summarized in Figure 5-6 to Figure 5-8 and Figure 5-10 to Figure 5-13 where each figure presents curves of specimens with the same number of BFRP layers. Figure 5-9 to Figure 5-14 present the average behaviour for each test series. Each cylinder is identified corresponding to type and thickness of the BFRP jacket as can be seen Table 4-3. The results of tested cylinder specimens are summarized by reporting the key parameters at milestones throughout the loading time. The results are summarised in Table 5-2 to Table 5-5. Each table includes the maximum axial load, F_{max}, the unconfined concrete strength at peak for the unconfined specimens, f_c, and the confined concrete strength at ultimate for the confined specimens, f_{cc}. The tables also show the confined concrete strength at the transition point B, f_{cc1}. Corresponding

strain at f_c is, $\varepsilon_{c1,}$ corresponding strain at f_{cc} is ε_{cu} and the corresponding strain at f_{cc1} is ε_{cc1}. The end of the stress-strain curve was defined as the point when the specimen had unloaded to a stress equal to 0,85 times the unconfined concrete strength f_c, in the case of unconfined specimens and 0,85 times the confined strength at jacket rupture f_{cc}, in the case of confined specimens. Table 5-3 and Table 5-5 also include the strength ratio f_{cc}/f_c, f_{cc1}/f_c and the strain ratio $\varepsilon_{cu}/\varepsilon_{c1}$, where f_c is the average unconfined concrete strength at peak and ε_{c1} is the corresponding average strain. The axial stress of the cylinder specimens was obtained by dividing the measured axial load by the average section area from the unconfined specimens. The axial strain of the specimens was obtained by dividing the measured bottom base movement by the average specimen´s height and therefore does not show strain values that can be compared to recommended design values by EC2 [25]. However, as the primary interest is in the strain enhancement the strain ratio is considered to show satisfactory results.

5.2.2.1 Specimens SBB

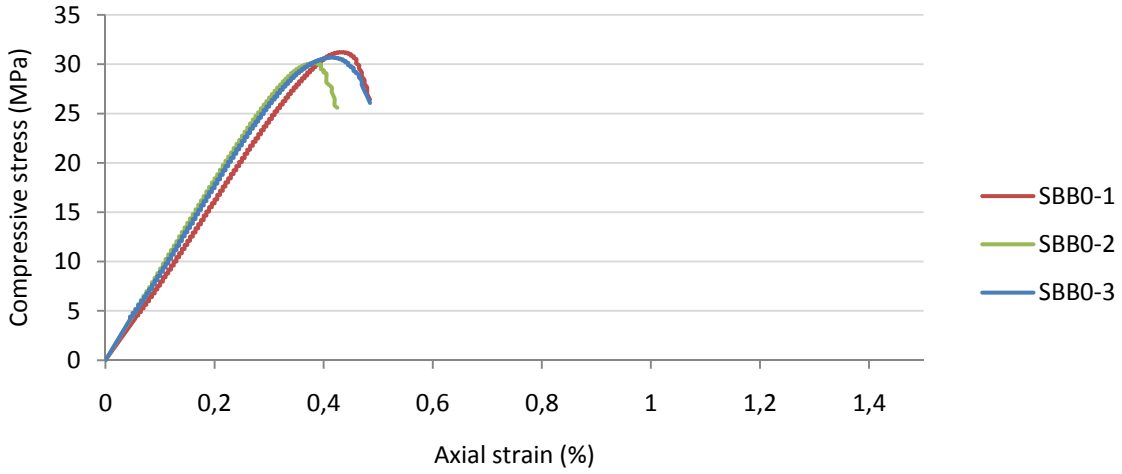

Figure 5-6: Axial stress-strain curves for plain cylinder specimens.

All unconfined specimens generally behaved in a similar manner. The specimens reached an average maximum compressive stress of 30,7 MPa and axial strain at ultimate of 0,47%. These results are considered to be a reference value of 1,0 for the following enhancement results.

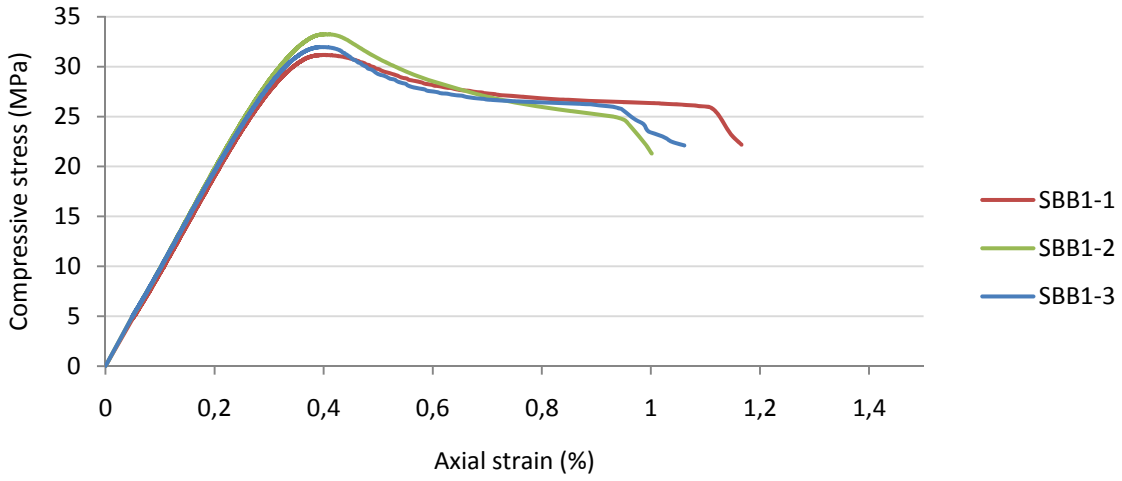

Figure 5-7: Axial stress-strain curves for confined cylinder specimens with one BFRP layer.

Stress enhancement ratio in specimens SBB1 at ultimate was 0,85, 0,82, and 0,85. The enhancement in strain at ultimate was 2,33, 2,30 and 2,27. Smooth rupture occurred in the middle region except in specimen SBB1-1 where the rupture expanded upwards with a loud sound.

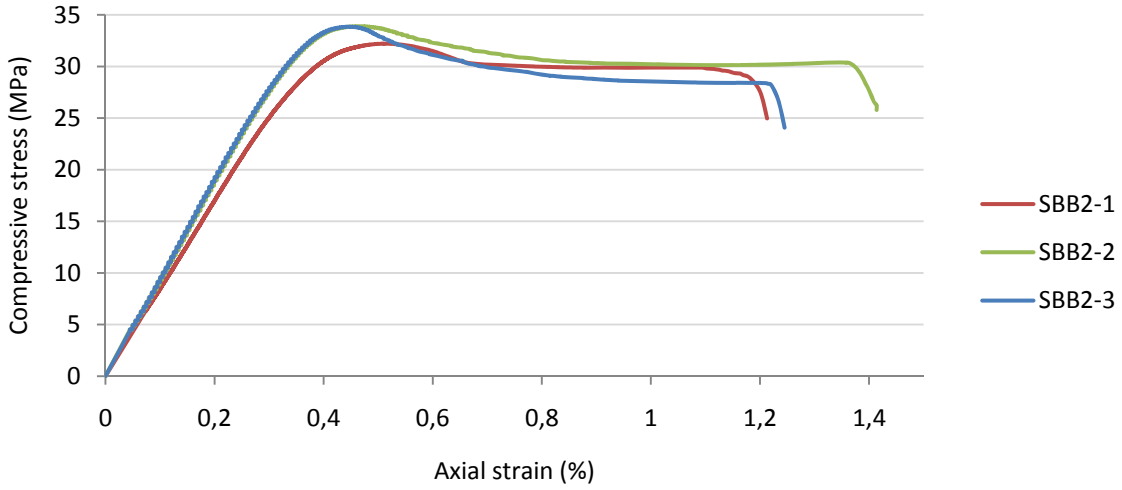

Figure 5-8: Axial stress- strain curves for confined cylinder specimens with two BFRP layers.

Stress enhancement ratio in specimens SBB2 at ultimate was 0,96, 0,99 and 0,92. The enhancement in strain at ultimate was 2,90, 2,55 and 2,62. A loud sound was noticed at rupture which occurred in the middle region. Specimen SBB2-1 showed lower slope up to the peak stress which can be explained by lesser amount of aggregates compared to the other cylinder specimens.

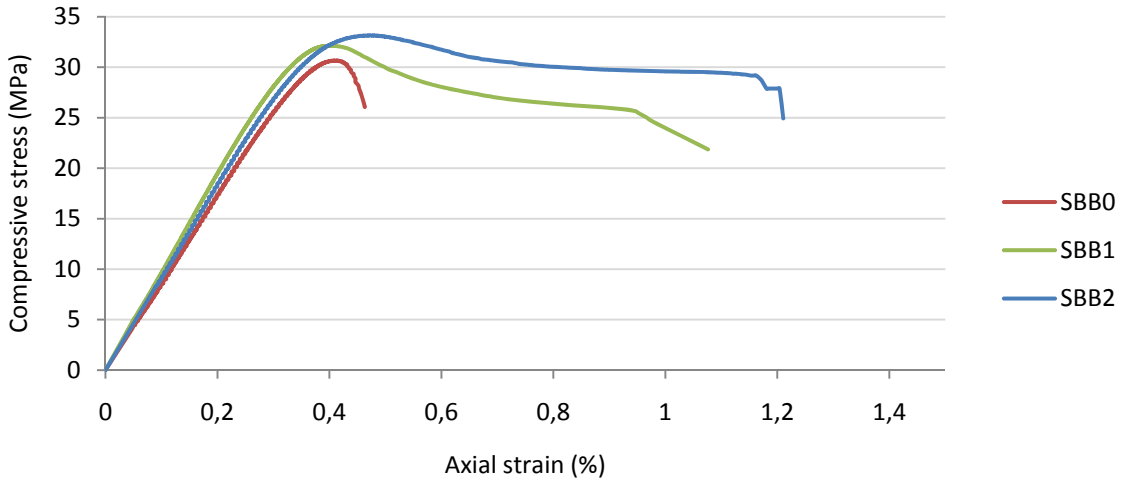

Figure 5-9: Average axial-stress strain curves for plain cylinders and cylinders confined with one and two layers.

Figure 5-9 shows that confined cylinder specimens with one and two layers achieved much higher axial strain than the cylinder specimens without BFRP jacket which resulted in a ductile behaviour with a descending curve.

Table 5-2: Results of plain cylinder specimens.

Specimen	**n**	**F_{max} (kN)**	**f_c (MPa)**	**ε_{c1} (%)**	**ε_{cu} (%)**
SBB0-1	0	245,1	31,21	0,44	0,49
SBB0-2	0	232,3	30,12	0,39	0,43
SBB0-3	0	237,1	30,68	0,42	0,49
Average		**238,2**	**30,67**	**0,41**	**0,47**

Table 5-3: Results of confined cylinder specimens.

Specimen	**n**	**F_{max} (kN)**	**f_{cc1} (MPa)**	**f_{cc} (MPa)**	**f_{cc1}/f_c**	**f_{cc}/f_c**	**ε_{cc1} (%)**	**ε_{cu} (%)**	**$\varepsilon_{cu}/\varepsilon_{c1}$**
SBB1-1	1	242,1	31,18	26,10	1,02	0,85	0,41	1,08	2,33
SBB1-2	1	258,1	33,24	25,06	1,08	0,82	0,40	0,92	2,30
SBB1-3	1	248,3	31,97	26,02	1,04	0,85	0,41	0,93	2,27
Average		**249,5**	**32,13**	**25,72**	**1,05**	**0,84**	**0,41**	**0,98**	**2,30**
SBB2-1	2	250,1	32,21	29,38	1,05	0,96	0,40	1,15	2,90
SBB2-2	2	263,2	33,89	30,34	1,11	0,99	0,51	1,31	2,55
SBB2-3	2	262,8	33,84	28,32	1,10	0,92	0,46	1,22	2,62
Average		**258,7**	**33,32**	**29,35**	**1,09**	**0,96**	**0,46**	**1,23**	**2,69**

5.2.2.2 Specimens SBU

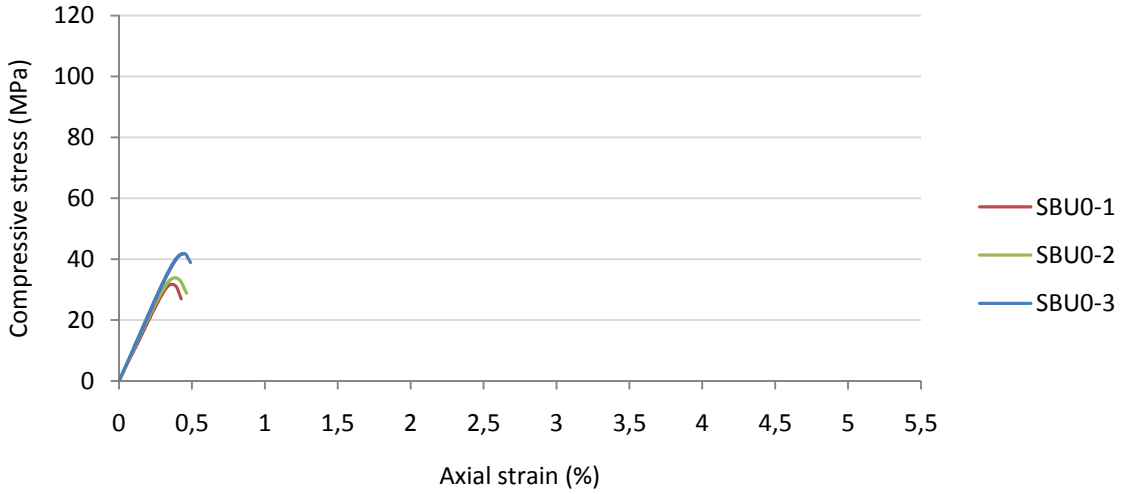

Figure 5-10: Axial stress-strain curves for plain cylinder specimens.

The average maximum compressive stress of the unconfined cylinders was 35,8 MPa and corresponding strain of 0,40 %. Specimen SBU0-3 reached a considerably higher strength than the other two which is surprising as the concrete used for casting of the cylinders was from the same container. As the reference specimens are only three it was decided not to exclude the dissimilar specimen where this difference could occur in other test series.

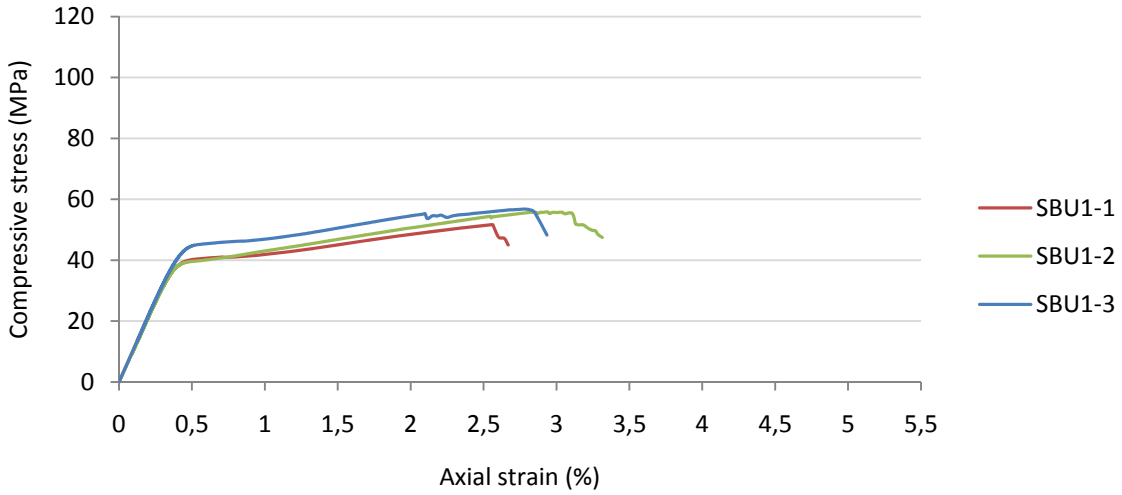

Figure 5-11: Axial stress-strain curves for confined cylinder specimens with one layer.

Stress enhancement in specimens SBU1 from the unconfined stress was 1,44, 1,55 and 1,59 and 6,40, 7,78 and 6,98 in strain. Similar difference in stress as for the unconfined specimens can be seen at the transition point in specimen SBU1-3. All specimens failed in a similar manner where the first rupture of fibre occurred in the middle region and the rest followed in an explosive way.

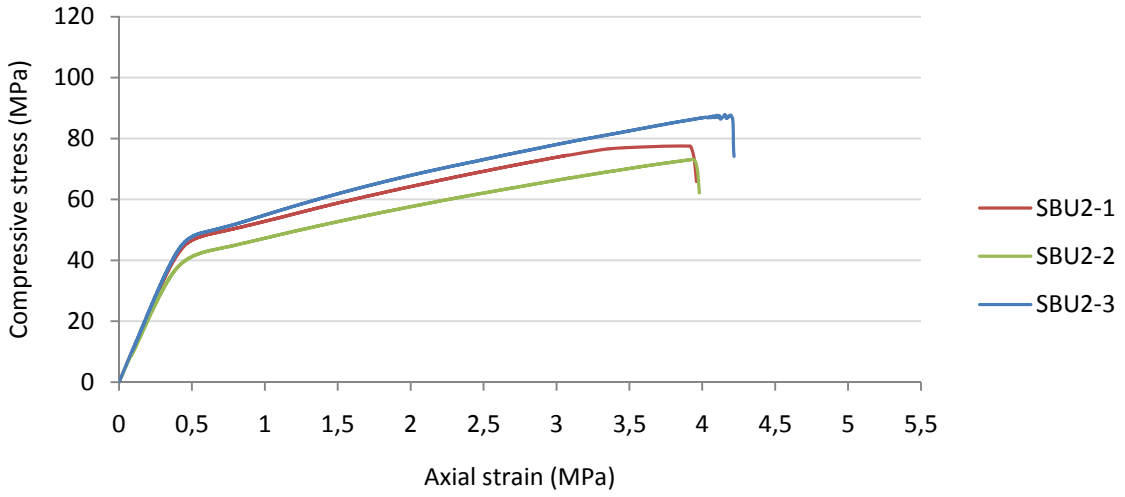

Figure 5-12: Axial stress strain-curves for confined cylinder specimens with two layers.

Stress enhancement in specimens SBU2 was 2,17, 2,04 and 2,44, corresponding strain enhancement was 9,82, 9,89 and 10,55. Failure modes of specimens SBU2-1 and SBU2-2 were a combination of rupture of fibres and delamination at the overlapping zone with a loud sound. Specimen failure of SBU2-3 was a tensile rupture in the middle region with a loud sound.

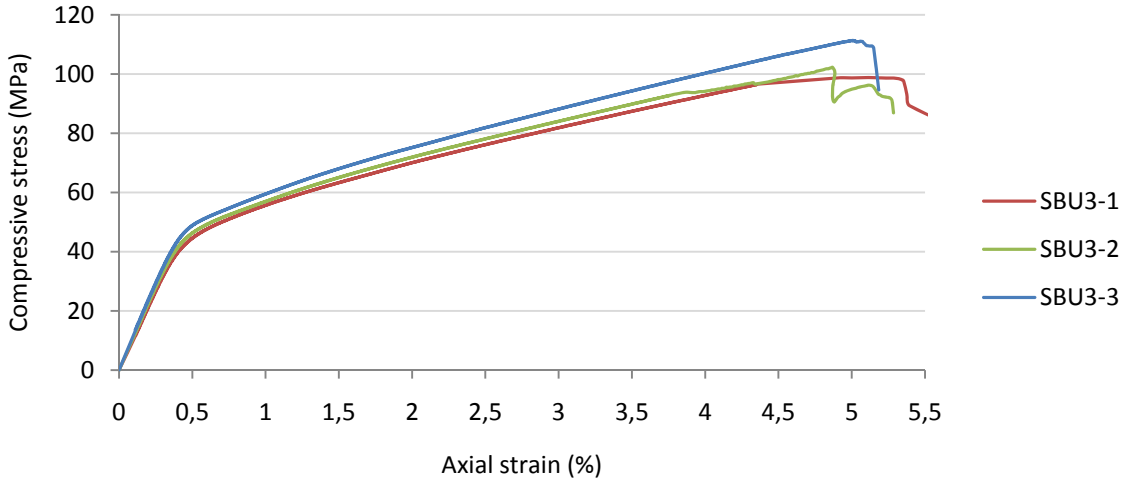

Figure 5-13: Axial stress-strain curves for confined cylinder specimens with three layers.

Stress enhancement in specimens SBU3 was 2,75, 2,85 and 3,11 and corresponding enhancement in strain was 13,32, 12,24 and 12,59. All specimens failed with tensile rupture in the middle region with a loud sound except for specimen SBU3-3 which also showed a delamination at the overlapping zone. The stress drop in specimen SBU3-2 is because of sudden rupture of fibre where the rest did not rupture immediately after. The stress increased again after the sudden drop and reached a second peak where the jacket ruptured with a loud sound.

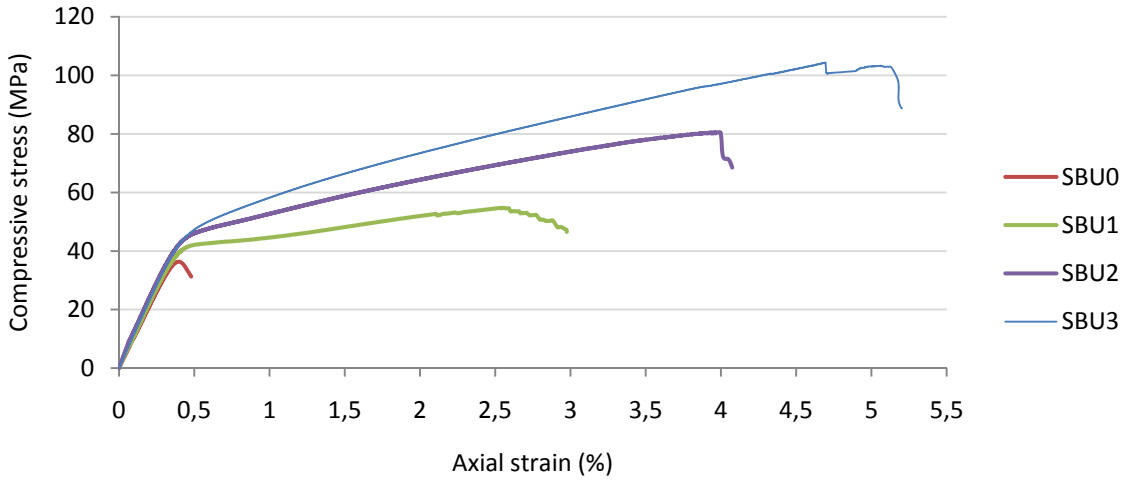

Figure 5-14: Average axial stress-strain curves for cylinder specimens of SBU test group. Good apparent of the great strength gain, both in compressive stress and axial strain with increased jacket thickness.

Table 5-4: Results of plain cylinder specimens.

Specimen	**n**	**F_{max} (kN)**	**f_c (MPa)**	**ε_{c1} (%)**	**ε_{cu} (%)**
SBU0-1	0	245,1	31,71	0,36	0,43
SBU0-2	0	232,3	33,89	0,38	0,51
SBU0-3	0	237,1	41,84	0,45	0,55
Average		**238,2**	**35,81**	**0,40**	**0,50**

Table 5-5: Results of confined cylinder specimens

Specimen	**n**	**F_{max} (kN)**	**f_{cc1} (MPa)**	**f_{cc} (MPa)**	**f_{cc1}/f_c**	**f_{cc}/f_c**	**ε_{cc1} (%)**	**ε_{cu} (%)**	**$\varepsilon_{cu}/\varepsilon_{c1}$**
SBU1-1	1	411,8	39,86	51,70	1,11	1,44	0,47	2,55	6,40
SBU1-2	1	442,3	39,46	55,53	1,10	1,55	0,48	3,10	7,78
SBU1-3	1	452,3	42,98	56,79	1,20	1,59	0,45	2,78	6,98
Average		**435,5**	**40,77**	**54,67**	**1,14**	**1,53**	**0,46**	**2,81**	**7,05**
SBU2-1	2	617,8	45,08	77,56	1,26	2,17	0,46	3,91	9,82
SBU2-2	2	582,9	40,67	73,18	1,14	2,04	0,48	3,94	9,89
SBU2-3	2	695,1	46,84	87,27	1,31	2,44	0,47	4,20	10,55
Average		**631,9**	**44,20**	**79,34**	**1,23**	**2,22**	**0,47**	**4,01**	**10,09**
SBU3-1	3	785,5	43,88	98,62	1,23	2,75	0,48	5,30	13,32
SBU3-2	3	814,2	45,46	102,22	1,27	2,85	0,48	4,87	12,24
SBU3-3	3	886,8	48,21	111,34	1,35	3,11	0,49	5,01	12,59
Average		**828,8**	**45,85**	**104,06**	**1,28**	**2,91**	**0,48**	**5,06**	**12,72**

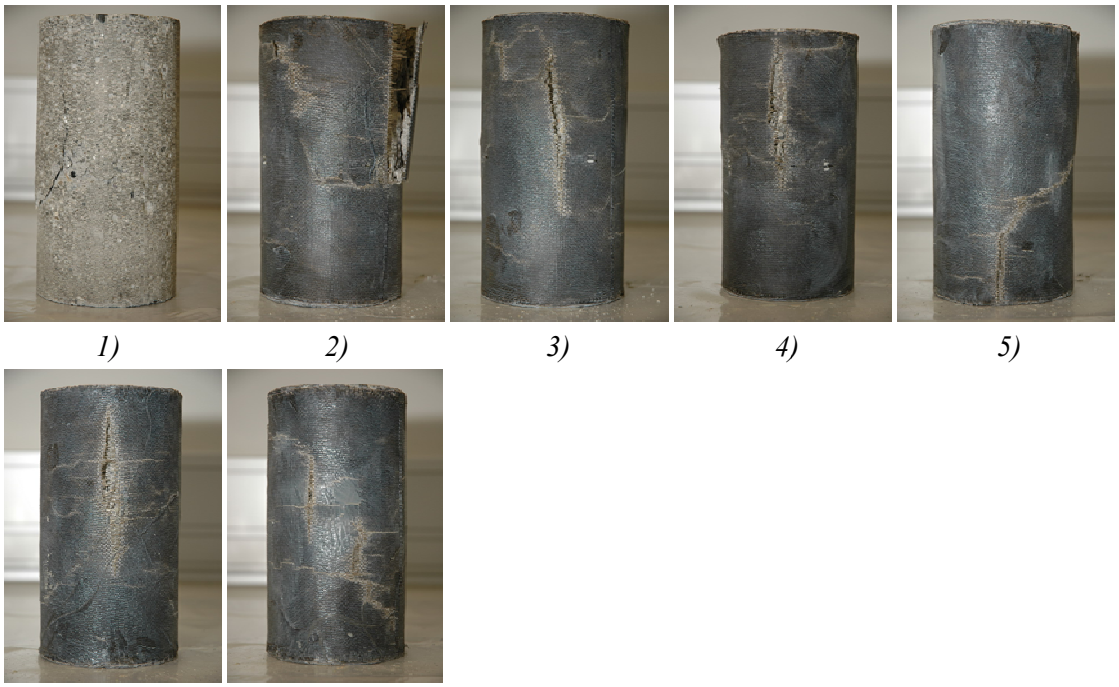

1) 2) 3) 4) 5)

6) 7)

Figure 5-15: Failure modes of specimens SBB: 1) Concrete failure SBU0-1, 2) Tensile rupture at the overlap end SBB1-1, 3) Tensile rupture SBB1-2, 4) Tensile rupture SBB1-3, 5) Tensile rupture SBB2-1, 6) Tensile rupture SBB2-2, 7) Tensile rupture SBB2-3.

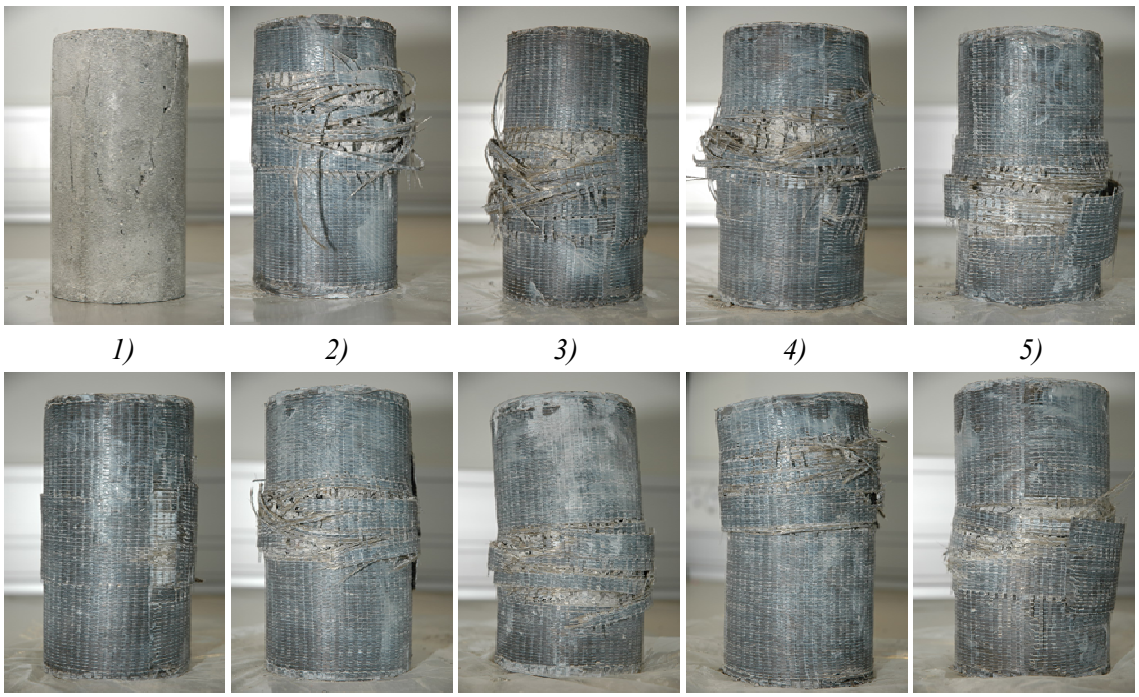

1) 2) 3) 4) 5)

6) 7) 8) 9) 10)

Figure 5-16: Failure modes of specimens SBU: 1) Concrete failure SBU0-3, 2) Explosive rupture SBU1-1, 3) Explosive rupture SBU1-2, 4) Explosive rupture SBU1-3, 5) Tensile rupture and delamination SBU2-1, 6) Tensile rupture and delamination SBU2-2, 7) Explosive rupture SBU2-3, 8) Explosive rupture SBU3-1, 9) Explosive rupture SBU3-2, 10) Tensile rupture and delamination SBU3-3.

5.2.3 Jacket Strain

The strain gauges did not give any data shortly after the jacket was fully activated and therefore did not give satisfactory results for estimating the actual rupture strain of the BFRP jacket. This can be caused by some error in computer reading as similar measurements were done successfully with another computer on the confined columns as shown in section 0. However, the following figure verifies quite well the behaviour of the BFRP jacket during the first branch of the loading state. The tensile strain in the jacket increases at an axial stress level slightly lower than the unconfined concrete strength f_c, and increases rapidly after reaching the unconfined concrete strength resulting in increase of the confinement pressure. Jacket strain behaviour of other specimens is shown in Figure 5-17.

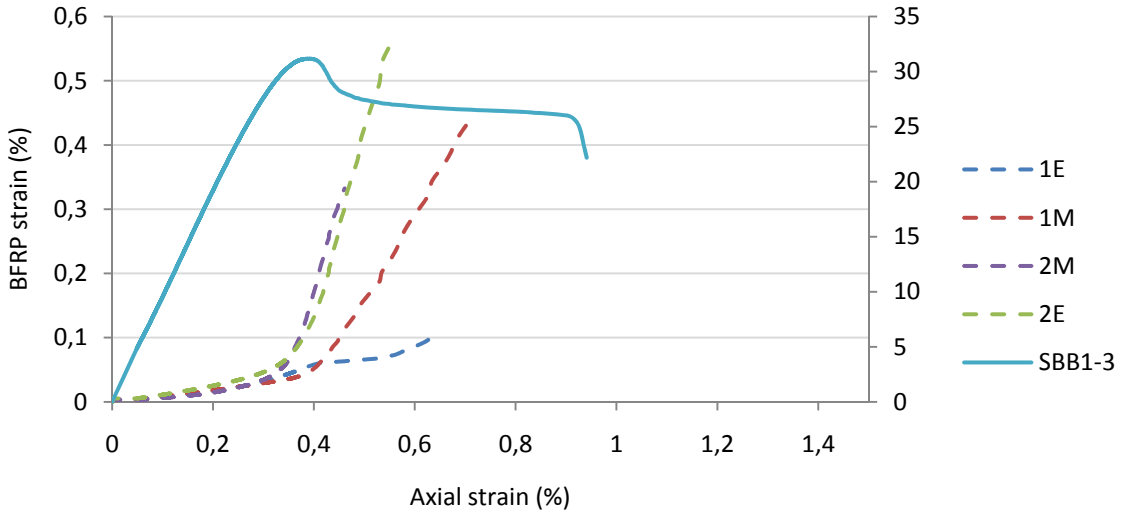

Figure 5-17: Axial stress-strain curve of specimen SBB1-3 and corresponding longitudinal strain in the BFRP jacket.

5.3 Column Specimens

5.3.1 General Behaviour and Mode of Failure

During the ascending part of loading up to the first peak load at transition point B, no visual cracks were seen in the concrete cover of the reference columns CA0 and CB0. Right after reaching the peak load, longitudinal bars buckled between hoops and the concrete separated in an explosive way. Since there was no plastic deformation in the reinforcement the columns failed in a brittle manner giving no warning of failure. In both columns the failure occurred at the top of the centre region between the uppermost hoop space of 180 mm.

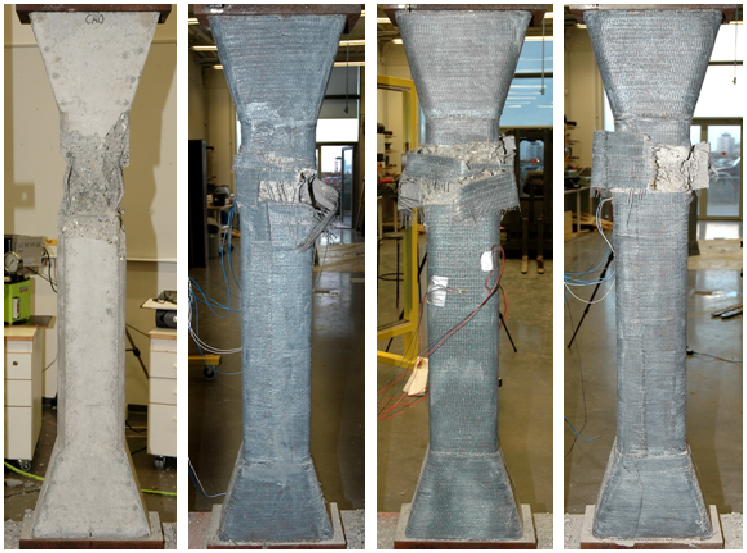

1) *2)* *3)* *4)*

Figure 5-18: Failure modes of columns from test group CA: 1) CA0, 2) CA1, 3) CA2, 4) CA3.

As in the confined cylinder specimens the stress-strain behaviour of BFRP confined columns was similar at the ascending part of loading and the load capacity at first peak increased with more BFRP thickness. After reaching the load capacity at first peak, all columns except CB3 exhibited a rapid descending slope while the BFRP jacket activated and started to resist the concrete dilation and buckling of the longitudinal bars. With the BFRP jacket fully activated, the load capacity started to increase again in a stress-strain behaviour of a hardening response with increase in axial strain. Column CA1 however did not increase its load capacity after the BFRP jacket was fully activated but retained it constant until the jacket ruptured. Instead of a rapid descend slope after first peak, column CB3 kept the axial resistance at peak constant which then further increased until the jacket ruptured. Columns with increased axial load capacity generally reached a second peak where the maximum confined load capacity was reached and first rupture of fibres occurred. Load capacity at ultimate was where the BFRP jacket failed resulting in failure of the columns. Considering the prediction of increase in axial load capacity by the confinement ratio MCR, columns CB2 and CB3 could be expected to increase their load capacity with a MCR of 0,17 and 0,25 respectively. However, confined load capacity increased or reached the unconfined load capacity in all columns except in CA1.

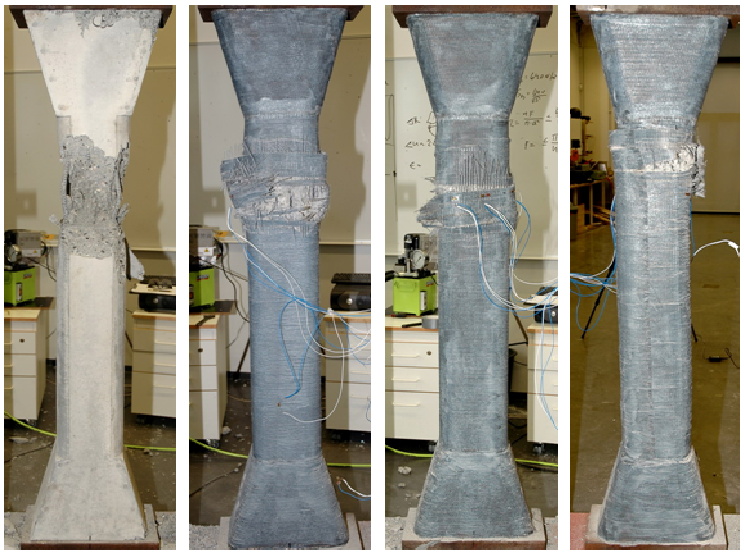

1) 2) 3) 4)

Figure 5-19: Failure modes of columns from test group CB: 1) CB0, 2) CB1, 3) CB2, 4) CB3.

Crack sounds in the jacket were observed after reaching the first peak load while the jacket was activating in all columns. At the second branch of the stress-strain curve horizontal cracks were observed in the BFRP jackets at side faces in the upper centre region of the columns. These cracks were caused by the axial deformation of the columns and did not have a visible effect on the confinement strength as the cracks occurred parallel to the main fibres. As the axial deformation and dilation increased, more crack sounds could be heard until the first fibre rupture was observed. Axial strain generally continued to increase with decrease in axial load capacity and buckling of longitudinal bars until next fibres ruptured which resulted in rupture of the jacket. Right before the jacket ruptured, white patches began to show at the rupture location which indicated a plastic flow of the resin.

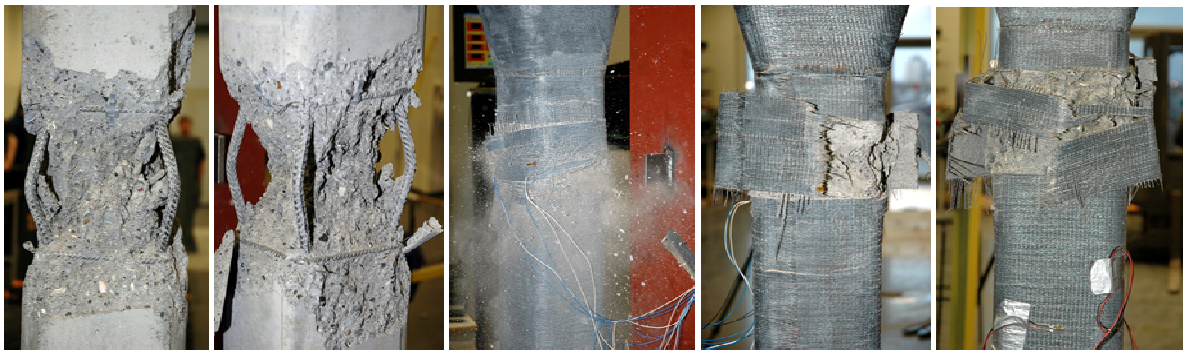

1) 2) 3) 4) 5)

Figure 5-20: Failure modes: 1) Local buckling of longitudinal bars, 2) Symmetric buckling of longitudinal bars, 3) BFRP jacket during failure, 4) BFRP jacket rupture at corner 1C, 5) BFRP jacket failure at corners 2C and 3C.

Fibre rupture generally occurred at the curvature changing point of the corners. Delamination was observed in the overlap for columns CA1 and CB1 before the jacket rupture but did not result in rupture of fibres and therefore had no affect on the confined load capacity. All columns failed at the uppermost hoop space of 180 mm.

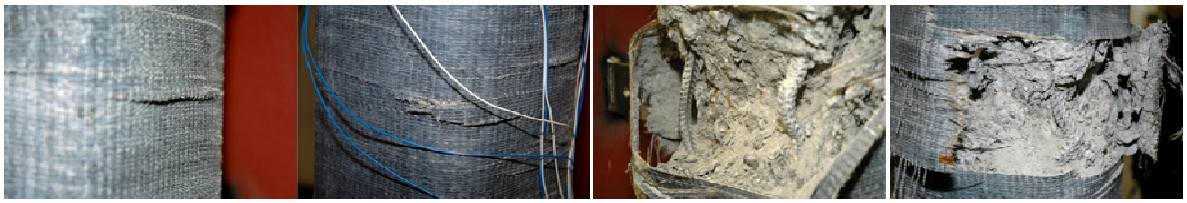

1) *2)* *3)* *4)*

Figure 5-21: Failure close ups: 1) Horizontal crack in BFRP jacket during loading, 2) BFRP jacket started to rupture, 3) buckling of longitudinal bars, 4) BFRP jacket rupture and buckling of longitudinal bars.

5.3.2 Axial Load versus Axial Strain Response

Axial load versus axial strain behaviour of concrete columns are summarized in Figure 5-22 to Figure 5-25 where each figure presents columns with the same number of BFRP layers. Each column is identified corresponding to thickness of the BFRP jacket and corner radius as can be seen in Table 4-6. The results of tested columns are summarized by reporting the key parameters at milestones throughout the loading time in Table 5-6 and Table 5-7. Each table includes the unconfined axial load capacity at first peak where F_c is for the unconfined columns and F_{cc1} is for the confined columns, the confined axial load capacity at jacket rupture F_{cc} and the load capacity at failure of the unconfined columns F_{cu}. Corresponding strain at F_c is ε_{c1}, at F_{cu} is ε_{cu}, at F_{cc1} is ε_{cc1}, and at F_{cc} is ε_{cu}. For comparison of the performance of confined columns to the unconfined columns, the strength ratio F_{cc}/F_c and the strain ratio $\varepsilon_{cu}/\varepsilon_{c1}$ is shown. The axial strain was obtained in the same manner as for the cylinder specimens and therefore only the strain ratio is considered to show satisfactory results.

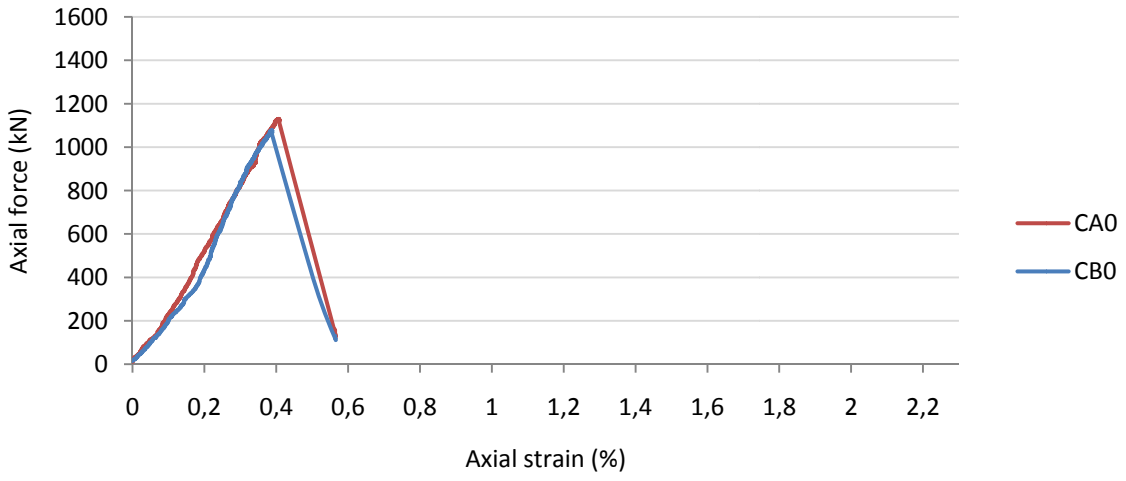

Figure 5-22: Axial load versus axial strain curves for unconfined columns.

Figure 5-22 shows very well the brittle failure of the unconfined columns right after reaching the maximum load capacity. Column CA0 reached axial load capacity of 1129,5 kN at a strain level of 0,346% and column CB0 reached axial load capacity of 1076,7 kN at a strain level of 0,343%. As the cross-section of CB0 was smaller than CA0, it reached a lower load capacity as expected.

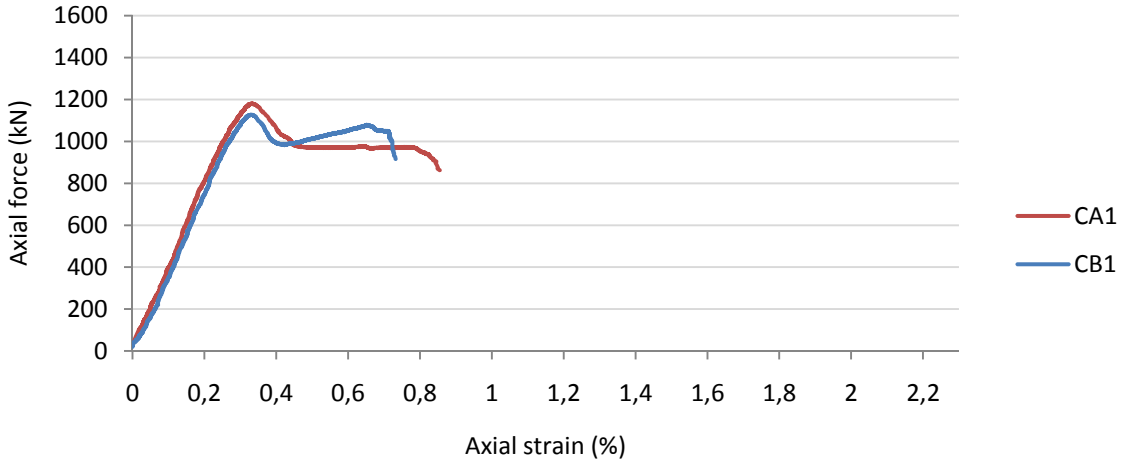

Figure 5-23: Axial load versus axial strain curves for confined columns with one BFRP layer.

Columns CA1 and CB1 reached load capacity at first peak a bit higher than the unconfined columns or at 1179,4 kN and 1127,1 kN, respectively. Strength enhancement of CA1 was 0,86 and 2,26 in strain. Column CB1 reached the unconfined strength with a ratio of 1,0 and strain enhancement of 1,91 where the first fibres ruptured. At ultimate the strength ratio was 0,97 and 2,07 in strain. In column CA1, rupture occurred at the overlap corner and corner 1C. First fibres ruptured at corner 1C and shortly after total jacket rupture occurred at the same time at corners 1C and 3C in column CB1.

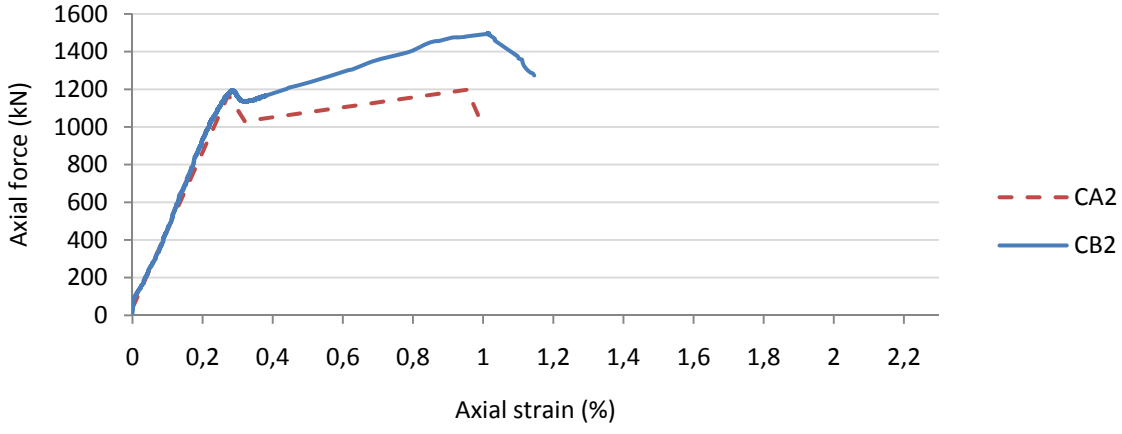

Figure 5-24: Axial load versus axial strain curves for confined columns with two BFRP layers.

When testing column CA2, a computer error occurred in the data reading resulting in inaccurate test results. The load capacity at milestones was estimated from a video file where the manometer on the hydraulic pressure could be seen. The axial strain was estimated from the displacement data recorded by the computer. At first peak, columns CA2 and CB2 reached 1169,7 kN and 1193,2 kN load capacity. Both columns reached the

unconfined strength at second peak with a strength ratio of 1,06 for CA2 and 1,39 for CB2. Corresponding strain ratios were 2,74 and 2,95. Corner 3C first ruptured in column CA2 followed with a total jacket rupture at corner 2C. In column CB2, first rupture occurred at corner 2C which resulted in total jacket rupture at corners 2C and 1C.

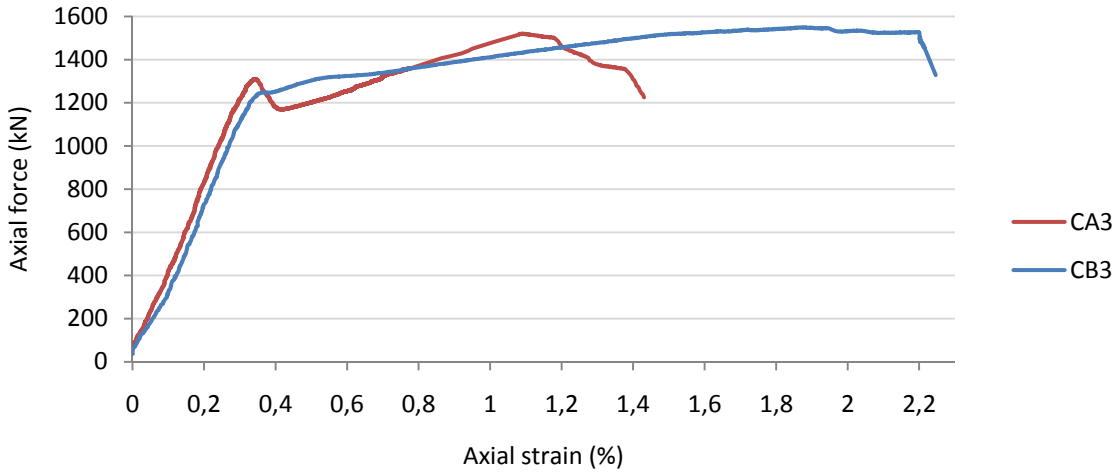

Figure 5-25: Axial load versus axial strain curves for confined columns with three BFRP layers.

Columns CA3 and CB3 reached a load capacity at first peak of 1310,1 kN and 1209,5 kN respectively. Column CA3 gained the load capacity of 1,35 where first rupture occurred at corner 1C at strain ratio of 3,14. The load capacity reduced while axial strain increased until the rupture at 1C extended vertically at strength ratio of 1,20 and strain ratio of 3,98. Column CB3 showed good hardening response as no drop in the load capacity occurred after first peak. At ultimate the strength ratio was 1,42 and the corresponding strain ratio 6,40. The jacket rupture occurred at corner 1C. Unlike for all the others columns a bending moment seemed to appear as the heavily reinforced upper region of the column moved aside the vertical axis as in the case of load eccentricity.

Table 5-6: Results of unconfined columns.

Column	n	F_c (kN)	F_{cu} (kN)	ε_{c1} (%)	ε_{cu} (%)
CA0	0	1129,5	1111,1	0,346	0,348
CB0	0	1076,7	1068,5	0,343	0,344

Table 5-7: Results of confined columns.

Column	n	F_{cc1} (kN)	F_{cc} (kN)	F_{cc1}/F_c	F_{cc}/F_c	ε_{cc1} (%)	ε_{cu} (%)	$\varepsilon_{cu}/\varepsilon_{c1}$
CA1	1	1179,4	971,2	1,04	0,86	0,332	0,783	2,26
CA2*	2	1169,7	1197,6	1,04	1,06	0,270	0,950	2,74
CA3	3	1310,1	1355,7	1,16	1,20	0,344	1,378	3,98
CA3×	3	1310,1	1520,2	1,16	1,35	0,344	1,088	3,14
CB1	1	1127,1	1048,3	1,05	0,97	0,330	0,711	2,07
CB1×	1	1127,1	1078,4	1,05	1,0	0,330	0,655	1,91
CB2	2	1193,2	1497,2	1,11	1,39	0,286	1,014	2,95
CB3	3	1209,5	1527,3	1,12	1,42	0,332	2,198	6,40

5.3.3 Jacket Strain

The same type of strain gauges was used to measure the longitudinal strain in the BFRP jacket as in the cylinder specimens. Unlike the cylinder specimens, the strain gauges gave a good data reading until failure of the BFRP jacket. The data reading was done with the same computer as for the tensile coupon specimens. It is therefore believed that the computer program used for reading strain in the BFRP jacket on the cylinder specimens had some effect on the data reading which did not give any data at failure of the jackets.

Strain values of the BFRP jacket at ultimate failure are shown in Table 5-8, in which 1C, 2C, 3C and 1M stand for the centre of corners 1 to 3 and middle of the side face. The distribution of strain gauges is shown in Figure 4-16. In addition to the strain values, R_{max} is shown which is the ratio of the maximum strain of each column to the average ultimate tensile strain that was obtained from the flat coupon tensile test. The results in Table 5-8 show that columns confined with one BFRP layer gave the highest ratio which reached the same strain level obtained from the tensile test. This strain level did not have a linear strain increase as at the end, drastic increase was observed which is not according to the strain behaviour of the tensile test specimens. Table 5-8 verifies that the ratio varies with the corner radius as the strain ratio is higher in columns with larger corner radius. The low ratio in column CA2 was expected as the strain gauges were placed below the rupture area. Jacket strain behaviour of other column specimens is shown in Appendix A.

* Estimated value because of computer error in data reading.
× Value corresponding to the maximum confined load capacity.

Table 5-8: BFRP strains at failure.

Column	r	1C (%)	2C (%)	3C (%)	1M (%)	R_{max}	Place of rupture
CA1	20	2,583	2,388	1,834	1,864	0,95	1C
CA2	20	0,188	0,250*	0,414	0,941	0,35	3C
CA3	20	0,151	0,704	0,553	1,683	0,62	1C
CB1	35	2,228	1,561	2,858	2,930	1,08	1C
CB2	35	1,507	1,731	1,748	1,867	0,69	2C
CB3	35	1,107	1,259	1,526	1,846	0,68	1C

Figure 5-26 shows very well the behaviour of the BFRP jacket as the strain linearly increased after reaching the first peak load capacity until the first rupture occurred in the jacket resulting in decrease in strain.

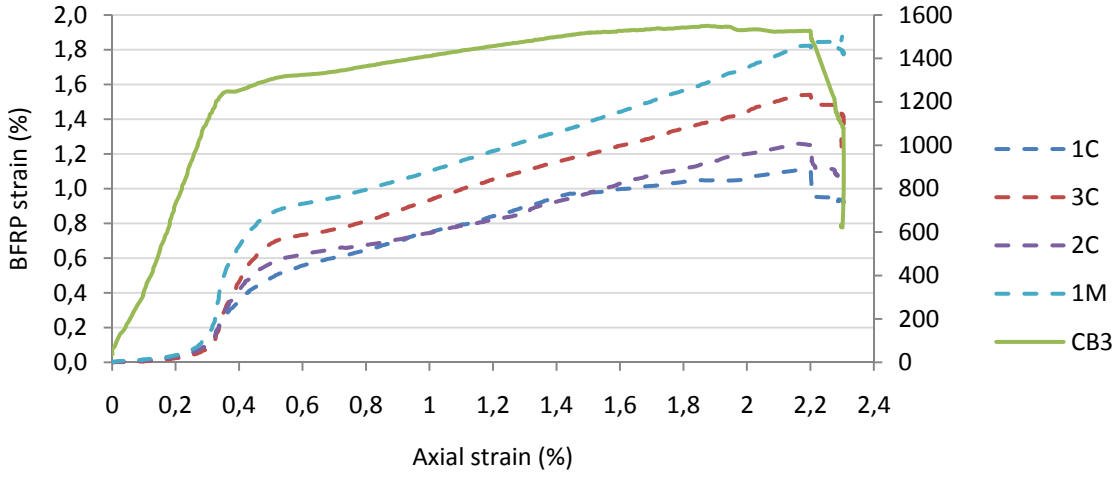

Figure 5-26: Axial load versus axial strain curve of column CB3 and corresponding longitudinal strain in the BFRP jacket.

* Value at the opposite side of 1M

6 Discussion

6.1 Confinement Effectiveness

6.1.1 Cylinder Specimens

The stress-strain behaviour of confined concrete cylinders mainly depends on the FRP confinement ratio as shown by several researchers and discussed in section 2.2.3 [30, 31]. The criterion set by Lam and Teng in equation (2.8) presents the minimum value of 0,07 for sufficient confinement to obtain a hardening response. Figure 6-1 presents the average results from the cylinder tests where each curve is separated by the corresponding confinement ratio. The results verify that BFRP confined concrete cylinders with confinement ratio above 0,17 can be expected to show a hardening response where the compressive stress continuously increases until jacket rupture and confined cylinders with confinement ratio of 0,06 or lesser show a softening response. Where the confinement ratio was calculated with the strain efficiency factor of 0,6 it can be assumed that it is an appropriate value for BFRP jackets based on the criterion for a strain softening or hardening behaviour.

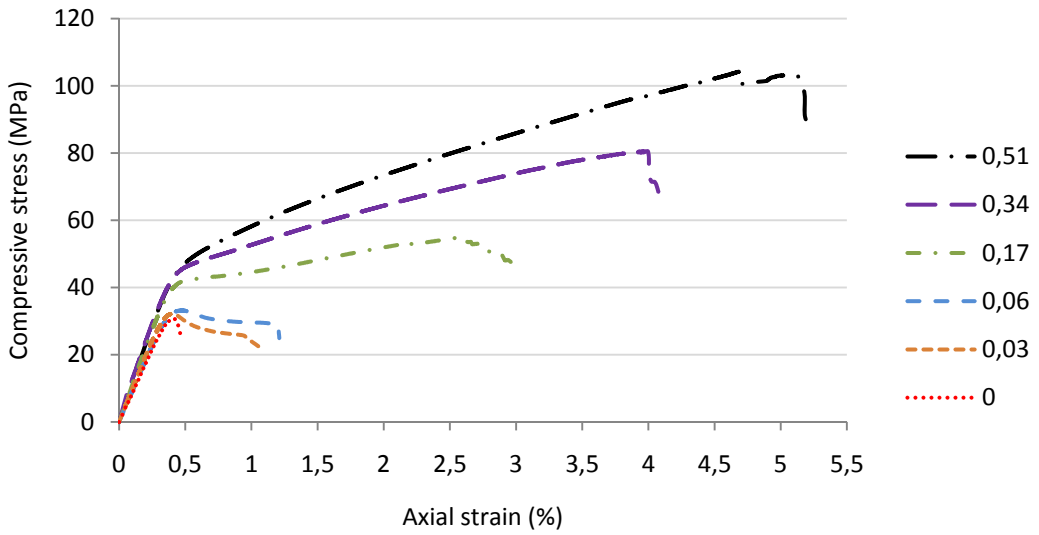

Figure 6-1: Stress-strain curves of cylinders with different confinement ratio, $f_{l,a}/f_c$, as indicated in legend.

Figure 6-2 shows the increase in confined concrete strength for a corresponding confinement ratio. It can be observed that to obtain enhancement in compressive stress the confinement ratio above 0,07 is valid according to the test results.

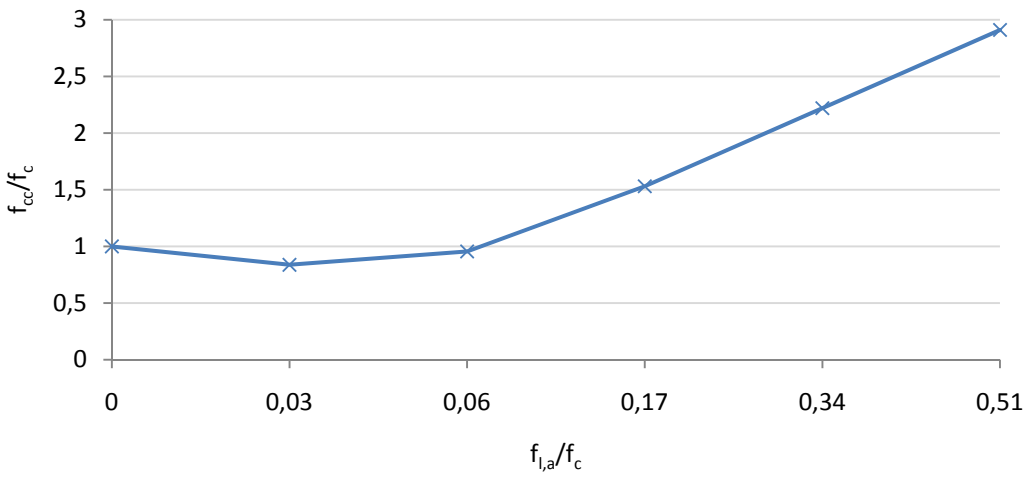

Figure 6-2: Variation of confined cylinders strength with confinement ratio.

To increase performance of structure in accidental actions, such as in earthquake events, the ability to resist large deformations is an important factor to prevent premature collapse of the structure. As Figure 6-3 shows, the deformability for resisting axial load increases greatly in proportion to increased confinement ratio. The lower increase slope in the beginning is because of lower ultimate strain capacity in the BAS 220 material used in specimens SBB.

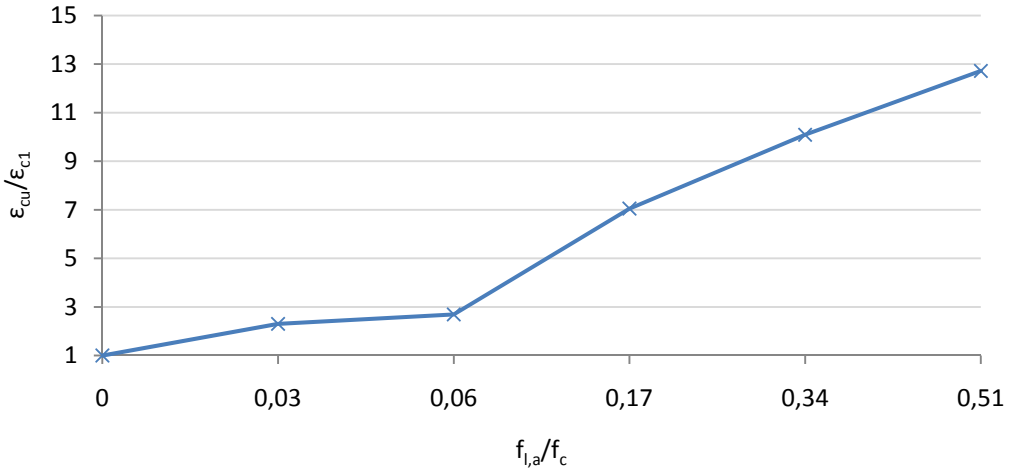

Figure 6-3: Variation of confined cylinders strain with confinement ratio.

It should be noted that as these tests are made with standard cylinders, the rapid gain in strength will not occur as determined with increased number of layers in columns of larger diameter. The confinement ratio and volumetric ratio is smaller and strengthening with one layer of BFRP will be lower [46].

6.1.2 Column Specimens

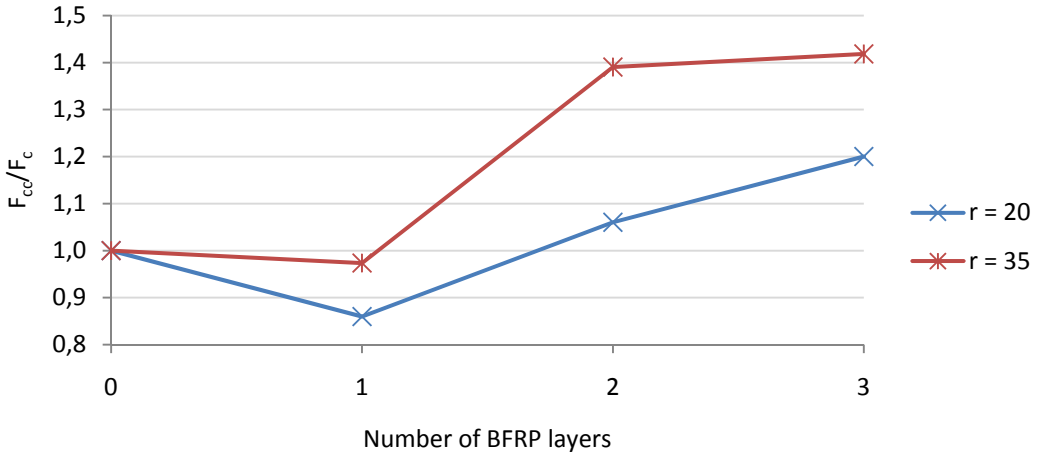

Figure 6-4: Variation of confined columns axial load capacity with increased number of layers. Corner radius of columns as indicated in legend.

It is observed that the presence of BFRP jacket increases the strength and strain of reinforced columns and the thickness of the BFRP jacket is clearly an important factor. This performance is also strongly influenced by the cross-section shape as the strength gain is not as evident as in the cylinders of circular sections. Figure 6-4 clearly shows that by rounding the corners more load capacity can be obtained with the same thickness of BFRP. This is due to a lower concentration of stresses at well rounded corners which results in a higher strain resistance in the BFRP as was shown in Table 5-8. By rounding the corners the effectively confined concrete core extends and the load capacity increases. Neither of the columns confined with one BFRP layer increased their unconfined load capacity as shown above, however as the number of layers increases the strength ratio enhances almost linearly in columns of corner radius of 20 mm. This is not the case in the columns of 35 mm corner radius as column CB3 seems to have sustained a load eccentricity which induces both axial compression and bending action. It has been shown that eccentric loading reduces the effectiveness of FRP jackets in axial strengthening which explains the lower increase in axial load capacity with three BFRP layers [47].

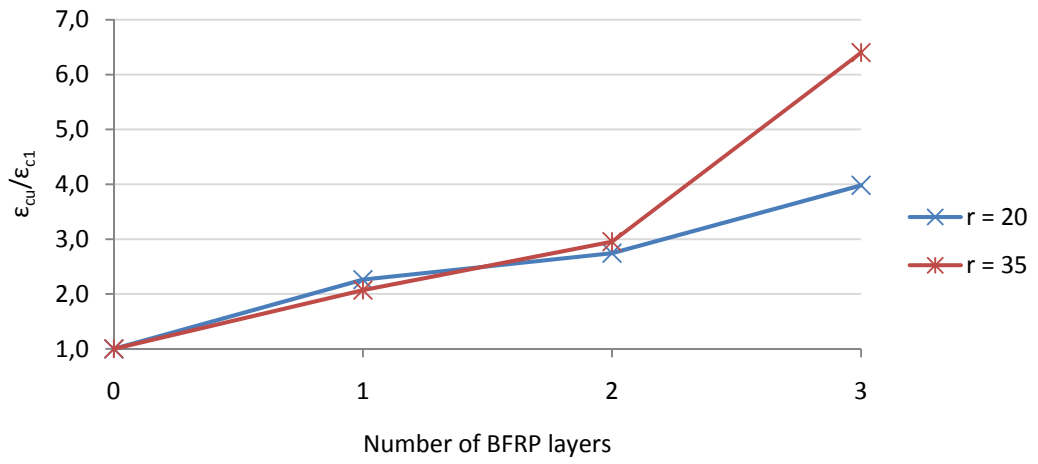

Figure 6-5: Variation of confined columns axial strain with increased number of layers.

In section 2.2.1, ductile behaviour was defined as the deformation capability of column under axial load. Figure 6-5 shows how the ductility increases with increased number of layers as the strain ratio reaches a value around 4,0 for the unconfined column of 20 mm corner radius. The drastic increase in strain from two layers to three layers in columns of 35 mm corner can be explained because of inaccurate strain measurements. Due to a bending moment in column CB3 it was not parallel to its vertical axis at failure. Therefore the movement of the compressive steel plate increases, resulting in over measured displacement compared to if the actual displacement would have been measured on the column itself. Therefore the great strain enhance in column CB3 should be taken with precaution. These results clearly show that for gaining increase in axial strain, rounded corners are not as effective factor as when increasing the compressive strength.

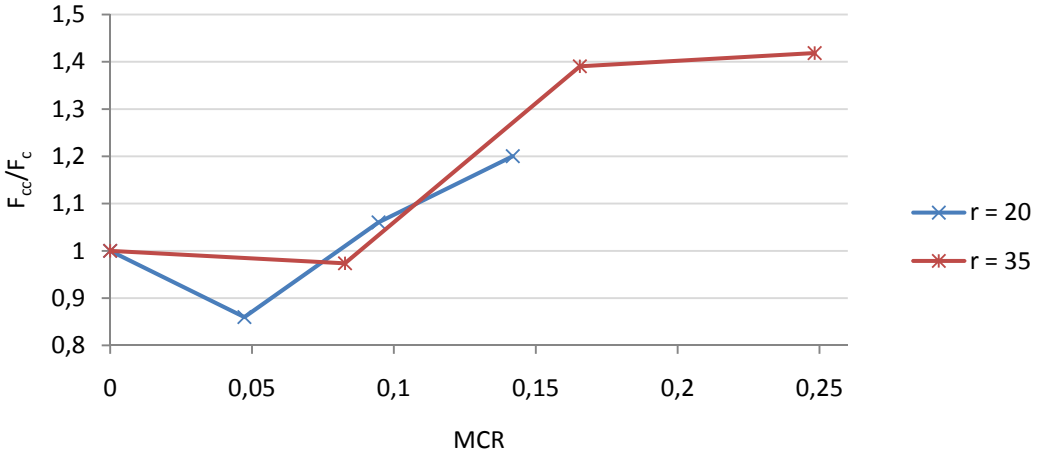

Figure 6-6: Variation of confined columns load capacity with confinement ratio MCR.

The confinement ratio MCR, defined by Mirmiran [36], suggested that enhancement in axial load capacity of confined columns should not be expected if the ratio is less than 0,15. As Figure 6-6 shows, the load capacity increases with MCR above 0,09. It can then be said that a reinforced column with corner radius of 20 mm to 35 mm can be expected to reach enhance in axial load capacity with MCR at least 0,10.

The jacket strain measurements reveal that by increasing corner radius, higher strain can be expected. The ratio of the measured strain in BFRP jackets on columns to the ultimate strain from tensile test reveal that the recommended strain efficiency factor of 0,6 provided by the Concrete Society gives a reasonable conservative approximation to the actual strain obtained on confined columns.

6.2 Comparison with Existing Models

6.2.1 Cylinder Specimens

To evaluate the performance of predicted compressive strength, f_{cc}, and ultimate strain, ε_{cu}, by the guidelines, calculations were done according to each guideline. Table 6-1 presents the calculated theoretical values where the enhancement ratio f_{cc}/f_c is the ratio between the calculated compressive stress of confined cylinder and the unconfined concrete strength obtained from the cylinder test. Aside are the experimental results for comparison. All safety and material factors were set equal to 1,0 to get as good results as possible. It should be noted that only the strain enhancement ratios were compared because of inaccuracy in the experimental values as previously mentioned.

Table 6-1: Theoretical values of confined compressive strength and strain and the corresponding experimental results.

			Theoretical				Experimental			
Guideline/ Specimen	**n**	**$f_{l,a}/f_c$**	**f_{cc} (Mpa)**	**f_{cc}/f_c**	**ε_{cu} (%)**	**$\varepsilon_{cu}/\varepsilon_{c1}$**	**f_{cc} (Mpa)**	**f_{cc}/f_c**	**ε_{cu} (%)**	**$\varepsilon_{cu}/\varepsilon_{c1}$**
ACI										
SBB1	1	0,03	32,96	1,07	0,26	1,29	25,72	0,84	0,98	2,30
SBB2	2	0,06	35,10	1,14	0,32	1,62	29,35	0,96	1,23	2,69
SBU1	1	0,17	45,19	1,26	0,49	2,44	54,67	1,53	2,81	7,05
SBU2	2	0,34	53,11	1,48	0,72	3,60	79,34	2,22	4,01	10,09
SBU3	3	0,51	59,98	1,68	0,92	4,62	104,06	2,91	5,06	12,72
Concrete Society										
SBB1	1	0,03	34,90	1,14	0,44	2,22	25,72	0,84	0,98	2,30
SBB2	2	0,06	39,10	1,27	0,54	2,69	29,35	0,96	1,23	2,69
SBU1	1	0,17	54,60	1,52	1,00	4,99	54,67	1,53	2,81	7,05
SBU2	2	0,34	73,30	2,05	1,65	8,23	79,34	2,22	4,01	10,09
SBU3	3	0,51	92,10	2,57	2,29	11,47	104,06	2,91	5,06	12,72
fib, exact										
SBB1	1	0,03	28,23	0,92	1,36	6,80	25,72	0,84	0,98	2,30
SBB2	2	0,06	36,20	1,18	1,74	8,70	29,35	0,96	1,23	2,69
SBU1	1	0,17	58,86	1,64	3,19	15,90	54,67	1,53	2,81	7,05
SBU2	2	0,34	79,12	2,21	4,29	21,40	79,34	2,22	4,01	10,09
SBU3	3	0,51	93,25	2,60	5,05	25,30	104,06	2,91	5,06	12,72
fib, practical										
SBB1	1	0,03	22,59	0,74	0,48	2,40	25,72	0,84	0,98	2,30
SBB2	2	0,06	29,40	0,96	0,52	2,60	29,35	0,96	1,23	2,69
SBU1	1	0,17	51,51	1,44	0,63	3,10	54,67	1,53	2,81	7,05
SBU2	2	0,34	69,88	1,95	0,72	3,60	79,34	2,22	4,01	10,09
SBU3	3	0,51	83,98	2,35	0,79	4,00	104,06	2,91	5,06	12,72

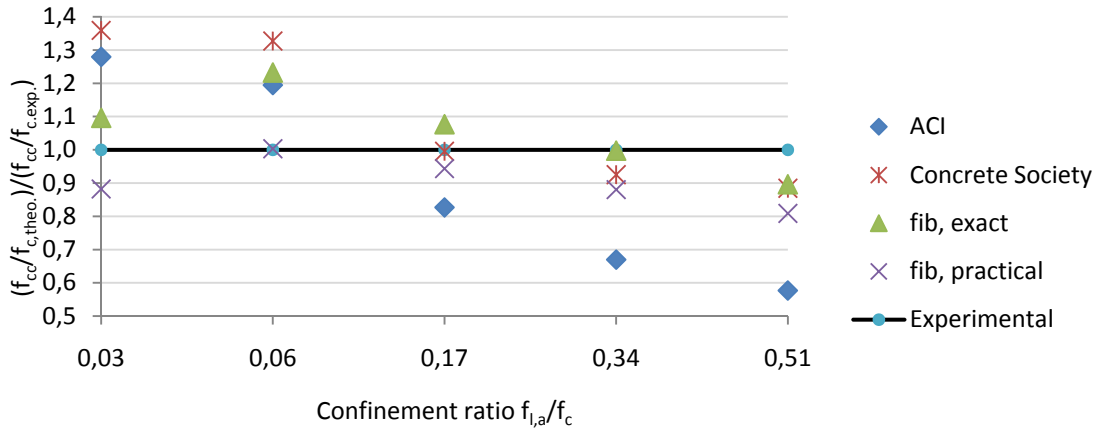

Figure 6-7: Guidelines performance. Ratio of theoretical compressive strength enhancement to experimental results of cylinders.

Figure 6-7 shows the comparison between the calculated and experimental results of the confined compressive strength. As no strain efficiency factor of the BFRP was estimated in this work the efficiency factor recommended by the Concrete Society was used in calculations by models provided by fib and the maximum strain value of 0,4% was used in ACI as recommended. All models overestimated the strength enhancement in specimens with confinement ratio under 0,17 except the practical model by fib. This could be expected in the calculation model by the Concrete Society where specimens SBB1 and SBB2 did not satisfy the criteria in (3.24) for a sufficient confinement and the calculation model was therefore not suitable for those specimens. Calculations by ACI varied from -40% to 30% for the confined strength. The estimation for the latter three specimens with the confinement ratio of 0,17 to 0,51 varied within a range of ±20% where the exact equation by fib and the equation by the Concrete Society showed the best approximation within a range of ±10%. Regarding all specimens, the best approximation was by the practical equation provided by fib. It can be seen in Figure 6-7 that as the confinement ratio increases with increased number of BFRP layers the predictive calculations underestimate the compressive strength.

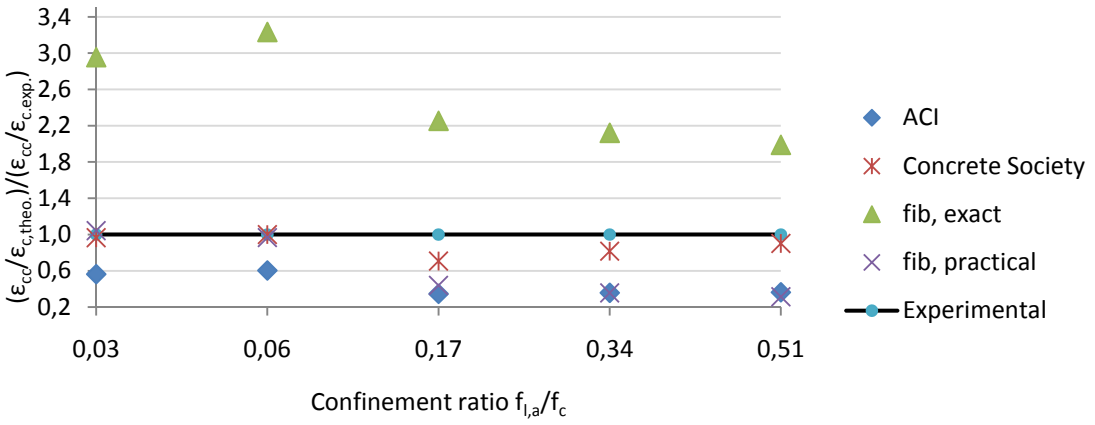

Figure 6-8: Guideline performance. Ratio of theoretical axial strain enhancement to experimental results of cylinders.

Figure 6-8 shows the comparison between the calculated and experimental results of axial strain. Calculations by the Concrete Society model did show a decent conservative approximation for all specimens with variation up to 30% but ACI underestimated the strain up to 64%. The fib model showed the least accuracy. It should be pointed out that this overestimation occurred even though the strain efficiency factor of 0,6 was considered in calculations with the exact model by fib.

6.2.2 Column Specimens

Table 6-2 presents the calculated confined axial load capacity N_{cc} and the ultimate strain ε_{cu} predicted by each guideline. Thereto are the theoretical enhancement ratios N_{cc}/N_c and $\varepsilon_{cu}/\varepsilon_{c1}$ where N_c is the maximum calculated load capacity of unconfined column and the corresponding strain ε_{c1}. Aside are the experimental results for comparison.

As the main purpose of calculations by guidelines was to see their accuracy in predicting the actual test results all safety factors were set equal to 1,0. Beside, no safety factors have been suggested for BFRP so it was decided not to consider any safety factors. Factors that take into account long term effects and unintended eccentricity were not included. Axial load capacity of columns were calculated by

$$N_c = f_c \cdot (A_g - A_{s,l}) + f_y \cdot A_{s,l} \tag{5.3}$$

$$N_{cc} = f_{cc} \cdot (A_g - A_{s,l}) + f_y \cdot A_{s,l} \tag{5.4}$$

Ratio of theoretical load capacity to experimental load capacity of columns CA0 and CB0 were 0,97 and 1,0 respectively.

Considering the strain efficiency factor k_ε, for reduced strain in the BFRP on confined columns, the factor of 0,6 provided by the Concrete Society was taken into account in the fib models calculations. The maximum strain value provided by the ACI was followed.

Table 6-2: Theoretical values of confined compressive strength, ultimate axial strain and the corresponding experimental results.

			Theoretical				Experimental			
Guideline/ Specimen	**n**	**MCR**	**N_{cc} (kN)**	**N_{cc}/N_c**	**ε_{cu} (%)**	**$\varepsilon_{cu}/\varepsilon_{c1}$**	**N_{cc} (kN)**	**N_{cc}/N_c**	**ε_{cu} (%)**	**$\varepsilon_{cu}/\varepsilon_{c1}$**
ACI										
CA1	1	0,05	1201,9*	1,09	0,34	1,68	971,2	0,86	0,78	2,26
CA2	2	0,09	1295,8*	1,18	0,45	2,27	1197,6	1,06	0,95	2,74
CA3	3	0,14	1382,7*	1,26	0,56	2,82	1520,2	1,35	1,38	3,98
CB1	1	0,08	1206,4*	1,12	0,37	1,84	1048,3	0,97	0,71	2,07
CB2	2	0,17	1318,9*	1,22	0,51	2,56	1497,2	1,39	1,01	2,95
CB3	3	0,25	1421,3*	1,31	0,65	3,23	1527,3	1,42	2,20	6,40
Concrete Society										
CA1	1	0,05	1243,5	1,13	0,69*	3,43	971,2	0,86	0,78	2,26
CA2	2	0,09	1387,4	1,26	1,02*	5,11	1197,6	1,06	0,95	2,74
CA3	3	0,14	1531,4	1,39	1,36*	6,79	1520,2	1,35	1,38	3,98
CB1	1	0,08	1258,5	1,16	0,77*	3,87	1048,3	0,97	0,71	2,07
CB2	2	0,17	1435,8	1,33	1,20*	5,98	1497,2	1,39	1,01	2,95
CB3	3	0,25	1613,1	1,49	1,62*	8,10	1527,3	1,42	2,20	6,40
fib, exact										
CA1	1	0,05	1071,3	0,97	4,36	21,80	971,2	0,86	0,78	2,26
CA2	2	0,09	1388,3	1,26	6,12	30,60	1197,6	1,06	0,95	2,74
CA3	3	0,14	1622,4	1,48	7,41	37,10	1520,2	1,35	1,38	3,98
CB1	1	0,08	1146,4	1,06	4,89	24,40	1048,3	0,97	0,71	2,07
CB2	2	0,17	1489,3	1,38	6,83	34,10	1497,2	1,39	1,01	2,95
CB3	3	0,25	1739,6	1,61	8,25	41,20	1527,3	1,42	2,20	6,40
fib, practical										
CA1	1	0,05	1126,4	1,02	1,34	2,40	971,2	0,86	0,78	2,26
CA2	2	0,09	1407,8	1,28	1,73	2,60	1197,6	1,06	0,95	2,74
CA3	3	0,14	1623,7	1,48	2,02	3,10	1520,2	1,35	1,38	3,98
CB1	1	0,08	1188,8	1,10	1,45	7,30	1048,3	0,97	0,71	2,07
CB2	2	0,17	1497,5	1,39	1,89	9,40	1497,2	1,39	1,01	2,95
CB3	3	0,25	1734,4	1,60	2,22	11,10	1527,3	1,42	2,20	6,40

* Not provided by the guideline.

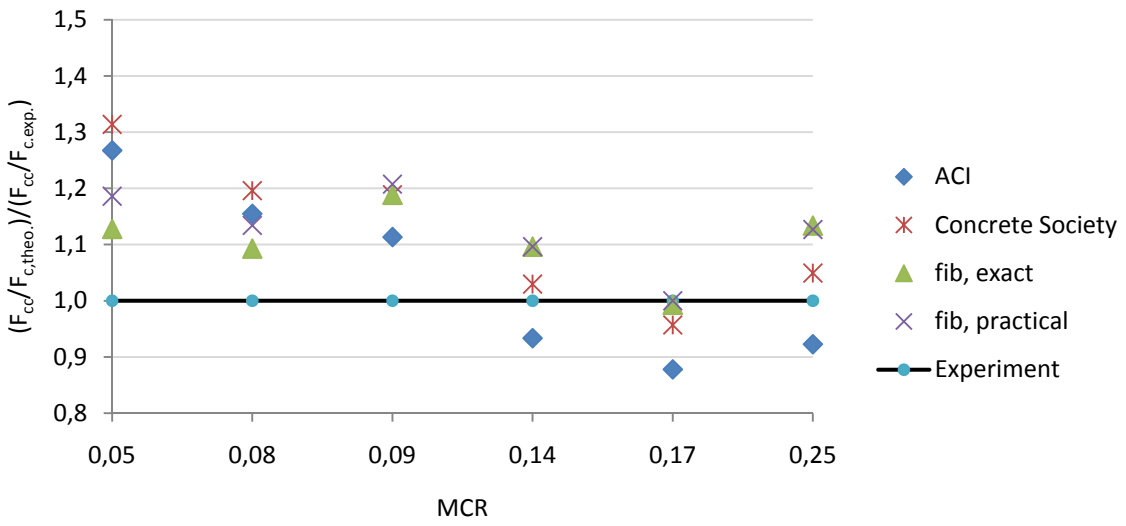

Figure 6-9: Guidelines performance. Ratio of theoretical load capacity enhancement to experimental results of columns.

The comparison between the calculated and experimental load capacity reveals that all guidelines gave acceptable results in predicting the axial load capacity. As noted in Table 6-2, ACI does not provide any recommendations on the use of FRP for axial strengthening of square and rectangular columns. However, these results show that by using the confined pressure calculated for increase in ductility, ACI predictions varied within a range of ±12% in the case of columns with MCR equal to 0,09 and higher. The model provided by the Concrete Society is only valid for a hardening response so the overestimation in columns with MCR equal to 0,05 and 0,08 of 20% and 31% is as expected. In other columns the predictions varied from -4% to 19%. Both models provided by fib gave the best approximation for all columns where the exact model varied from -1% to 19%.

According to this comparison, the exact model provided by fib gave the best predictions as it considered columns with both reduced and increased strength after reaching the unconfined strength.

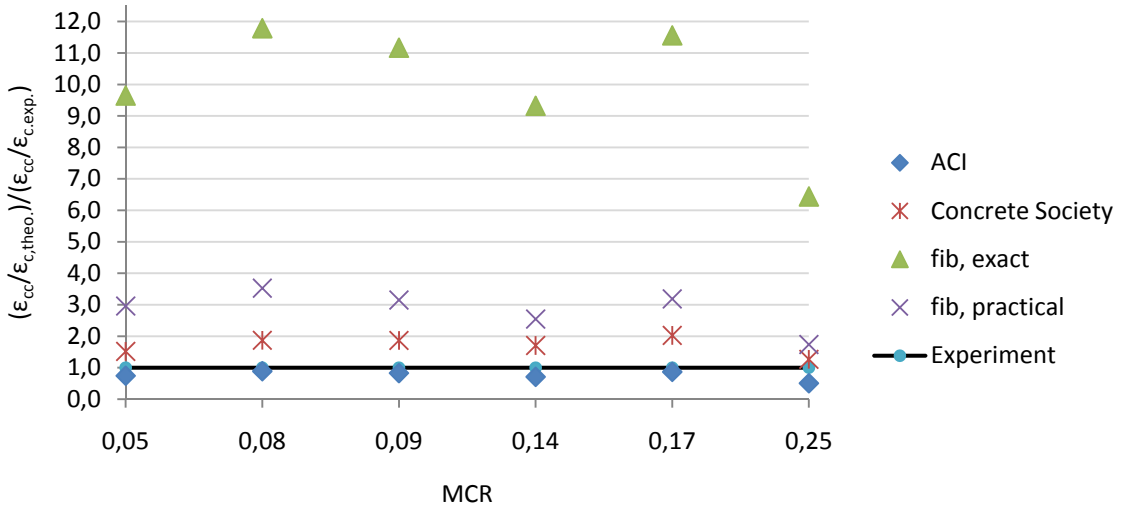

Figure 6-10: Guidelines performance. Ratio of theoretical axial strain enhancement to experimental results of columns.

The prediction of axial strain enhancement varied substantially between guidelines as Figure 6-10 shows. Despite the reduced strain used in calculations in the fib models, the strain enhancement was drastically overestimated. The Concrete Society does not provide recommendation for increased axial strain of square and rectangular columns so the overestimation of 25% to 100% could be expected. The best prediction was by the ACI where the ultimate strain of the BFRP was limited to 0,4%. The conservative prediction by ACI varied from -50% to -11%.

6.2.3 Guidelines Performance

The predictions of the confined cylinders strength reveal that all guidelines, except for the ACI, give reasonable accuracy of cylinders with a hardening response. In the case of strain enhancement predictions only the Concrete Society gives a reasonable accuracy as it is based directly on plain FRP confined cylinders. The large variance in predictions by ACI can be explained by the limited allowable FRP strain level of 0,4% which is not based on the actual FRP performance.

All guidelines can be considered to be able to predict the axial strength of BFRP confined reinforced columns of square cross-section with reasonable accuracy. This statement is only applicable for short columns with a sufficient confinement ratio for increase in axial strength. The theoretical to experimental strength enhancement ratio for square columns was best approximated by the exact model provided by fib. However, fib drastically overestimates the axial strain enhancement. This may be partly because of overestimation of internal damage of the concrete, such as cracking, which reduces the second modulus of concrete at ultimate. Regarding prediction of the axial strain enhancement, the ACI give the best approximation but with more scatter than in the prediction of the concrete cylinders.

In general, the scatter of the predictions for strain enhancement is much larger than for the strength enhancement. This reveals the uncertainty in strain predictions where effects of parameters such as type of aggregates, mix of concrete and the stiffness of the FRP jacket are difficult to represent.

7 Summary and Conclusions

In this work, the behaviour of BFRP confined plain and reinforced concrete specimens was investigated. The experimental results clearly demonstrate that BFRP wrapping can enhance the structural performance of concrete columns under axial loading.

The confinement effect is directly related to the shape of the cross-section. Circular specimens showed more distinct increase in compressive strength and axial strain capacity. Square columns generally suffer more increase in axial strain capacity rather than compressive strength.

The number of BFRP layers and the corner radius are the major parameters having effect on the behaviour of concrete columns. To enhance the confined behaviour, the stiffness of the BFRP jacket can be increased by applying additional layers and also by increasing the corner radius of square columns. Columns with corner radius of at least 20 mm can be expected to obtain increase in axial strength with sufficient confinement ratio.

Confinement effectiveness of circular columns can be estimated with the confinement ratio, $f_{l,a}/f_c$,. Increase in compressive strength can be expected for $f_{l,a}/f_c \geq 0{,}07$ as previously stated by Lam and Teng [30]. Increase in compressive strength of square columns can be expected for $MCR \geq 0{,}15$ according to Mirmiran [36]. However, from this experimental results, it can be concluded that BFRP confined columns can be expected to sustain enhance in compressive strength of $MCR \geq 0{,}10$.

The results of the experimental tests show that BFRP can give a good lateral confinement pressure to concrete columns. This effectiveness provides a good ductile behaviour and delays column failure even though the confinement ratio is low. This ability is important for example in the case of earthquake actions.

The comparison between the confined concrete strength predictions of different guidelines revealed the most accurate and the least accurate models of circular and non-circular cross-sections. This comparison however provides no indication of the safety limits offered by various guidelines. This is because no safety factors have been suggested for BFRP in structural strengthening and therefore it was not suitable to consider any safety factors in the calculations.

Predictions of confined cylinders were best obtained by the Concrete Society in the case of hardening response. Strain efficiency factor of 0,6 can be assumed to be an appropriate value for BFRP jacket as provided by the guideline but that should be verified by further research. All guidelines can be considered to be able to predict the axial strength of BFRP confined reinforced columns of square cross-section with reasonable accuracy. However, only the exact model by fib considers the decrease in compressive strength of columns with softening response. All models overestimate the axial strain enhancement of reinforced columns except the model provided by the ACI. The ACI prediction is however not based on actual rupture strain and therefore provides conservative prediction in axial strain.

7.1 Further Research

These experimental results provide a realistic behaviour of BFRP confined columns of circular and square cross-sections. To verify the strain efficiency of BFRP on concrete components a research should be done on a large number of concrete cylinders confined with different number of BFRP layers. Several strain gauges should be distributed around the cylinders to estimate the average ultimate strain observed on axially loaded specimens. In addition, tensile coupon tests should be done on specimens of variable thickness to compare with the same BFRP thickness on cylinder specimens. From this research, the strain efficiency factor could be examined and the tensile stress on BFRP tensile specimens of different thickness would reveal the accuracy in taking the ultimate stress as the product of applied number of layers and that obtained from tensile test on single BFRP layer.

Based on such research, a number of BFRP confined reinforced columns should be fabricated. The values obtained from the cylinders research should be used in the design of those columns and verified through testing of the columns. This research would improve the accuracy in predicting the confined strength by calculations as the efficiency of the BFRP would be better identified.

Axially compressed concrete columns rarely occur in practice. Columns, designed to carry only axial load, are expected to sustain bending action due to accidental load eccentricities, possible inaccuracy in construction and in the case of seismic action. To verify the BFRP confined columns efficiency for such actions, tests on columns under eccentric loading would be essential for practical application. Thereto, tests on columns under cyclic shear and bending while simultaneously subject to constant axial load to simulate earthquake action. However, such experimental work would require a more elaborate testing machine and would be more complicated in process.

References

[1] ACI Committee 440, "Guide for the Design and Construction of Externally Bonded FRP Systems for Strengthening Concrete Structures (ACI 440.2R-02)," American Concrete Institute, Farmington Hills, Mich, 2002.

[2] M. J. N. Priestley*, et al.*, *Seismic design and retrofit of bridges*. New York: John Wiley & Sons, Inc., 1996.

[3] A. Nanni and N. M. Bradford, "FRP jacketed concrete under uniaxial compression," *Construction and Building Materials,* vol. 9, pp. 115-124, 1995.

[4] H. Saadatmanesh*, et al.*, "Strength and Ductility of Concrete Columns Externally Reinforced With Fiber Composite Straps," *ACI Structural Journal,* vol. 91, pp. 434-447, 1994.

[5] M. Demers and K. W. Neale, "Confinement of reinforced concrete columns with fibre-reinforced composite sheets-an experimental study," *Canadian Journal of Civil Engineering.,* vol. 26, pp. 226-241, 1999.

[6] S. Pessiki*, et al.*, "Axial Behavior of Reinforced Concrete Columns Confined with FRP Jackets," *Journal of Composites for Construction,* vol. 5, pp. 237-245, 2001.

[7] S. Matthys*, et al.*, "Axial Load Behavior of Large-Scale Columns Confined with Fiber-Reinforced Polymer Composites," *ACI Structural Journal,* vol. 102, p. 258, 2005.

[8] F. Michael N and K. Homayoun, "Concrete Encased in Fiberglass-Reinforced Plastic," *ACI Structural Journal,* vol. 78, pp. 440-446, 1981.

[9] Y.-F. Wu and L.-M. Wang, "Unified Strength Model for Square and Circular Concrete Columns Confined by External Jacket," *Journal of Structural Engineering,* vol. 135, pp. 253-261, 2009.

[10] T. Turgay*, et al.*, "Compressive behavior of large-scale square reinforced concrete columns confined with carbon fiber reinforced polymer jackets," *Materials & Design,* vol. 31, pp. 357-364, 2010.

[11] M. N. Fardis and H. H. Khalili, "FRP-encased concrete as a structural material," *Magazine of Concrete Research,* vol. 34, pp. 191-202, 1982.

[12] J. B. Mander*, et al.*, "Theoretical Stress-Strain Model for Confined Concrete," *ASCE, Journal of Structural Engineering,* vol. 114, pp. 1804-1826, 1988.

[13] ACI Committee 440, "Guide for the Design and Construction of Externally Bonded FRP Systems for Strengthening Concrete Structures (ACI 440.2R-02)." Farmington Hills, Mich: American Concrete Institute (ACI), 2002.

[14] Concrete Society, "Design guidance for strengthening concrete structures using fibre composite materials," The Concrete Society, Wiltshire UK Technical Rep. No. 55, 2004.

[15] Fédération internationale du Béton (*fib*), "Externally bonded FRP reinforcment for RC structures," Inernational Federation for Structural Concrete, Lausanne, Switzerland, 2001.

[16] J. Sim, *et al.*, "Characteristics of basalt fiber as a strengthening material for concrete structures," *Composites Part B: Engineering,* vol. 36, pp. 504-512, 2005.
[17] S. Caijun and M. Yilung, *High-Performance Construction Materials: Science and Applications* vol. 1. Singapore: World Scientific Puplishing Co. Pte. Ltd., 2008.
[18] A. Bhagwan D and B. Lawrence J, *Analysis and Performance of Fiber Compostites* vol. 2. New York: John Wiley & Sons, Inc., 1990.
[19] C. B. Lawrance, *Composites for Construction: Structural Design with FRP Materials*. New Jersey USA: Wiley, 2006.
[20] G. Hota V.S, *et al.*, *Reinforced Concrete Design with FRP Composites*. New York: CRC Press, 2007.
[21] Z. Wu, *et al.* (05.09.2010). *Basalt FRP Composite as Reinforcements in Infrastructure*. Available: http://wjoe.hebeu.edu.cn/ICCE-17%20proceedings%20Hawaii%20USA/Wu,%20Zhishen%20(Ibaraki%20U.,%20Hitachi,%20Japan)%20%201135.pdf
[22] K. Van de Velde, *et al.* (08.09.2010). *Basalt Fibres as Reinforcement for Composites*. Available: http://basaltex.com/en/r-d.aspx
[23] M. Wang, *et al.*, "Chemical Durability and Mechanical Properties of Alkali-proof Basalt Fiber and its Reinforced Epoxy Composites," *Journal of Reinforced Plastics and Composites,* vol. 27(4), pp. 393-407, 2008.
[24] T. Paulay and M. J. N. Priestley, *Seismic design of reinforced conrete and masonry buildings*. New York: John Wiley & Sons, Inc., 1992.
[25] CEN, "Eurocode 2: Design of concrete structures-Part 1-1: General rules and rules for buildings," European Committe for Standardization, Brussels,2004.
[26] F. E. Richart, *et al.*, "A study of the failure of concrete under combined compressive stresses," Engineering Experiment Station Bulletin No. 190, Urbana, 1928.
[27] G. Wu, *et al.*, "Strength and ductility of concrete cylinders confined with FRP composites," *Construction and Building Materials,* vol. 20, pp. 134-148, 2006.
[28] F. E. Richart, *et al.*, "A study of the failure of concrete under combined compressive stresses," Engineering Experiment Staion Bulletin No. 190, Urbana1928.
[29] L. Lam and J. G. Teng, "Strength Models for Fiber-Reinforced Plastic-Confined Concrete," *Journal of Structural Engineering,* vol. 128, pp. 612-623, 2002.
[30] L. Lam and J. G. Teng, "Design-oriented stress–strain model for FRP-confined concrete," *Fibre-reinforced polymer composites in construction,* vol. 17, pp. 471-489, 2003.
[31] M. R. Spoelstra and G. Monti, "FRP-Confined Concrete Model," *Journal of Composites for Construction,* vol. 3, pp. 143-150, 1999.
[32] P. Rochette and P. Labossiere, "Axial Testing of Rectangular Column Models Confined with Composites," *ASCE J. Compos. for Constr.,* vol. 4, pp. 129-136, 2000.

[33] L.-M. Wang and Y.-F. Wu, "Effect of corner radius on the performance of CFRP-confined square concrete columns: Test," *Engineering Structures,* vol. 30, pp. 493-505, 2008.

[34] L. Lam and J. G. Teng, "Design-oriented stress-strain model for FRP-confined concrete in rectangular columns," *Journal of Reinforced Plastics and Composites,* vol. 22, p. 1149, 2003.

[35] L. Chung-Sheng*, et al.*, "Analytical Model for Fiber-Reinforced Polymer-Jacketed Square Concrete Columns in Axial Compression," *Structural Journal,* vol. 107, pp. 208-217, 2010.

[36] A. Mirmiran*, et al.*, "Effect of column parameters on FRP-confined concrete," *Journal of Composites for Construction,* vol. 2, pp. 175-185, 1998.

[37] X. Yang*, et al.*, "Shape Effect on the Performance of Carbon Fiber Reinforced Polymer Wraps," *Journal of Composites for Construction,* vol. 8, pp. 444-451, 2004.

[38] D. Cusson and P. Paultre, "High-Strength Concrete Columns Confined by Rectangular Ties," *Journal of Structural Engineering,* vol. 120, pp. 783-804, 1994.

[39] R. Eid*, et al.*, "Normal- and High-Strength Concrete Circular Elements Wrapped with FRP Composites," *Journal of Composites for Construction,* vol. 13, pp. 113-124, 2009.

[40] Fédération internationale du Béton (*fib*), "Externally bonded FRP reinforcment for RC structures," Inernational Federation for Structural Concrete, Lausanne, Switzerland2001.

[41] ASTM, "Standard Test Method for Tensile Properties of Polymer Matrix Composite Materials," American Society for Testing and Materials, West Conshohocken, USA,2008.

[42] CEN, "ÍST EN 12390-3:2009: Testing hardened concrete - Part 3: Compressive strength of test specimens," Staðlaráð Íslands, 2009.

[43] B. S. Institution, "BS 1881-121:1983: Testing concrete. Method for determination of static modulus of elasticity in compression," 1983.

[44] J. Friðriksson, "Togstyrkur á skeytingum járna í steyptum bitum," B.Sc., Reykjavik University, 2010.

[45] P. V. Bjarnason and A. Konráðsson, "Ductility and Strength of Rectangular Confined Concrete Columns made of Icelandic Concrete," Reykjavik University, Iceland. 2010.

[46] O. Chaallal*, et al.*, "Circular Columns Confined with FRP: Experimental versus Predictions of Models and Guidelines," *Journal of Composites for Construction,* vol. 10, pp. 4-12, 2006.

[47] J. Li and M. N. S. Hadi, "Behaviour of externally confined high-strength concrete columns under eccentric loading," *Composite Structures,* vol. 62, pp. 145-153, 2003.

Appendix A

Jacket Strain

Following figures show the strain enhancement in the BFRP jackets on corresponding concrete specimens. Two figures only show the BFRP strain with increased time.

Cylinder Specimens

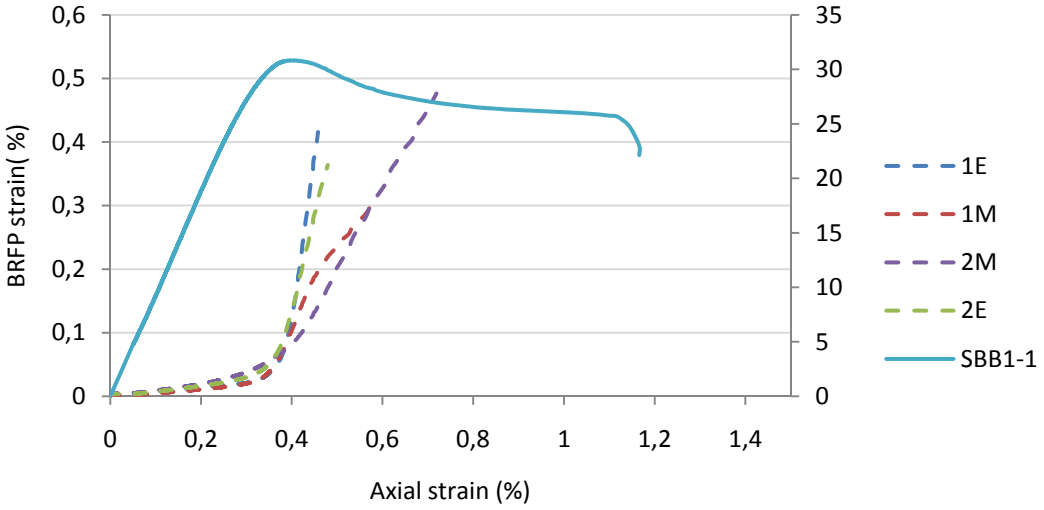

Axial stress-strain curve of specimen SBB1-1 and corresponding longitudinal strain in the BFRP jacket.

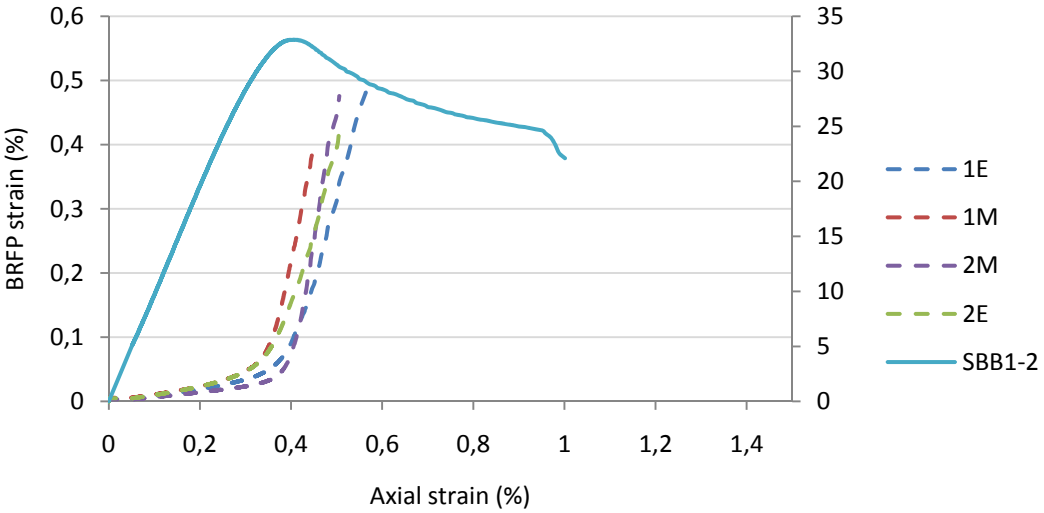

Axial stress-strain curve of specimen SBB1-2 and corresponding longitudinal strain in the BFRP jacket.

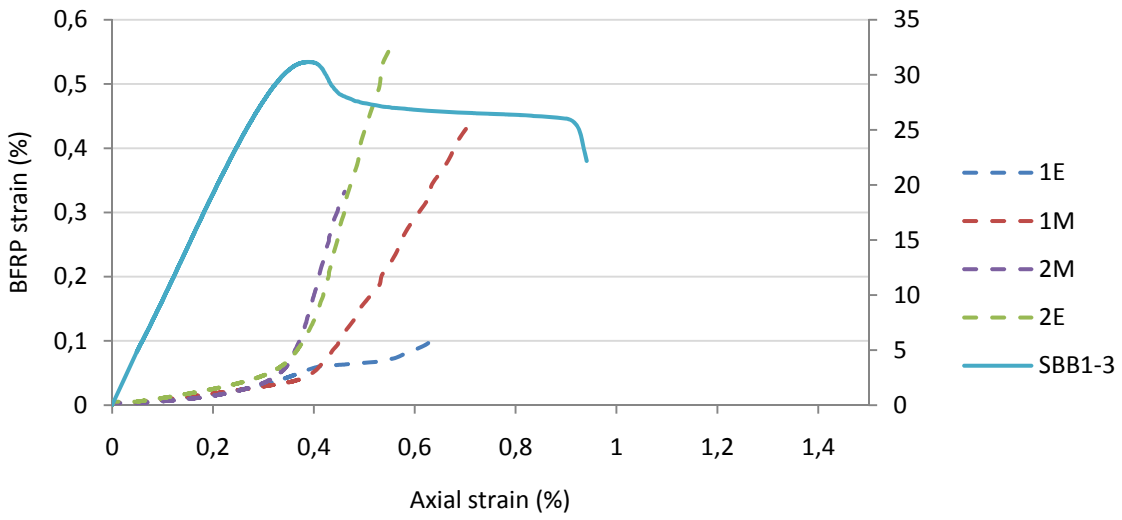

Axial stress-strain curve of specimen SBB1-3 and corresponding longitudinal strain in the BFRP jacket.

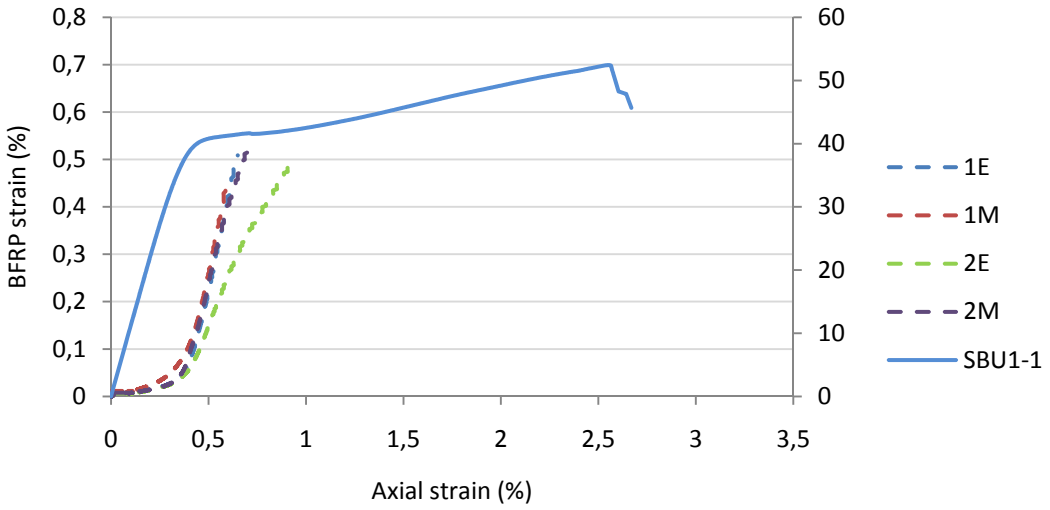

Axial stress-strain curve of specimen SBU1-1 and corresponding longitudinal strain in the BFRP jacket.

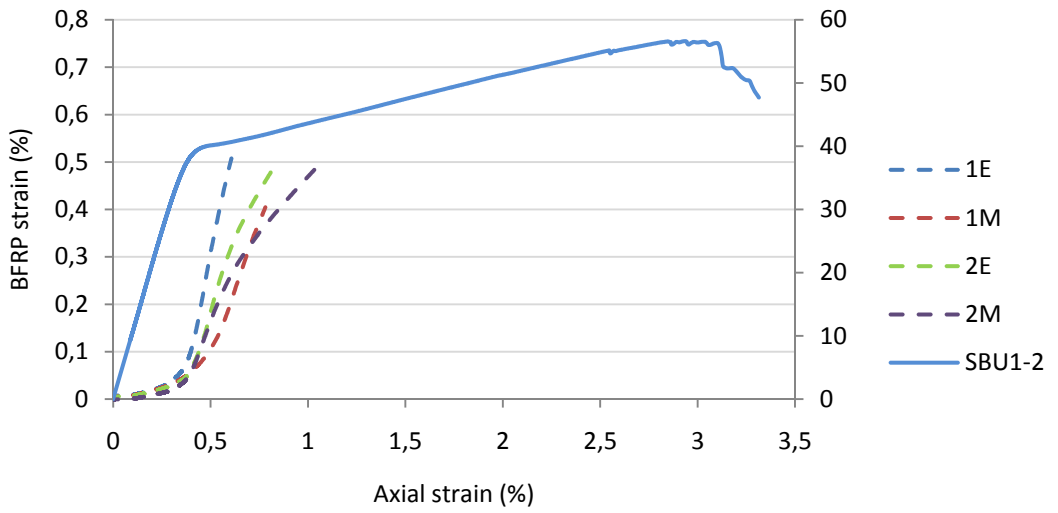

Axial stress-strain curve of specimen SBU1-2 and corresponding longitudinal strain in the BFRP jacket.

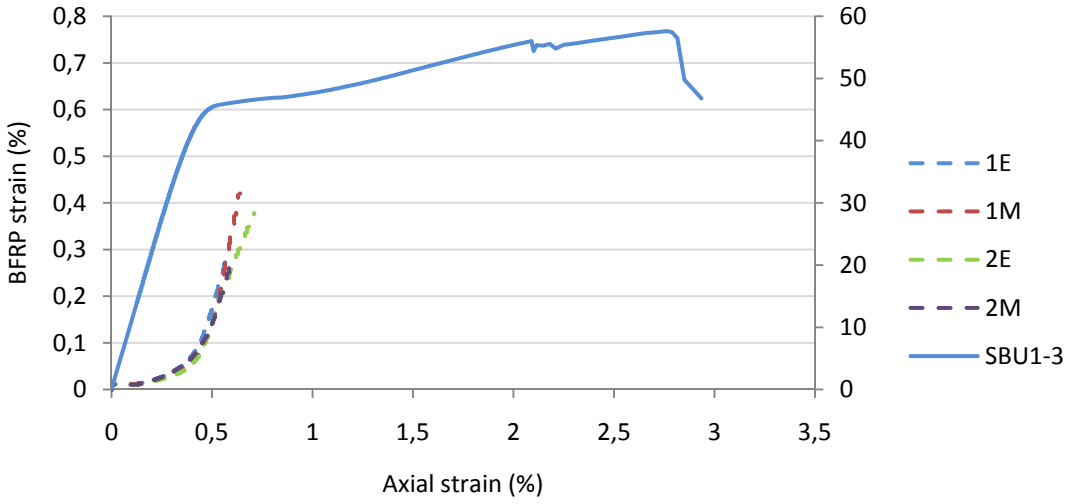

Axial stress-strain curve of specimen SBU1-3 and corresponding longitudinal strain in the BFRP jacket.

Square Columns

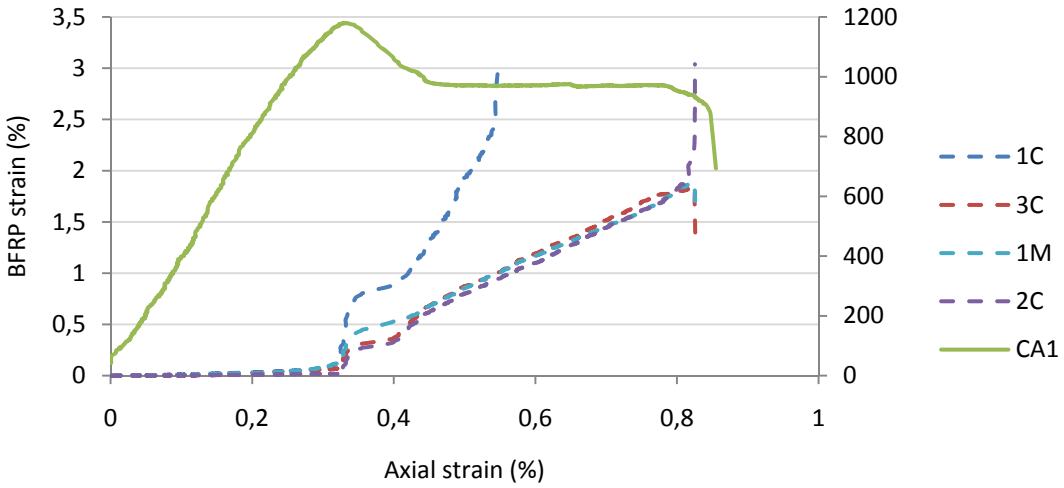

Axial load versus axial strain curves for column CA1 and corresponding longitudinal strain in the BFRP jacket.

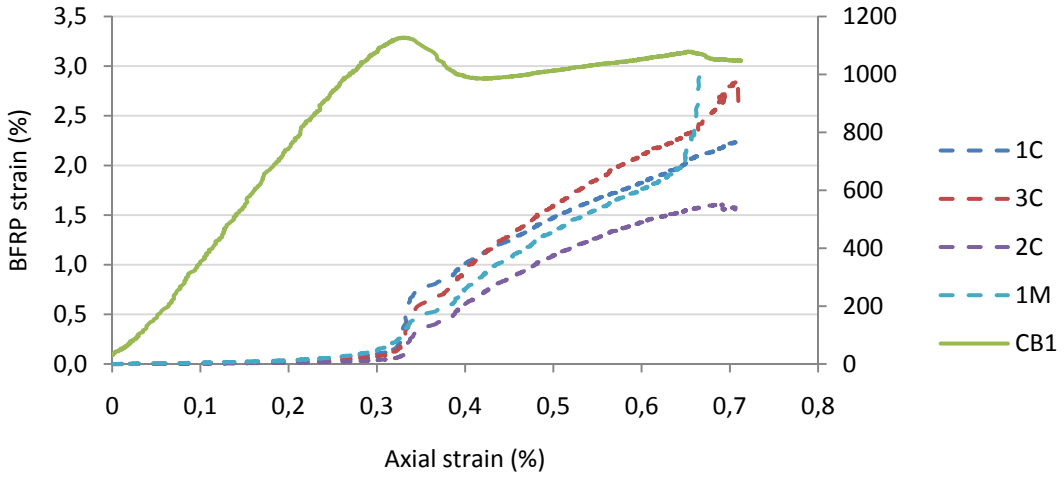

Axial load versus axial strain curves for column CB1 and corresponding longitudinal strain in the BFRP jacket.

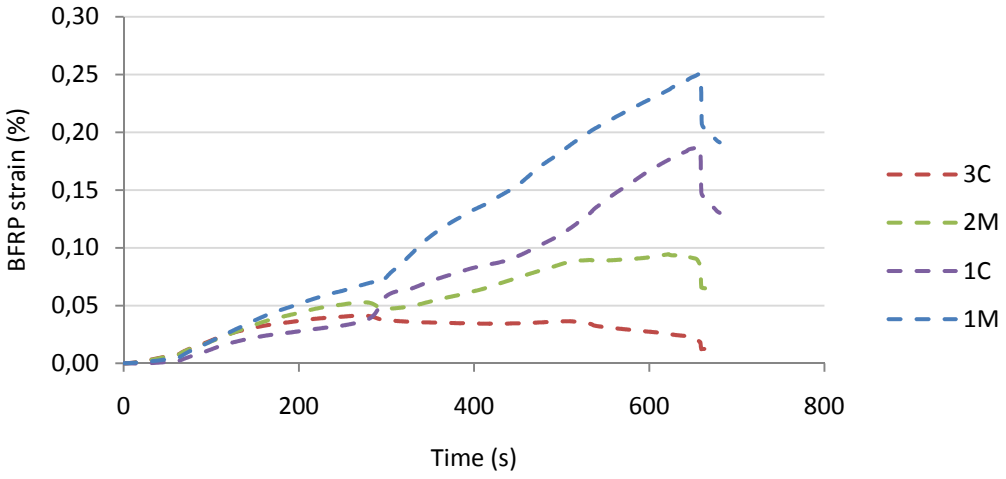

Longitudinal strain in the BFRP jacket on column CA2 with increased time.

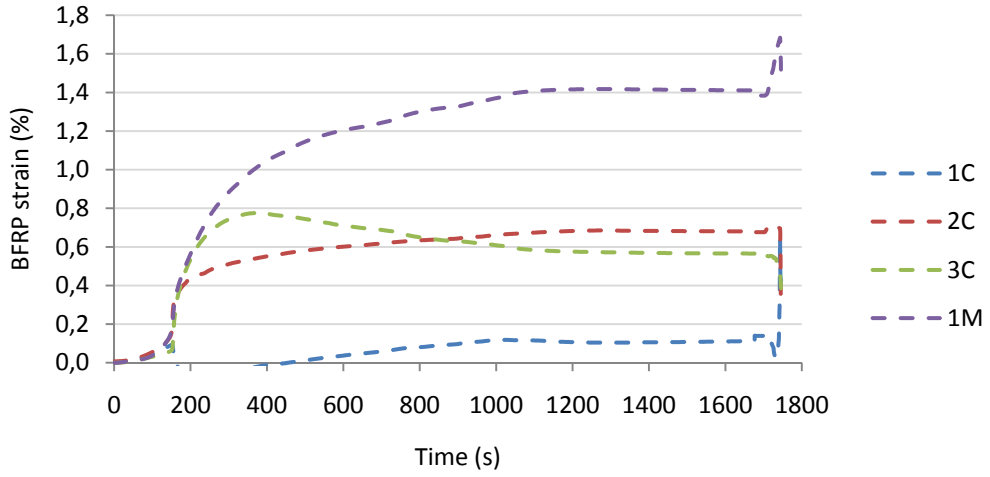

Longitudinal strain in the BFRP jacket on column CA3 with increased time.

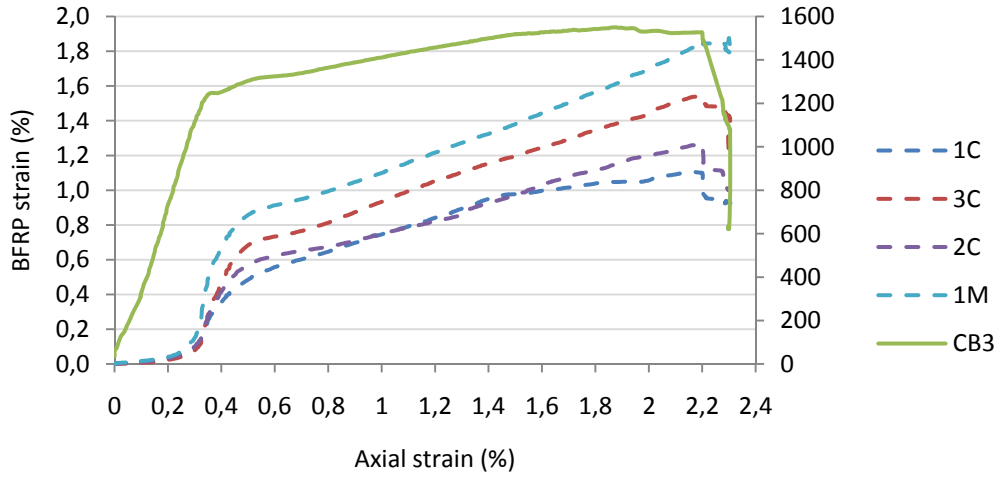

Axial load versus axial strain curve of column CB3 and corresponding longitudinal strain in the BFRP jacket.

Appendix B

Unsuccessful Cylinder Specimens

Three cylinders were partially wrapped with three 40 mm straps forming one number of layers. Those cylinders were designed with wrong strength properties of the BFRP material which resulted in little increase in axial strain.

Specimen	f_c^* (Mpa)	n	$t_{f,tot.}$ (mm)	$f_{l,a}/f_c$	ρ_f (%)	Number of specimens
S-BB1-P	30,7	1	0,2	0,02	0,4	3

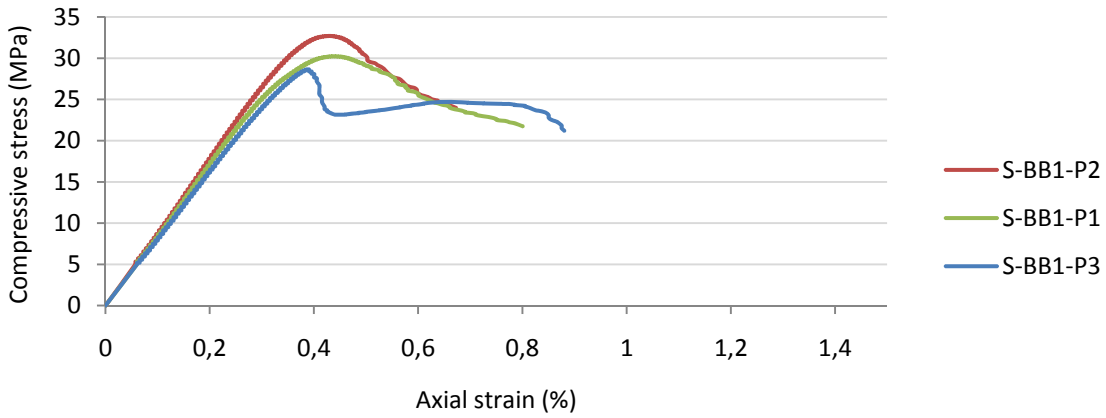

Axial stress-strain curve of unsuccessful partially wrapped specimens.

Partially wrapped specimen after failure.

* Concrete strength determined by standard cylinder test.

Appendix C

Calculation according to Guidelines

Calculation of Confined Cylinders, *AC1 440*

Cylinder specimen	Confined with BAS 220 material		
Diameter	D =	100	mm
Height	h =	200	mm
Cross-section area	A =	7854	mm^2
Concrete			
Compressive strength	f_c =	30,7	Mpa
Modulus of elasticity	E_c =	27721	Mpa
Compressive strain	ε_{c1} =	0,002	0,2 %
BFRP jacket			
Nominal thickness	t_f =	0,2	mm
Number of layers	n =	1	
Total nominal thickness	$t_{f,all}$ =	0,2	mm
Elastic modulus	E_f =	21033	Mpa
Ult. tensile strength	f_f =	310,85	Mpa
BFRP reinforcement ratio	ρ_f =	0,008	0,8 %
Rupture strain of BFRP jacket			
Ult. tensile strain	ε_f =	0,0194	1,9 %
	$0{,}75\varepsilon_f \cdot C_E$ =	0,01455	
Actual rupture strain	$\varepsilon_{f,a}$ =	0,004	0,4 %
Strengthening calculations			
Confining pressure	$f_{l,a}$ =	0,34	Mpa
Confinement ratio	$f_{l,a}/f_c$ =	0,01	
Compressive strength	f_{cc} =	33,0	Mpa
Gain in strength	f_{cc}/f_c =	1,07	
Ultimate strain	ε_{cu} =	0,0026	0,26 %
Gain in strain	$\varepsilon_{cu}/\varepsilon_{c1}$ =	1,29	

Main results of confined cylinders with different number of layers.

Specimen	**n**	**ρ_f**	**$f_{l,a}$ (Mpa)**	**$f_{l,a}/f_c$**	**f_{cc} (Mpa)**	**f_{cc}/f_c**	**ε_{cu}**	**$\varepsilon_{cu}/\varepsilon_{c1}$**	**N_{cc} (kN)**	**Tons**
SBB1	1	0,008	0,3	0,01	32,96	1,07	0,0026	1,29	258,8	26,4
SBB2	2	0,016	0,7	0,02	35,10	1,14	0,0032	1,62	275,7	28,1

Specimen	Confined with BAS UNI 600 material		
Diameter	D =	100	mm
Height	h =	200	mm
Cross-section area	A =	7854	mm^2
Concrete			
Compressive strength	f_c =	35,8	Mpa
Modulus of elasticity	E_c =	29029	Mpa
Compressive strain	ε_{c1} =	0,002	0,2 %
BFRP jacket			
Nominal thickness	t_f =	0,65	mm
Number of layers	n =	1	
Total nominal thickness	$t_{f,all}$ =	0,65	mm
Elastic modulus	E_f =	28870	Mpa
Ult. tensile strength	f_f =	760,34	Mpa
BFRP reinforcement ratio	ρ_f =	0,013	1,3 %
Rupture strain of BFRP jacket			
Ult. tensile strain	ε_f =	0,0271	2,7 %
	$0{,}75\varepsilon_f \cdot C_E$ =	0,020333	
Actual rupture strain	$\varepsilon_{f,a}$ =	0,004	0,4 %
Strengthening calculations			
Confining pressure	$f_{l,a}$ =	0,75	Mpa
Confinement ratio	$f_{l,a}/f_c$ =	0,02	
Compressive strength	f_{cc} =	40,7	Mpa
Gain in strength	f_{cc}/f_c =	1,14	
Ultimate strain	ε_{cu} =	0,0036	0,36 %
Gain in strain	$\varepsilon_{cu}/\varepsilon_{c1}$ =	1,78	

Main results of confined cylinders with different number of layers.

Specimen	**n**	**ρ_f**	**$f_{l,a}$ (Mpa)**	**$f_{l,a}/f_c$**	**f_{cc} (Mpa)**	**f_{cc}/f_c**	**ε_{cu}**	**$\varepsilon_{cu}/\varepsilon_{c1}$**	**N_{cc} (kN)**	**Tons**
SBU1	1	0,026	1,5	0,04	45,19	1,26	0,0049	2,44	354,9	36,2
SBU2	2	0,052	3,0	0,08	53,11	1,48	0,0072	3,60	417,1	42,5
SBU3	3	0,078	4,5	0,13	59,98	1,68	0,0092	4,62	471,1	48,0

Calculation of Confined Cylinders, The Concrete Society

Cylinder specimen	Confined with BAS 220 material		
Diameter	D =	100	mm
Height	h =	200	mm
Cross-section area	A =	7854	mm^2
Concrete			
Compressive strength	f_c =	30,7	Mpa
Modulus of elasticity	E_c =	27721	MPa
Compressive strain	ε_{c1} =	0,002	0,2 %
BFRP jacket			
Nominal thickness	t_f =	0,2	mm
Number of layers	n =	1	
Total nominal thickness	$t_{f,all}$ =	0,2	mm
Elastic modulus	E_f =	21033	Mpa
Ult. tensile strength	f_f =	319,85	Mpa
BFRP reinforcement ratio	ρ_f =	0,008	0,80 %
Rupture strain of BFRP jacket			
Ult. tensile strain	ε_f =	0,0194	1,94 %
Effiency factor	k_ε =	0,6	
Actual rupture strain	$\varepsilon_{f,a}$ =	0,01164	1,16 %
Strengthening calculations			
Confining pressure	$f_{l,a}$ =	1,28	Mpa
Confinement ratio	$f_{l,a}/f_c$ =	0,04	
Confinement criteria		0,089	Mpa
Compressive strength	f_{cc} =	34,9	Mpa
Gain in strength	f_{cc}/f_c =	1,14	
Ultimate strain	ε_{cu} =	0,0044	0,44 %
Gain in strain	$\varepsilon_{cu}/\varepsilon_{c1}$ =	2,22	

Main results of confined cylinders with different number of layers.

Specimen	**n**	**ρ_f (%)**	**$f_{l,a}$ (Mpa)**	**$f_{l,a}/f_c$**	**f_{cc} (Mpa)**	**f_{cc}/f_c**	**$\varepsilon_{cu}/\varepsilon_{c1}$**	**ε_{cu}**	**N_{cc} (kN)**	**Tons**
S1	1	0,008	1,3	0,04	34,9	1,14	2,2	0,0044	274,2	27,9
S2	2	0,016	2,6	0,08	39,1	1,27	2,7	0,0054	307,2	31,3

Cylinder specimen	Confined with BAS UNI 600 material		
Diameter	D =	100	mm
Height	h =	200	mm
Cross-section area	A =	7854	mm^2
Concrete			
Compressive strength	f_c =	35,8	Mpa
Modulus of elasticity	E_c =	29029	MPa
Compressive strain	ε_{c1} =	0,002	0,2 %
BFRP jacket			
Nominal thickness	t_f =	0,65	mm
Number of layers	n =	1	
Total nominal thickness	$t_{f,all}$ =	0,65	mm
Elastic modulus	E_f =	28870	Mpa
Ult. tensile strength	f_f =	760,34	Mpa
BFRP reinforcement ratio	ρ_f =	0,026	2,60 %
Rupture strain of BFRP jacket			
Ult. tensile strain	ε_f =	0,02711	2,71 %
Effiency factor	k_ε =	0,6	
Actual rupture strain	$\varepsilon_{f,a}$ =	0,016266	1,63 %
Strengthening calculations			
Confining pressure	$f_{l,a}$ =	9,88	Mpa
Confinement ratio	$f_{l,a}/f_c$ =	0,28	
Confinement criteria		0,293	Mpa
Compressive strength	f_{cc} =	54,6	Mpa
Gain in strength	f_{cc}/f_c =	1,52	
Ultimate strain	ε_{cu} =	0,0100	1,00 %
Gain in strain	$\varepsilon_{cu}/\varepsilon_{c1}$ =	4,99	

Main results of confined cylinders with different number of layers.

Specimen	**n**	**ρ_f (%)**	**$f_{l,a}$ (Mpa)**	**$f_{l,a}/f_c$**	**f_{cc} (Mpa)**	**f_{cc}/f_c**	**$\varepsilon_{cu}/\varepsilon_{c1}$**	**ε_{cu}**	**N_{cc} (kN)**	**Tons**
SBU1	1	0,026	9,9	0,28	54,6	1,52	5,0	0,0100	428,6	43,7
SBU2	2	0,052	19,8	0,55	73,3	2,05	8,2	0,0165	575,9	58,7
SBU3	3	0,078	29,7	0,83	92,1	2,57	11,5	0,0229	723,3	73,7

Calculation of Confined Cylinders, fib – exact

Cylinder specimen	Confined with BAS 220 material		
Diameter	D =	100	mm
Height	h =	200	mm
Cross-section area	A =	7854	mm^2
Concrete			
Compressive strength	f_c =	30,7	Mpa
Modulus of elasticity	E_c =	27721	MPa
Compressive strain	ε_{c1} =	0,002	0,2 %
BFRP jacket			
Nominal thickness	t_f =	0,2	mm
Number of layers	n =	1	
Total nominal thickness	$t_{f,all}$ =	0,2	mm
Elastic modulus	E_f =	21033	Mpa
Ult. tensile strength	f_f =	310,85	Mpa
Confinem. effectivness.	k_e =	1,0	
BFRP reinforcement ratio	ρ_f =	0,008	0,80 %
Rupture strain of BFRP jacket			
Ult. tensile strain	ε_f =	0,0194	1,94 %
Effiency factor	k_ε =	0,6	
Actual rupture strain	$\varepsilon_{f,a}$ =	0,0116	1,16 %
Strengthening calculations			
Confining pressure	$f_{l,a}$ =	0,98	Mpa
Confinement ratio	$f_{l,a}/f_c$ =	0,03	
	f_{cc}^* =	37,01	Mpa
	ε_{cc}^* =	0,004	
	E_{cc} =	9125,9	MPa
	β =	528,74	
Ultimate strain	ε_{cu} =	0,01	
Compressive strength	f_{cc} =	28,23	Mpa
Gain in strength	f_{cc}/f_c =	0,92	
Gain in strain	$\varepsilon_{cu}/\varepsilon_{c1}$ =	6,78	

Main results of confined cylinders with different number of layers.

Specimen	**n**	**ρ_f**	**$f_{l,a}$ (Mpa)**	**$f_{l,a}/f_c$**	**f_{cc} (Mpa)**	**f_{cc}/f_c**	**ε_{cu}**	**$\varepsilon_{cu}/\varepsilon_{co}$**	**N_{cc} (kN)**	**Tons**
SBB1	1	0,008	1,0	0,03	28,2	0,92	0,0136	6,8	221,7	22,6
SBB2	2	0,016	2,0	0,06	36,2	1,18	0,0174	8,7	284,3	29,0

Cylinder specimen	Confined with BAS UNI 600 material		
Diameter	D =	100	mm
Height	h =	200	mm
Cross-section area	A =	7854	mm^2
Concrete			
Compressive strength	f_c =	35,8	Mpa
Modulus of elasticity	E_c =	29029	MPa
Compressive strain	ε_{c1} =	0,002	0,2 %
BFRP jacket			
Nominal thickness	t_f =	0,65	mm
Number of layers	n =	1	
Total nominal thickness	$t_{f,all}$ =	0,65	mm
Elastic modulus	E_f =	28870	Mpa
Ult. tensile strength	f_f =	760,3	Mpa
Confinem. effectivness.	k_e =	1,0	
BFRP reinforcement ratio	ρ_f =	0,026	2,60 %
Rupture strain of BFRP jacket			
Ult. tensile strain	ε_f =	0,0271	2,71 %
Effiency factor	k_ε =	0,6	
Actual rupture strain	$\varepsilon_{f,a}$ =	0,0163	1,63 %
Strengthening calculations			
Confining pressure	$f_{l,a}$ =	6,10	Mpa
Confinement ratio	$f_{l,a}/f_c$ =	0,17	
	f_{cc}^* =	66,70	Mpa
	ε_{cc}^* =	0,01	
	E_{cc} =	6273,8	MPa
	β =	452,65	
Ultimate strain	ε_{cu} =	0,03	
Compressive strength	f_{cc} =	58,86	Mpa
Gain in strength	f_{cc}/f_c =	1,64	
Gain in strain	$\varepsilon_{cu}/\varepsilon_{c1}$ =	15,94	

Main results of confined cylinders with different number of layers.

Specimen	**n**	**ρ_f**	**$f_{l,a}$ (Mpa)**	**$f_{l,a}/f_c$**	**f_{cc} (Mpa)**	**f_{cc}/f_c**	**ε_{cu}**	**$\varepsilon_{cu}/\varepsilon_{c1}$**	**N_{cc} (kN)**	**Tons**
SBU1	1	0,026	6,1	0,17	58,9	1,64	0,0319	15,9	462,3	47,1
SBU2	2	0,052	12,2	0,34	79,1	2,21	0,0429	21,4	621,4	63,3
SBU3	3	0,078	18,3	0,51	93,2	2,60	0,0505	25,3	732,4	74,7

Calculation of Confined Cylinders, fib – practical

Cylinder specimen	Confined with BAS 220 material		
Diameter	D =	100	mm
Height	h =	200	mm
Cross-section area	A =	7854	mm^2
Concrete			
Compressive strength	f_c =	30,7	Mpa
Modulus of elasticity	E_c =	27721	MPa
Compressive strain	ε_{c1} =	0,002	0,2 %
BFRP jacket			
Nominal thickness	t_f =	0,2	mm
Number of layers	n =	1	
	$t_{f,all}$ =	0,2	mm
Elastic modulus	E_f =	21033	Mpa
Ult. tensile strength	f_f =	310,85	Mpa
Confinem. effectivness.	k_e =	1,0	
BFRP reinforcement ratio	ρ_f =	0,008	0,80 %
Rupture strain of BFRP jacket			
Ult. tensile strain	ε_f =	0,0194	1,94 %
Effiency factor	k_ε =	0,6	
Actual rupture strain	$\varepsilon_{f,a}$ =	0,0116	1,16 %
Strengthening calculations			
Confining pressure	$f_{l,a}$ =	0,98	Mpa
Confinement ratio	$f_{l,a}/f_c$ =	0,03	
	$'f_{l,a}$ =	0,03	
	$'E_c$ =	903,0	
Compressive strength	f_{cc} =	22,6	Mpa
Ultimate strain	ε_{cu} =	0,0087	
Gain in strength	f_{cc}/f_c =	0,74	
Gain in strain	$\varepsilon_{cu}/\varepsilon_{c1}$ =	4,35	

Main results of confined cylinders with different number of layers.

Specimen	**n**	**ρ_f**	**$f_{l,a}$ (Mpa)**	**$f_{l,a}/f_c$**	**f_{cc} (Mpa)**	**f_{cc}/f_c**	**ε_{cu}**	**$\varepsilon_{cu}/\varepsilon_{co}$**	**N_{cc} (kN)**	**Tons**
SBB1	1	0,008	0,98	0,03	22,59	0,74	0,005	2,4	177,4	18,1
SBB2	2	0,016	1,96	0,06	29,40	0,96	0,0052	2,6	230,9	23,5

Cylinder specimen	Confined with BAS UNI 600 material		
Diameter	D =	100	mm
Height	h =	200	mm
Cross-section area	A =	7854	mm^2

Concrete			
Compressive strength	f_c =	35,8	Mpa
Modulus of elasticity	E_c =	29029	MPa
Compressive strain	ε_{c1} =	0,002	0,2 %

BFRP jacket			
Nominal thickness	t_f =	0,65	mm
Number of layers	n =	1	
Total nominal thickness	$t_{f,all}$ =	0,65	mm
Elastic modulus	E_f =	28870	Mpa
Ult. tensile strength	f_f =	760,3	Mpa
Confinem. effectivness.	k_e =	1,0	
BFRP reinforcement ratio	ρ_f =	0,026	2,60 %

Rupture strain of BFRP jacket			
Ult. tensile strain	ε_f =	0,0271	2,71 %
Effiency factor	k_ε =	0,6	
Actual rupture strain	$\varepsilon_{f,a}$ =	0,0163	1,63 %

Strengthening calculations			
Confining pressure	$f_{l,a}$ =	6,10	Mpa
Confinement ratio	$f_{l,a}/f_c$ =	0,17	
	$'f_{l,a}$ =	0,17	
	$'E_c$ =	810,9	
Compressive strength	f_{cc} =	51,5	Mpa
Ultimate strain	ε_{cu} =	0,0176	
Gain in strength	f_{cc}/f_c =	1,44	
Gain in strain	$\varepsilon_{cu}/\varepsilon_{c1}$ =	8,81	

Main results of confined cylinders with different number of layers.

Specimen	**n**	**ρ_f**	**$f_{l,a}$ (Mpa)**	**$f_{l,a}/f_c$**	**f_{cc} (Mpa)**	**f_{cc}/f_c**	**ε_{cu}**	**$\varepsilon_{cu}/\varepsilon_{co}$**	**F_{cc} (kN)**	**Tons**
SBU1	1	0,026	6,10	0,17	51,51	1,44	0,0063	3,1	404,6	41,2
SBU2	2	0,052	12,21	0,34	69,88	1,95	0,0072	3,6	548,8	55,9
SBU3	3	0,078	18,31	0,51	83,98	2,35	0,0079	4,0	659,6	67,2

Calculation of Confined Columns, AC1 440

Column	Confined with BAS UNI 600 material		
Width	b =	180	mm
Width	h =	180	mm
Corner radius	r =	20	mm
Cross-section area	A_g =	32057	mm^2
Concrete			
Compressive strength	f_c =	25,8	Mpa
Modulus of elasticity	E_c =	21423	Mpa
Compressive strain	ε_{c1} =	0,002	0,2 %
Steel reinforcement			
Longitudinal bars	ø =	**K12**	mm
Number of bars	K12	4	psc.
Cross-section area	$A_{s,l}$ =	452,4	mm^2
Reinforcement ratio	ρ_l =	1,41	%
Yield strength	f_y =	628	Mpa
Transverse bars	ø =	**K8**	mm
Hoop spacing	s =	180	mm
Cross-section area	$A_{s,t}$ =	100,5	mm^2
Reinforcement ratio	ρ_t =	0,31	%
BFRP jacket			
Nominal thickness	t_f =	0,65	mm
Number of layers	n =	1	
Total nominal thickness	$t_{f,all}$ =	0,65	mm
Elastic modulus	E_f =	28870	Mpa
Ult. tensile strength	f_f =	760,3	MPa
BFRP reinforcement ratio	ρ_f =	0,014	1,4 %
Rupture strain of BFRP jacket			
Ult. tensile strain	ε_f =	0,02711	2,7 %
	$0{,}75\varepsilon_f \cdot C_E$ =	0,0203	
Allowable strain by ACI	ε_{fe} =	0,004	$0{,}004 \leq 0{,}75\varepsilon_{fu}$
Strengthening calculations			
Shape factor	k_s =	0,59	
Confining pressure	$f_{l,a}$ =	0,49	Mpa
Confinement ratio	$f_{l,a}/f_c$ =	0,02	
Compressive strength	f_{cc} =	29,04	Mpa
Gain in strength	f_{cc}/f_c =	1,13	
Ultimate strain	ε_{cu} =	0,003	0,3 %
Gain in strain	$\varepsilon_{cu}/\varepsilon_{c1}$ =	1,68	
Axial compressive strength	N_{cc} =	1201,9	kN

Main results of confined columns with different number of layers and corner radius.

Column	**n**	**ρ_f**	**$f_{l,a}$ (Mpa)**	**f_{cc} (Mpa)**	**f_{cc}/f_c**	**ε_{cu}**	**$\varepsilon_{cu}/\varepsilon_{c1}$**	**N_{cc} (kN)**	**N_{cc}/N_c**	**Tons**
CA1	1	0,0144	0,49	29,0	1,13	0,0034	1,68	1201,9	1,09	122,4
CA2	2	0,0289	0,99	32,0	1,24	0,0045	2,27	1295,8	1,18	132,0
CA3	3	0,0433	1,48	34,8	1,35	0,0056	2,82	1382,7	1,26	140,8
CB1	1	0,0144	0,62	29,9	1,16	0,0037	1,84	1206,4	1,12	122,9
CB2	2	0,0289	1,25	33,5	1,30	0,0051	2,56	1318,9	1,22	134,3
CB3	3	0,0433	1,87	36,8	1,43	0,0065	3,23	1421,3	1,31	144,7

Calculation of Confined Columns, The Concrete Society

Column	Confined with BAS UNI 600 material		
Width	b =	180	mm
Width	h =	180	mm
Corner radius	r =	20	mm
Cross-section area	A_g =	32057	mm^2
Concrete			
Compressive strength	f_c =	25,8	Mpa
Modulus of elasticity	E_c =	21423	MPa
Compressive strain	ε_{c1} =	0,002	0,20 %
Steel reinforcement			
Longitudinal bars	ø =	**K12**	mm
Number of bars	K12	4	psc.
Cross-section area	$A_{s,l}$ =	452,4	mm^2
Reinforcement ratio	ρ_l =	1,41	%
Yield strength	f_y =	628	MPa
Transverse bars	ø =	**K8**	mm
Hoop spacing	s =	180	mm
Cross-section area	$A_{s,t}$ =	100,5	mm^2
Reinforcement ratio	ρ_t =	0,31	%
BFRP jacket			
Nominal thickness	t_f =	0,65	mm
Number of layers	n =	1	
Total nominal thickness	$t_{f,all}$ =	0,65	mm
Elastic modulus	E_f =	28870	Mpa
Ult. tensile strength	f_f =	760,34	MPa
BFRP reinforcment ratio	ρ_f =	0,0144	1,44 %
Rupture strain			
Ulr. Tensile strain	ε_f =	0,02711	2,71 %
Effiency factor	k_ε =	0,6	
Actual rupture strain	$\varepsilon_{f,a}$ =	0,0163	1,63 %
Strengthening calculations			
Shape factor	k_s =	0,59	
Confining pressure	$f_{l,a}$ =	3,883	Mpa
Confinement ratio	$f_{l,a}/f_c$ =	0,15	
Confinement criteria		0,31	MPa
Compressive strength	f_{cc} =	30,36	Mpa
Gain in strength	f_{cc}/f_{cu} =	0,94	
Ultimate strain	ε_{cu} =	0,0084	
Gain in strain	$\varepsilon_{cu}/\varepsilon_{co}$ =	4,19	
Axial compressive strength	N_{cc} =	1243,5	kN

Main results of confined columns with different number of layers and corner radius.

Columns	**n**	**ρ_f (%)**	**$f_{l,a}$ (Mpa)**	**f_{cc} (Mpa)**	**f_{cc}/f_c**	**ε_{cu}**	**$\varepsilon_{cu}/\varepsilon_{c1}$**	**N_{cc} (kN)**	**N_{cc}/N_c**	**Tons**
CA1	1	0,0144	3,88	30,4	1,18	0,0069	3,43	1243,5	1,13	126,8
CA2	2	0,0289	7,77	34,9	1,35	0,0102	5,11	1387,4	1,26	141,4
CA3	3	0,0433	11,65	39,5	1,53	0,0136	6,79	1531,4	1,39	156,1
CB1	1	0,0144	3,88	31,5	1,22	0,0077	3,87	1258,5	1,16	128,3
CB2	2	0,0289	7,77	37,3	1,44	0,0120	5,98	1435,8	1,33	146,4
CB3	3	0,0433	11,65	43,0	1,67	0,0162	8,10	1613,1	1,49	164,4

Calculation of Confined Columns, fib-exact

Column	Confined with BAS UNI 600 material		
Width	b =	180	mm
Width	h =	180	mm
Corner radius	r =	20	mm
Cross-section area	A_g =	32057	mm^2
Concrete			
Compressive strength	f_c =	25,8	Mpa
Modulus of elasticity	E_c =	21423	MPa
Compressive strain	ε_{c1} =	0,002	0,2 %
Steel reinforcement			
Longitudinal bars	ø =	**K12**	mm
Number of bars	K12	4	psc.
Cross-section area	$A_{s,l}$ =	452,4	mm^2
Reinforcement ratio	ρ_l =	1,41	%
Yield strength	f_y =	628	MPa
Transverse bars	ø =	**K8**	mm
Hoop spacing	s =	180	mm
Cross-section area	$A_{s,t}$ =	100,5	mm^2
Reinforcement ratio	ρ_t =	0,31	%
BFRP jacket			
Nominal thickness	t_f =	0,65	mm
Number of layers	n =	1	
Total nominal thickness	$t_{f,all}$ =	0,65	mm
Elastic modulus	E_f =	28870	Mpa
Ult. tensile strength	f_f =	760,34	MPa
BFRP reinforcement ratio	ρ_f =	0,0144	1,44 %
Rupture strain			
Ult. tensile strain	ε_f =	0,02711	2,71 %
Efficiency factor	κ_ε =	0,6	
Actual rupture strain	$\varepsilon_{f,a}$ =	0,016266	1,63 %
Strengthening calculations			
Shape factor	k_s =	0,59	
Confining pressure	$f_{l,a}$ =	1,99	Mpa
Confinement ratio	$f_{l,a}/f_c$ =	0,08	
	f_{cc}^* =	37,51	MPa
	ε_{cc}^* =	0,0065	
	E_{cc} =	5737,1	MPa
	β =	1122,19	
Ultimate strain	ε_{cu} =	0,0436	
Compressive strength	f_{cc} =	24,91	Mpa
Gain in strength	f_{cc}/f_c =	0,965	
Gain in strain	$\varepsilon_{cu}/\varepsilon_{c1}$ =	21,80	

Main results of confined columns with different number of layers and corner radius.

Column	**n**	**ρ_f**	**$f_{l,a}$ (Mpa)**	**$f_{l,a}/f_c$**	**f_{cc} (Mpa)**	**f_{cc}/f_c**	**ε_{cu}**	**$\varepsilon_{cu}/\varepsilon_{c1}$**	**N_{cc} (kN)**	**N_{cc}/N_c**	**Tons**
CA1	1	0,0144	1,99	0,08	24,9	0,97	0,0436	21,8	1071,3	0,97	109,2
CA2	2	0,0289	3,98	0,15	34,9	1,35	0,0612	30,6	1388,3	1,26	141,5
CA3	3	0,0433	5,97	0,23	42,3	1,64	0,0741	37,1	1622,4	1,48	165,4
CB1	1	0,0144	2,51	0,10	27,9	1,08	0,0489	24,4	1146,4	1,06	116,9
CB2	2	0,0289	5,01	0,19	39,0	1,51	0,0683	34,1	1489,3	1,38	151,8
CB3	3	0,0433	7,52	0,29	47,1	1,83	0,0825	41,2	1739,6	1,61	177,3

Calculation of Confined Columns, fib-practical

Column	Confined with BAS UNI 600 material		
Width	b =	180	mm
Width	h =	180	mm
Corner radius	r =	20	mm
Cross-section area	A_g =	32057	mm^2
Concrete			
Compressive strength	f_c =	25,8	Mpa
Modulus of elasticity	E_c =	21423	MPa
Compressive strain	ε_{c1} =	0,002	0,2 %
Steel reinforcement			
Longitudinal bars	ø =	**K12**	mm
Number of bars	K12	4	psc.
Cross-section area	$A_{s,l}$ =	452,4	mm^2
Reinforcement ratio	ρ_l =	1,41	%
Yield strength	f_y =	628	MPa
Transverse bars	ø =	**K8**	mm
Hoop spacing	s =	180	mm
Cross-section area	$A_{s,t}$ =	100,5	mm^2
Reinforcement ratio	ρ_t =	0,31	%
BFRP jacket			
Nominal thickness	t_f =	0,65	mm
Number of layers	n =	1	
Total nominal thickness	$t_{f,all}$ =	0,65	mm
Elastic modulus	E_f =	28870	Mpa
Ult. tensile strength	f_f =	760,34	MPa
BFRP reinforcement ratio	ρ_f =	0,0144	1,44 %
Rupture strain			
Ult. tensile strain	ε_f =	0,02711	2,71 %
Efficiency factor	κ_ε =	0,6	
Actual rupture strain	$\varepsilon_{f,a}$ =	0,016266	1,63 %
Strengthening calculations			
Shape factor	k_s =	0,59	
Confining pressure	$f_{l,a}$ =	1,99	Mpa
Confinement ratio	$f_{l,a}/f_c$ =	0,08	
	$f_{l,a}'$ =	0,0771	
	E_c' =	830,35	
Compressive strength	f_{cc} =	26,65	Mpa
Gain in strength	f_{cc}/f_c =	1,033	
Ultimate strain	ε_{cu} =	0,0134	
Gain in strain	$\varepsilon_{cu}/\varepsilon_{c1}$ =	6,69	

Main results of confined columns with different number of layers and corner radius.

Column	**n**	**ρ_f**	**$f_{l,a}$ (Mpa)**	**$f_{l,a}/f_c$**	**f_{cc} (Mpa)**	**f_{cc}/f_c**	**ε_{cu}**	**$\varepsilon_{cu}/\varepsilon_{c1}$**	**N_{cc} (kN)**	**N_{cc}/N_c**	**Tons**
CA1	1	0,0144	1,99	0,08	26,7	1,03	0,0134	6,7	1126,4	1,02	114,8
CA2	2	0,0289	3,98	0,15	35,6	1,38	0,0173	8,6	1407,8	1,28	143,5
CA3	3	0,0433	5,97	0,23	42,4	1,64	0,0202	10,1	1623,7	1,48	165,5
CB1	1	0,0144	2,51	0,10	29,3	1,13	0,0145	7,3	1188,8	1,10	121,2
CB2	2	0,0289	5,01	0,19	39,3	1,52	0,0189	9,4	1497,5	1,39	152,7
CB3	3	0,0433	7,52	0,29	46,9	1,82	0,0222	11,1	1734,4	1,60	176,8

Appendix D

Reference Cylinders

Reference cylinders from test group SBB.

Specimen	D*(mm)	H (mm)	W (kg)	ρ (kg/m^3)	N (kg)	f_c (Mpa)	Age (days)
SBB0-1	100	200	-	-	24.985	31,2	29
SBB0-2	99,1	200,0	3,46	2.244	23.680	30,1	29
SBB0-3	99,2	200,1	3,48	2.248	24.169	30,7	29
Average	99,4	200,0	3,5	2.246	24.278	30,7	

Reference cylinders from test group SBU.

Specimen	D*(mm)	H (mm)	W (kg)	ρ (kg/m^3)	N (kg)	f_c (Mpa)	Age (days)
SBU0-1	101,0	200,1	3,73	2.325	25.896	31,7	39
SBU0-2	100,1	200,6	3,71	2.352	27.198	33,9	39
SBU0-3	101,0	201,1	3,85	2.387	34.169	41,8	39
Average	100,7	200,6	3,8	2.354	29.088	35,8	

Reference cylinders for columns.

Specimen	D*(mm)	H (mm)	W (kg)	ρ (kg/m^3)	N (kg)	f_c (Mpa)	Age (days)
C1	99,6	200,3	3,34	2.142	19.800	24,9	135
C2	99,5	200,4	3,36	2.158	18.950	23,9	135
C3	99,2	200,5	3,31	2.137	22.400	28,4	135
Average	99,4	200,4	3,3	2.148	20.383	25,8	

Reference cylinders for columns, estimation of elastic modulus..

Specimen	D*(mm)	H (mm)	W (kg)	ρ (kg/m^3)	E (MPa)	Age (days)
C1	149,4	318,0	11,3	2.027	20.515	135
C2	149,0	300,6	11,2	2.127	23.572	135
C3	148,9	300,5	11,1	2.125	20.180	135
Average	149,1	306,4	11,2	2.093	21.422	

* Average dimension of each cylinder.

Appendix E

Tensile Coupon Test Specimens

Measured dimension on tensile coupon test specimens.

	End 1		Middle		End 2		Average	
	w*	t×	w	t	w	t	w	t
Specimen	(mm)	(mm)	(mm)	(mm)	(mm)	(mm)	(mm)	(mm)
BAS 220								
BB-1	24,9	0,55	24,5	0,55	24,35	0,55	24,58	0,55
BB-2	26,65	0,6	25,8	0,5	25,35	0,5	25,93	0,53
BB-3	24,05	0,7	24,4	0,45	25,1	0,6	24,52	0,58
BB-4	25,55	0,6	27,4	0,65	21,0	0,65	24,65	0,63
BB-5	22,95	0,5	23,3	0,5	21,55	0,4	22,60	0,47
Average							**24,46**	**0,55**
BAS 600								
BU-1	23,75	1,5	23,2	1,25	23,95	1,2	23,63	1,32
BU-2	24,1	1,5	23,15	1,25	22,85	1,25	23,37	1,33
BU-3	23,6	1,45	22,4	1,1	26,1	1,35	24,03	1,30
BU-4	22,3	1,45	22,1	1,05	24,4	1,2	22,93	1,23
BU-5	25,5	1,3	22,95	1,35	25	1,15	24,48	1,27
Average							**23,69**	**1,29**

Estimation of volume fraction in the BFRP composite.

Specimen	Weigth of dry fibre *(g)*	Weigth of fibre in a matrix *(g)*	Weight of matrix *(g)*	Density of fibres (g/m^3)	Density of matrix (g/m^3)	Volume fraction of fibres, V_f (%)
BAS 220						
1	0,72	1,45	0,730	2,7	1,3	32,2
2	0,72	1,44	0,712	2,7	1,3	32,5
3	0,72	1,55	0,830	2,7	1,3	29,5
Average						**31,4**
BAS 600						
1	2,15	4,47	2,318	2,7	1,3	30,9
2	2,15	5,17	3,018	2,7	1,3	25,6
3	2,15	4,67	2,518	2,7	1,3	29,1
Average						**28,5**

* Width
× Thickness